TECHNISCHE UNIVERSITÄT MÜNCHEN

Wissenschaftszentrum Weihenstephan für Ernährung, Landnutzung und Umwelt (WZW)

Lehrstuhl für Biochemische Pflanzenpathologie

Cyclic nucleotide signaling in *Arabidopsis thaliana* and the identification of cGMP binding proteins

Katharina Meier

Vollständiger Abdruck der von der Fakultät Wissenschaftszentrum Weihenstephan für Ernährung, Landnutzung und Umwelt der Technischen Universität München zur Erlangung des akademischen Grades eines

Doktors der Naturwissenschaften

genehmigten Dissertation.

Vorsitzender: Univ.-Prof. Dr. R. Hückelhoven

Prüfer der Dissertation: 1. Univ.-Prof. Dr. J. Durner

2. Univ.-Prof. Dr. B. Poppenberger-Sieberer

Die Dissertation wurde am 20.10.2016 bei der Technischen Universität München eingereicht und durch die Fakultät Wissenschaftszentrum Weihenstephan für Ernährung, Landnutzung und Umwelt am 20.01.2017 angenommen.

I Table of Contents

II Abbreviations

ABA	Abscisic acid
ANP	Atrial natriuretic peptide
AP	Alkaline phosphatase
ATP	Adenosine triphosphate
BR	Brassinosteroid
cAMP	Cyclic adenosine monophosphate
cCMP	Cyclic cytidine monophosphate
CGBP	cGMP binding protein
cGMP	Cyclic guanosine monophosphate
CNGC	Cyclic nucleotide gated channel
cNMP	Cyclic nucleotide monophosphate
cUMP	Cyclic uridine monophosphate
DEX	Dexamethasone
EDRF	Endothelial-derived relaxant factor
FT-ICR	Fourier-transform-ion-cyclotron-resonance
GA	Gibberellic acid
GC	Guanylate cyclase
GTP	Guanosine triphosphate
GDP	Guanosine diphosphate
GMP	Guanosine monophosphate
H	Hour
HPLC-MS/MS	High performance liquid chromatography tandem mass spectrometry
IAA	Indole-3-acetic acid
IPTG	Isopropyl-β-D-thiogalactopyranosid
LB	Luria-Bertani
LOD	Limit of detection
LOQ	Limit of quantification
MES	2-(N-morpholino)ethanesulfonic acid
mgf	Mascot generic files
Min	Minute
MS	Murashige and Skoog
NDPK	Nucleoside diphosphate kinase
Ni-NTA	Nickel-2, 2′, 2″-Nitrilotriacetic acid
NOS	Nitric oxide synthase

OD	Optical density
ON	Over night
PAGE	Polyacrylamide gel electrophoresis
PAMP	Pathogen associated molecular patterns
PCR	Polymerase chain reaction
PDE	Phosphodiesterase
pGC	Particulate guanylate cyclase
PKA	Protein kinase A
PKG	Protein kinase G
qPCR	Quantitative PCR
ROS	Reactive oxygen species
Rpm	Rounds per minute
PSII	Photosystem II
SDS	Sodium dodecyl sulfate
sGC	Soluble guanylate cyclase
STa	Heat-stable enterotoxins
TRIS	2-Amino-2-hydroxymethyl-propane-1,3-diol
TBS	TRIS-buffered Saline
TBST	TRIS-buffered Saline and Tween 20

III List of Figures

IV List of Tables

V Summary

Cyclic nucleotides are important second messengers in the mammalian system and have been shown to function in various signal transduction processes. The most studied cNMPs are 3’5’-cGMP and -cAMP, being involved in processes such as smooth muscle relaxation, phototransduction, neural regeneration and germ cell proliferation. Increasing evidence suggests that additionally 3’5’-cUMP and -cCMP might function as second messengers in mammals. Furthermore, 2’3’-cNMPs were shown to be involved in signal transduction processes and were suggested to play a role in apoptosis. In plants, the most studied cyclic nucleotide is 3’5’-cGMP. It was shown to be involved in various processes, such as chloroplast development, stomata opening, cell cycle progression and stress responses. However, the existence of downstream targets of cGMP in plants needs to be clarified. Furthermore, also 3’5’-cAMP was shown to be present in plants and was suggested to be involved in cell cycle progression as well as defense and stress responses. In contrast, the exact signaling role of 2’3’-cNMPs as well as 3’5’-cCMP and 3’5’-cUMP in plants remains largely unknown.

In this study, the regulation of 3’5’- and 2’3’-cNMP levels was investigated during cell death events as well as in response to nitric oxide (NO) and auxin signaling. Two different methods, fourier-transform-ion-cyclotron-resonance (FT-ICR) mass spectrometry and high performance liquid chromatography tandem mass spectrometry (HPLC-MS/MS), were applied. To induce a hypersensitive response (HR) *pDEX:AvrRPM1-HA* mutants plants were used. These plants contain the *Pseudomonas avirulence (Avr)* gene, under the control of a dexamethasone (DEX)-inducible promotor. Through treatment with DEX the expression of *AvrRPM1* is initiated leading to the simulation of an avirulent pathogen attack. Furthermore, *Arabidopsis thaliana* Col-0 plants were fumigated with NO_2 since it was shown that NO_2 causes cell damage or cell death when applied in high concentrations. Additionally, the role of cNMPs in response to stress and hormone signaling was investigated. Therefore cNMP regulation was examined after treatment with the NO-donor SNP and the phytohormone auxin (IAA). NO was previously shown to induce defense gene expression as well as cell death. Furthermore, 3’5’-cGMP levels were shown to be increased in response to NO and IAA. In this study, using HPLC-MS/MS, it was shown that rather 2’3’-cNMP levels but not 3’5’-cNMPs are up-regulated during HR and NO_2-induced cell death, as well as in SNP- and IAA-induced responses. This result suggested a distinct role for 2’3’-cNMPs in these signaling processes. In response to treatment with the phytohormone IAA, only 2’3’-cCMP levels were increased suggesting that this cyclic nucleotide might be involved in the regulation of plant development and growth.

The second aim of this study was the identification of guanylate cyclases (GCs) in plants. Therefore, an assay was established to measure cGMP formation from plant protein extract. The biochemical purification of potential GCs failed. CGMP formation measured in protein extracts from soil grown *A. thaliana* and *Hordeum vulgare* plants was shown to be the result of a contamination with rhizosphere organisms. CGMP formation in protein extracts from sterile grown plants was not detectable.

The third part of this study was the identification of cGMP target proteins. A phosphodiesterase (PDE) resistant version of cGMP-agarose was used to purify cGMP binding proteins (CGBPs). After incubation of *A. thaliana* protein extracts with the cGMP-agarose, bound proteins were analyzed and quantified using mass spectrometry. This experiment resulted in the identification of 5 potential CGBPs. The most prominent candidate was HP29b, a protein of unknown function located in the chloroplast. Two T-DNA insertion lines of this candidate were analyzed for flavonol and chlorophyll content, as well as photosynthetic activity in response to UV-B radiation. It was demonstrated that both mutant lines showed decreased flavonol and chlorophyll contents but no differences in photosynthetic activity could be detected. Therefore an involvement of HP29b in flavonol and chlorophyll biosynthetic processes as well as in phototransduction processes was concluded.

Taken together, this study opens a new perspective on cNMP signaling in the plant system. It is suggested that not only 3’5’-cGMP and -cAMP, are part of the plant signaling cascade, but also 2’3’-cNMPs might be involved in important signaling processes such as cell death, HR and stress signaling. Additionally, potential downstream targets of cGMP have been identified. The most prominent candidate being a protein located in the chloroplast suggests that the cGMP signaling cascade in plants might include additional pathways compared to the mammalian system.

1 Introduction

1.1 Guanosine 3’5’-cyclic monophosphate signaling across the tree of life

1.1.1 The history of cGMP research

The need of every cell to respond to internal and external signals causes the requirement of a multitude of signaling mechanisms. One of them includes signal transduction via the second messenger 3’5’-cyclic guanosine monophosphate (3’5’-cGMP). A detailed overview on the history of cGMP-research was given by Kots et al. (2009) as well as Lemtiri-Chlieh et al. (2011). Hardman and Sutherland (1969) were able to identify the producing enzyme, the guanylate cyclase (GC), showing that cGMP is a product of the conversion of guanosine triphosphate (GTP). Further investigation revealed the existence of certain isoforms of GCs, categorized in soluble (sGC) and membrane bound (pGC) GCs (Goridis & Morgan, 1973; Kimura & Murad, 1974, 1975a, 1975b). Additionally, in the early seventies further progress was made in the identification of cGMP specific degrading enzymes, the phosphodiesterases (PDE), from various tissue of rat and bovine (Beavo et al., 1970; Cheung, 1971; Kakiuchi et al., 1971; Thompson & Appleman, 1971). It was now clear that cGMP levels in cells and tissue are regulated, but the specific underlying regulatory processes remained unknown. Progress in this field was achieved by further studies. It was shown that endothelial-derived relaxant factor (EDRF) causes an increase in cGMP levels resulting in smooth muscle relaxation (Furchgott & Zawadzki, 1980; Rapoport et al., 1983; Rapoport & Murad, 1983). Later on it was shown that EDRF in fact is nitric oxide (NO) (Ignarro et al., 1987). These studies led to the current understanding of the pathway of sGC activation and function and were awarded with the Nobel Prize in 1998. The second pathway investigated was based on the finding that a peptide, the atrial natriuretic peptide (ANP), also leads to increased cGMP levels (Hamet et al., 1984; Waldman et al., 1984). These studies gave strong impulse in research of particulate guanylate cyclase (pGC) identification and characterization (reviewed by Kots et al., 2009). Today it is known that ANP is the direct activator of certain isoforms of pGCs.

Research on cGMP and cGMP signaling is still ongoing. Because of its importance in many different pathways and tissues it became an interesting target in drug development. One prominent example was the development of a specific inhibitor for a cGMP specific PDE, called sildenafil, mostly known under its trade mark name Viagra®. Briefly, inhibition of cGMP degrading PDE5 caused an increase of cGMP levels followed by smooth muscle relaxation in the penile erectile tissue allowing the blood flow into the *corpus cavernosum* leading to an erection.

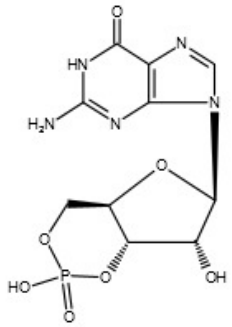

Figure 1: Chemical structure of 3'5'-cGMP.

About the same time, when PDEs where discovered in the mammalian system, scientists became interested in cGMP signaling in plants. PDE activity was discovered in several different species and tissue including common bean (*Phaseolus vulgaris*), pea (*Pisum sativum*) seedlings and spinach (*Spinacea oleracea*) chloroplasts (Brown et al., 1977; Brown et al., 1980; Lin & Varner, 1972). Although these findings were thought to be very interesting, cGMP occurrence and signaling in plants was controversial for a long time. This was mainly due to the fact, that concentrations measured were considerably lower compared to animal tissue and extraction was much more difficult and laborious (Lemtiri-Chlieh et al., 2011; Newton & Smith, 2004). Further, detection was hindered by cross-reactions of plant tissue specific compounds with immunoassay kits (Lemtiri-Chlieh et al., 2011). After cGMP was clearly identified applying mass spectrometry technology, the existence of cGMP in plants was no longer questioned (Newton et al., 1989). Remaining doubts on the second messenger role of cGMP in plants were cleared when first evidence occurred that a similar activation mechanism like in the mammalian system is present. In 1994, it was shown that gaseous NO increases cGMP levels in spruce (*Picea abies*) needles (Pfeiffer et al., 1994). These findings together with studies showing an involvement of cGMP in photosynthesis laid the foundation for acceptance and further research on plant cGMP signaling (Bowler et al., 1994; Neuhaus et al., 1997). By now, one NO-dependent and one NO-independent sGC, as well as several pGCs were proposed (Kwezi et al., 2007; Ludidi & Gehring, 2003; Meier et al., 2010; Mulaudzi et al., 2011). However, the function of these proteins as GCs is still being questioned, mainly because of irreproducible results and considerably low activities compared to mammalian GCs (Ashton, 2011; Bojar et al., 2014). In fact, purified soluble GC from bovine lung was shown to exhibit an activity of 2100 nmol/ mg protein/ min upon activation with NO. In contrast, the suggested NO-activated GC from *Arabidopsis thaliana*, NOGC1, showed an activity of only 22.5 pmol/ mg protein/ min upon activation (Humbert et al., 1990; Mulaudzi et al., 2011).

Besides eukaryotes, cGMP signaling was also found in the bacterial system. Convincing results for cGMP signaling in bacteria were shown by de Alda et al. (2000), demonstrating similar concentrations of cGMP in cyanobacteria strain *Synechocystis sp.* PCC 6803. They

further identified a bacterial GC (Cya2) in this organism. In another study, specific GC activity of Cya2 was demonstrated (Rauch et al., 2008). Another important finding in bacterial cGMP research was the description of a physiological role of cGMP in prokaryotes. Marden et al. (2011) were able to demonstrate that cGMP controls cyst development in *Rhodospirillum centenum* and identified the corresponding GC. Taken together, cGMP signaling in bacteria still needs investigation to fully understand the underlying mechanisms. Nevertheless, it was clearly demonstrated that cGMP signaling pathways are indeed present in certain species.

1.1.2 cGMP signaling in mammals

In mammals, cGMP is produced from GTP either by sGCs or pGCs. Both forms are activated independently by different signaling molecules (Figure 3). The pGCs are homodimers with a extracellular ligand binding site consisting of two domains at the N-terminus, a transmembrane- and juxtamembrane domain, as well as a kinase homology domain connected to the intracellular catalytic domain via a hinge region (Figure 2) (Lucas et al., 2000). Upon ligand binding, the juxtamembrane closes the extracellular domain, causing the reorientation of the kinase homology domain, which can now bind adenosine triphosphate (ATP) triggering a conformational change leading to activation of the GC-catalytic domain (He et al., 2001; Labrecque et al., 2001; Potter & Hunter, 2001; Schaap, 2005).

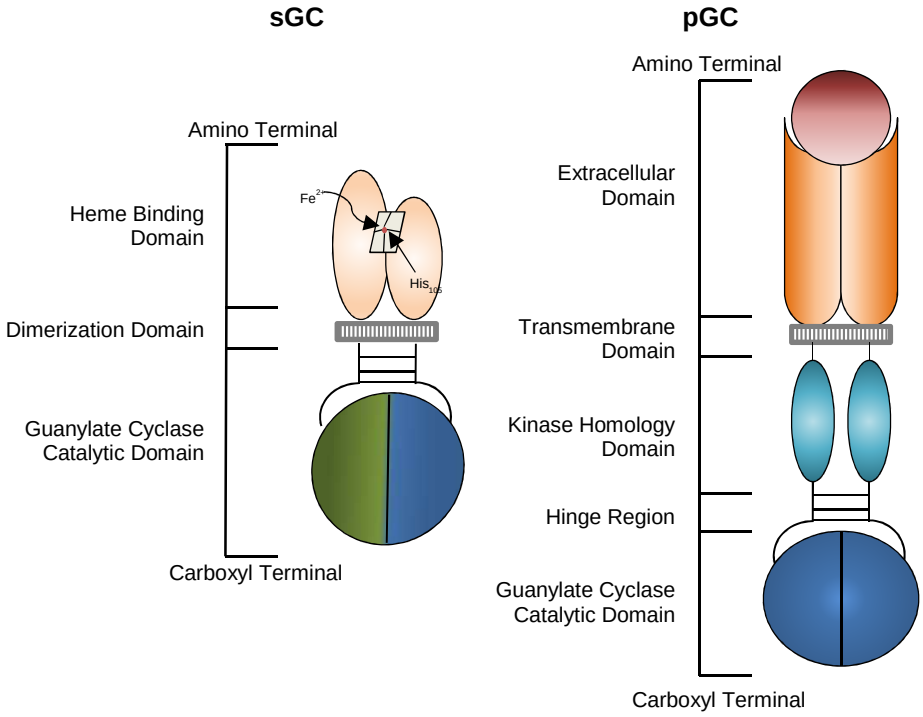

Figure 2: Domain structure of sGC and pGC.
SGCs are heterodimers containing a regulatory heme-binding domain at the N-terminus, a dimerization domain and a catalytic domain at the C-terminus. PGCs are homodimers with a single ligand binding site consisting of two extracellular domains at the N-terminus, a transmembrane- and juxtamembrane domain, as well as a kinase homology domain connected to the intracellular catalytic domain by a hinge region. Figure modified after Lucas et al. (2000).

The sGCs are usually heterodimers and consist of two subunits, the α- and the β- subunit each containing a GC-catalytic domain at the carboxyl (C)- terminus and a heme-binding domain at the amino (N)- terminus (Figure 2) (Kamisaki et al., 1986; Koesling et al., 1990; Nakane et al., 1988; J. R. Stone & Marletta, 1994). SGCs are activated by NO. In general, NO production is initiated by a calcium signal leading to the formation of a calcium/calmodulin complex with the NO-synthase (NOS) in the initiation cell. Produced NO then diffuses into the target cell where it activates sGC by binding to the heme-moiety which leads to the conversion of GTP to cGMP using Mg^{2+} as a cofactor (Derbyshire & Marletta, 2012).

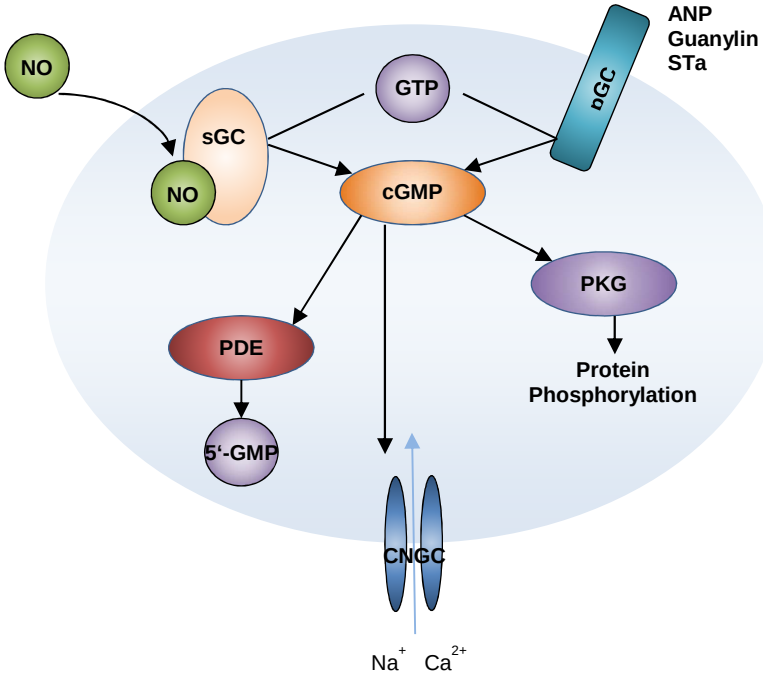

Figure 3: Signal transduction pathway of 3'5'-cGMP in mammalian cells.
Activation of sGC by NO and pGC by ANPs, guanilin or heat-stable enterotoxins (STa) lead to conversion of GTP to cGMP. Signal transduction occurs via activation of PKG followed by phosphorylation of target proteins or activation of CNGCs. cGMP is degraded to 5'-GMP by PDEs. Figure modified after Beavo and Brunton (2002).

CGMP functions as a second messenger and can activate cGMP dependent protein kinases (PKGs) leading to phosphorylation of target proteins followed by changes in transcription (Figure 3). Other cGMP induced mechanism are the activation of cyclic nucleotide gated ion channels (CNGCs) and the degradation of cGMP by PDEs (Beavo & Brunton, 2002).

In mammals, many physiological processes have been shown to be regulated by cGMP. These processes include smooth muscle relaxation in diverse tissue and regulation of the vascular tone, intestinal fluid and electrolyte homeostasis, as well as phototransduction (Lucas et al., 2000).

1.1.3 cGMP signaling in plants

The existence of cGMP in plants is now generally accepted. However, the detailed role in signaling is poorly understood. In higher plants cGMP was shown to play an important role in various biological processes in different plant species. For example, Bowler et al. (1994) demonstrated that cGMP together with Ca^{2+} is involved in chloroplast development. CGMP was also connected to phytochrome phototransduction in soybean and the regulation of the phenylpropanoid pathway in *A. thaliana* (Chory, 1994; Pietrowska-Borek & Nuc, 2013; Suita et al., 2009). Further, Durner et al. (1998) demonstrated that cGMP levels increase upon treatment with NO and are part of the NO-induced defense gene induction in tobacco. CGMP was further linked to be involved in NO-induced cell death in *A. thaliana* suspension cultures (Clarke et al., 2000). Moreover, it was shown that cGMP induces stomata opening by its influence on ion fluxes (Cousson, 2010; Cousson & Vavasseur, 1998; Pharmawati et al., 2001; Wang et al., 2013). Interestingly, cGMP was also shown to be involved in stomata opening in response to atrial natriuretic peptide (ANP) from rat (Pharmawati et al., 1998; Pharmawati et al., 2001). Additionally, cGMP has been shown to be involved in other hormone signal transduction pathways, for example in response to abscisic acid (ABA), brassinosteroids (BRs) or gibberellic acid (GA) (Dubovskaya et al., 2011; Kwezi et al., 2007; Penson et al., 1996). Moreover, it was suggested to be involved in auxin signaling during *A. thaliana* root growth and development (Nan et al., 2014). Its role in adventitious root formation was shown for mung beans (*Vigna radiate*) and cucumber (*Cucumis sativus*) (S. Li & Xue, 2010; Pagnussat et al., 2003). Further, a microarray analysis on *A. thaliana* roots after cGMP treatment revealed transcriptional activation of a variety of different cation transporters (Maathuis, 2006). Increases in cGMP were observed in response to various biotic and abiotic stimuli, including salt and osmotic stresses, pathogen infection or exposure to ozone (Donaldson et al., 2004; Ederli et al., 2008; Meier et al., 2009; Pasqualini et al., 2009).

Taken together, in the last 20 years a lot of research left no doubt about the existence and importance of cGMP and cGMP signaling in plants (Figure 4). Furthermore, based on the connection between NO or ANP and cGMP it is even suggested that similar signal transduction mechanisms compared to the mammalian signaling cascades might exist in plants (Figure 4).

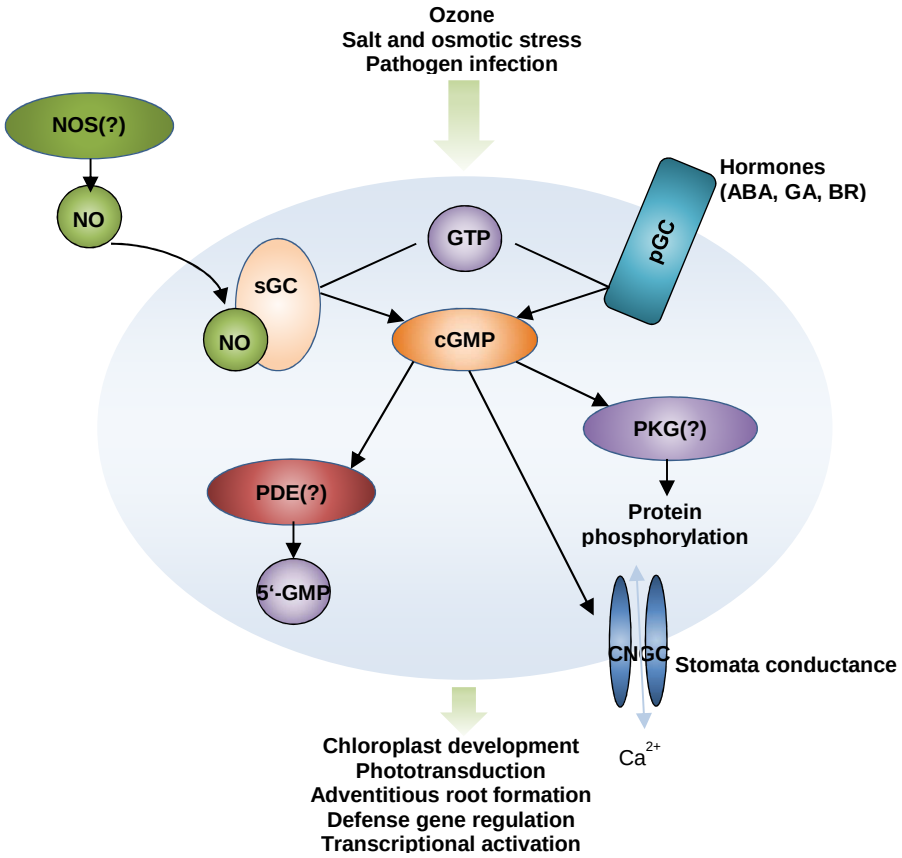

Figure 4: cGMP signaling in plants.
cGMP levels increase in response to ozone, salt and osmotic stress, pathogen infection and diverse hormones through the activation of sGC or pGC. The increase in cGMP results in the activation of CNGCs followed by stomata opening. Further, cGMP influences chloroplast development, phototransduction, adventitious root formation, defense gene induction and transcription. Downstream components, PKG and PDE, are not identified in plants.

1.1.4 Approaches for the identification of NOS, GCs and PDEs in plants

Despite the diverse functions of cGMP in signaling and the occurrence in response to various stresses, enzymes involved in production, signal transduction and degradation of cGMP have not been identified to date.

Until today, the exact mechanism behind the NO/cGMP signaling cascade is not completely understood in plants. This is mainly due to the fact that bioinformatics approaches based on mammalian search motifs for NOS failed to identify the corresponding genes in plants. It is not clear how NO is primarily produced in plants nor if an analog to the mammalian NOS exists. Still, there is plenty of evidence for the existence and function of NO in plants (Astier & Lindermayr, 2012; Fröhlich & Durner, 2011; Yoshioka et al., 2009).

In case of sGC, the situation seems similar to NOS. BLAST searches for annotated sGC sequences from other species do not result in any matches in plants, which likely is the result of a high level of divergence in plant sGCs (Ludidi & Gehring, 2003). Using an adjusted and

highly variable search motif for the GC-catalytic center of 14 amino acids, two forms of sGCs have been described in plants, a NO sensitive (NOGC1) and a NO insensitive sGC (AtGC1) (Ludidi & Gehring, 2003; Mulaudzi et al., 2011). Further, based on this motif, several receptor kinases were suggested to have GC-activity when partially expressed, including brassinosteroid insensitive1 (BRI1), phytosulfokine receptor (PSKR1), pathogen peptide1 receptor (PEPR1) and wall associated kinase like 10 (WAKL10) (Kwezi et al., 2007; Kwezi et al., 2011; Meier et al., 2010; Qi et al., 2010). All of these receptor kinases are suggested to have a GC-catalytic center embedded within the intracellular kinase domain (Irving et al., 2012). These findings were very interesting, albeit controversial because of the comparably low activity *in vitro* and *in vivo*, irreproducible activity when expressing a bigger fragment of the protein or the missing evidence for activity *in vivo* (Ashton, 2011; Bojar et al., 2014).

One element of downstream signaling of cGMP in mammals are CNGCs. In plants, bioinformatics approaches identified 20 different CNGCs in *A. thaliana*, some of them shown to be directly activated or regulated on the transcriptional level by cGMP (Kaplan et al., 2007; Maathuis, 2006; Wang et al., 2013).

Although transcriptional changes caused by cGMP, as they occur in the mammalian system in response to PKG activation, can be observed in plants too, the presence of a cGMP dependent protein kinase remains unclear (Bastian et al., 2010; Bridges et al., 2005; Maathuis, 2006; Penson et al., 1996). However, direct or indirect influences of cGMP on protein signature or protein phosphorylation status, were shown (Isner et al., 2012; Ordoñez et al., 2014). This indicates that a similar signal transduction cascade, as it was shown in vertebrates, might be present in plants.

In higher plants, no cGMP degrading enzyme could be identified by either BLAST searches or by biochemical purification processes, although PDE activity has been observed in crude protein extracts from various plant species, including pea (*Pisum sativum*), tomato (*Lycopersicon esculentum)*, spinach (*Spinacea oleracea*) and *A. thaliana* (Abel et al., 2000; Brown et al., 1979; Dubovskaya et al., 2011; Gross & Durner, 2016; Lin & Varner, 1972).

One approach to identify cGMP binding proteins like PKGs and PDEs in mammals could be the purification from plant extracts using cGMP immobilized on agarose beads. The purification of various cGMP binding proteins was already demonstrated for rat tissue (Kim & Park, 2003). Further, using cAMP agarose, purification of cAMP target proteins was performed using bovine heart tissue (Hanke et al., 2011). First approaches using plant material from *A. thaliana* and oat were performed, suggesting nucleoside-diphosphate kinases (NDPK) being a main target of cGMP (Dubovskaya et al., 2011; Dubovskaya & Volotovski, 2004). This result seems likely, since cGMP and NDPKs were shown to play a role in the same pathways, such as light-, hormone-, and stress-signaling (Dubovskaya et al., 2011). However, cGMP dependent activity for NDPKs could not be demonstrated yet.

The identification of the key enzymes upstream and downstream of cGMP will be a necessary and challenging task for the future to unravel the role and function of cGMP in plants.

1.2 Adenosine 3’5’-cyclic monophosphate signaling

In the mammalian system GTP-binding protein coupled receptors, also called 7-transmembrane domain receptors (7TM receptor), were shown to release the $G_s\alpha$ subunit upon binding of a specific agonist, such as different hormones or neurotransmitters (Beavo & Brunton, 2002; Daniel et al., 1998). The $G_s\alpha$ therefore activates membrane bound ACs (mAC), which convert ATP to cAMP (Figure 6). Another form of ACs are soluble ACs (sAC). This enzyme is regulated by bicarbonate anions and is located in the cytoplasm and in cellular organelles (Tresguerres et al., 2011). Once produced, cAMP can activate PKAs resulting in an alteration of protein phosphorylation as well as changes in gene transcription (Daniel et al., 1998). Another effect of cAMP is the activation of CNGCs, thereby regulating ion fluxes (Beavo & Brunton, 2002). cAMP is degraded by PDEs, with the rate of activity of PDEs being particularly important in the modulation of cAMP signaling (Daniel et al., 1998).

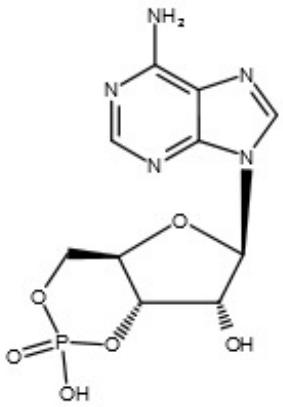

Figure 5: Chemical structure of 3’5’-cAMP

CAMP research in the field of plants is still controversial since many key components up- and downstream of cAMP need to be identified and their specific functions need to be demonstrated. However, cAMP-dependent Protein kinase (PKAs) activities were demonstrated in duckweed (*Lemna paucicostata*), maize (*Zea mays*), coconut (*Cocos nucifera*) and petunia (*Petunia hybrida* var. Old Glory Blue), although purification of the enzyme to homogeneity was not performed (Janistyn, 1988, 1989; Kato et al., 1983; Polya et al., 1991). Furthermore, cAMP degrading PDEs were also found in plants and have been

partially purified, for example from runner bean (*Phaseolus vulgaris*) or spinach (*Spinacea oleracea*) (Brown et al., 1975; Brown et al., 1979; Newton & Smith, 2004). Therefore, by now the presence of cAMP in plants is generally accepted and many different physiological roles of cAMP have been suggested, including involvement in ion transport, cell cycle progression, defense and stress responses as well as activation of PAL and CHS (Anderson et al., 1992; Bolwell, 1992; Choi & Xu, 2010; Ehsan et al., 1998; Kurosaki et al., 1987; Lemtiri-Chlieh et al., 2011; Pietrowska-Borek & Nuc, 2013; Smith, 1996).

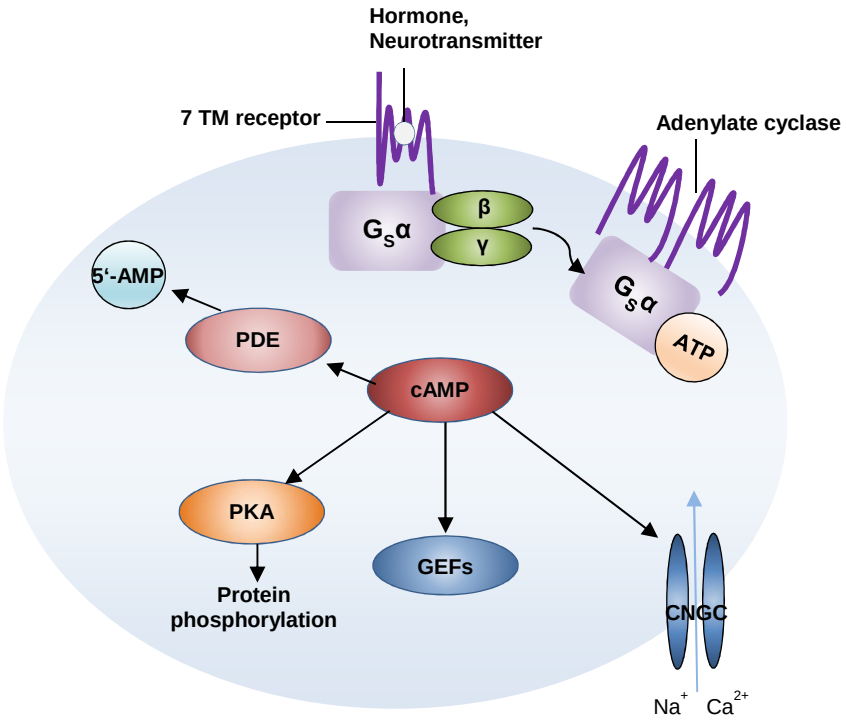

Figure 6: Signal transduction pathway of 3'5'-cAMP in mammalian cells.
Upon binding of suitable hormones or neurotransmitter to the 7TM receptor the Gsα subunit is released and activates AC which converts ATP to cAMP. CAMP can activate PKAs resulting in altered protein phosphorylation, CNGCs leading to ion fluxes or GEFs causing GTPase activation. CAMP is degraded by PDEs. Figure modified after Beavo and Brunton (2002).

1.3 Cytidine- and uridine- 3'5'-cyclic monophosphate signaling

In contrast to cAMP and cGMP the existence and the second messenger function of 3'5'-cyclic cytidine monophosphate (3'5'-cCMP) and 3'5'-cyclic uridine monophosphate (3'5'-cUMP) was debated for decades (Figure 7). Until recently, research input in the field of these nucleotides was considerable low compared to cAMP and cGMP. An interesting summary on the history and function of cCMP and cUMP was given by Beste and Seifert (2013) and Seifert (2015).

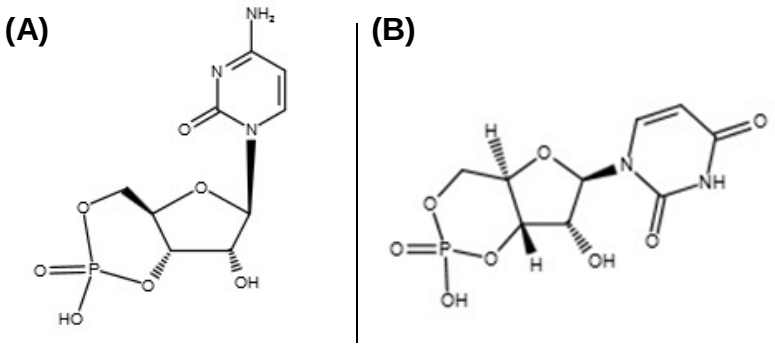

Figure 7: Chemical structure of 3'5'-cCMP and -cUMP.
The chemical structures are demonstrated for cCMP (A) and cUMP (B).

In 2004, Gille et al. demonstrated that sGC from bovine lung is capable of converting UTP to cUMP. cCMP and cUMP production by sGC was further shown to be stimulated by NO (Bähre et al., 2014; Beste et al., 2011). Additionally, it was shown by Hasan et al. (2014) that sAC but not membrane bound ACs are able to produce cCMP as well as cUMP. Attempts to identify downstream components revealed that both cyclic nucleotide monophosphates (cNMPs) are able to activate PKA and PKG (Wolter et al., 2014; Wolter et al., 2011). Moreover, cCMP and cUMP have been shown to activate hyperpolarization-activated cyclic nucleotide-gated channels, as well as multidrug resistance proteins (MRPs) (Akimoto et al., 2014; Laue et al., 2014; Zong et al., 2012). Studies investigating the degradation of cCMP and cUMP have shown that cCMP can be hydrolyzed by PDE7A1 and cUMP by PDE3A and PDE3B (Monzel et al., 2014).

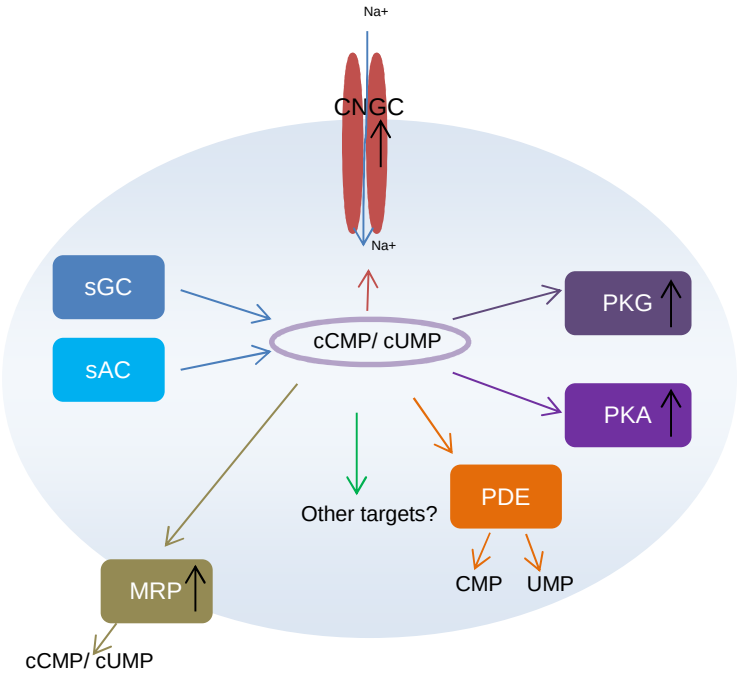

Figure 8: Proposed signaling cascade of the potential second messengers cCMP and cUMP.
CCMP and cUMP are generated by sGC/ sAC and can activate CNGC, PKG/ PKA. Multidrug resistance-associated proteins (MRPs) might function as cCMP/ cUMP transporters. Both nucleotides can be degraded by PDEs. Figure modified after Beste and Seifert (2013).

After the development of highly sensitive methods, such as high performance liquid chromatography tandem mass spectrometry (HPLC-MS/MS), cCMP and cUMP were identified in several different mammalian cell lines as well as in different tissues (Burhenne et al., 2011; Hartwig et al., 2014). Although the last years revealed many signaling components of these cNMPs, not much is known about their physiological function. Using a cell-permeable analog of cCMP it was suggested that this cNMP might be involved in cell proliferation, vascular relaxation and inhibition of platelet aggregation in mice (Desch et al., 2010; Newton, 1995; Seifert, 2015). Furthermore, for cUMP a potential role in cell death induction was shown (Seifert, 2015). Nevertheless, more investigation is required to solve the exact signaling mechanism of these potential second messengers.

In plants, the presence of both cyclic nucleotides was investigated in pea (*Pisum sativum*) roots already in 1989 (Newton et al., 1989). It was suggested that cCMP and cUMP are present at low levels in non-meristematic tissues, whereas higher concentrations of cCMP were found in meristemic tissues. This led to the conclusion that cCMP might be an important component in cell proliferation, as it was also suggested for mammalian tissue (Newton, 1995). Yet, as mentioned before, the sensitivity of measuring methods at this time was comparably low and these results should be interpreted carefully. Measuring cNMPs in various cell culture and tissue of different species using HPLC-MS/MS, Hartwig et al. (2014) demonstrated the occurrence of cAMP, cGMP and cUMP but not cCMP in leaves of *A. thaliana*. However, cCMP was shown to be present in tobacco (*Nicotiana tabacum*) BY-2 cells (Richards et al., 2002). Marondedze et al. (2015) suggested a role for cCMP in ROS signaling in plants. ROS are partially reduced or activated derivatives of oxygen (including NO, H_2O_2 or O_2^-) which can induce oxidative destruction of cells in certain concentrations but also play a role in different signaling cascades, such as pathogen defense and programmed cell death (Apel & Hirt, 2004; Marondedze et al., 2015; Mittler et al., 2004). Therefore, a tight regulation of ROS levels in cells is indispensable. Although natural occurrence of cCMP is not confirmed in *A. thaliana*, Marondedze et al. (2015) investigated the possible role of cCMP in ROS signaling by incubation of *A. thaliana* cell culture with cell permeable cCMP, showing an induction of ROS production.

1.4 2’3’-cyclic nucleotide monophosphates

In comparison to theirs 3’5’-isomers very little is known about the origin, function and biological relevance of 2’3’-cNMPs (Figure 9). The 2’3’-isomer of cAMP was found in perfused rat kidney and smooth muscle cells and was shown to be excreted by kidney (Jackson, 2011; Jackson et al., 2009). These studies suggested that 2’3’-cAMP is derived

from RNA degradation and acts as an intracellular toxin which can induce apoptosis. To prevent this effect, 2'3'-cAMP gets degraded to 2'-AMP and 3'-AMP. Further, Jackson et al. (2011) demonstrated that 2'3'-cAMP inhibits proliferation of preglomerular vascular smooth muscle cells and glomerular mesangial cells from rat.

A similar mechanism was suggested for 2'3'-cGMP by Sokurenko et al. (2015), demonstrating it to be an intermediate of RNA degradation by RNases. They further also suggested a role for 2'3'-cGMP in apoptosis.

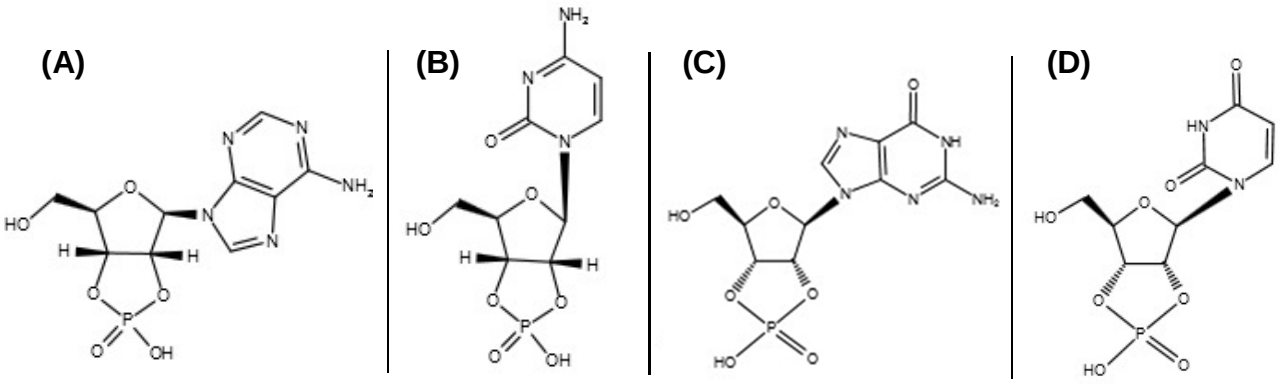

Figure 9: Chemical structure of 2'3'-cyclic nucleotide monophosphates.
The chemical structures of 2'3'-cGMP (A), 2'3'-cAMP (B), 2'3'cCMP (C) and 2'3'-cUMP (D) are demonstrated.

In another study, considerably high concentrations of 2'3'-cGMP, -cCMP and –cUMP were detected in diverse mice tissue, including murine heart, kidney, spleen, liver, pancreas and lung, (Burhenne et al., 2013). In this study it was demonstrated that concentrations of the 2'3'-isomers of cGMP are up to 5-fold higher than the 3'5'-isomers. Additionally, 2'3'- cGMP, -cAMP, -cCMP and –cUMP were detected in human kidney- and T-cell lymphoma cell lines (Bähre & Kaever, 2014). Considering the high concentration of 2'3'-cNMPs, it was suggested that RNA degradation might not be the only source of these nucleotides (Bähre & Kaever, 2014).

In plants, Richards et al. (2002) demonstrated the presence of 2'3'-cAMP,-cGMP and –cCMP in tobacco BY-2 cells. Additionally it was shown that upon wounding of *A. thaliana* 2'3'-cAMP and -cGMP levels strongly increase, while 3'5'-cAMP and -cGMP were below the limit of detection, suggesting a role of 2'3'-cNMPs in stress responses (Van Damme et al., 2014).

Taken together, information on the origin and mode of action of 2'3'-cNMPs is scarce in comparison to 3'5'-cNMPs. Therefore, the implementation of further studies is inevitable to validate their potential role as a second messenger.

1.5 Aim of this study

The first aim of this thesis was the investigation of cyclic nucleotide monophosphate (cNMP) signaling in plants. Therefore, different biotic and abiotic stimuli were applied to study the possible occurrence and kinetics of cNMPs in hypersensitive response (HR), NO_2-induced cell death, as well as NO and auxin treatment. For the induction of a HR, *pDEX:AvrRPM1-HA* mutants plants were used. These plants contain the *Pseudomonas avirulence (Avr)* gene, under the control of a dexamethasone (DEX)-inducible promotor. Through treatment with DEX the expression of *AvrRPM1* is initiated leading to the simulation of an avirulent pathogen attack without the need of an actual infection. To study the levels of the different cNMPs in response to NO_2-induced cell death, *A. thaliana* Col-0 plants were fumigated with NO_2. Furthermore, liquid cultured *A. thaliana* seedlings were treated with the NO-donor SNP and with Indole-3-acetic acid (IAA), a plant hormone of the auxin class. The existence and kinetics of cNMPs, in particular guanosine 3'5'- and 2'3'-cyclic monophosphate, were examined in treated and untreated plants using two different methods: fourier-transform-ion-cyclotron-resonance (FT-ICR) mass spectrometry and high performance liquid chromatography tandem mass spectrometry (HPLC-MS/MS).

The second aim of this study was the identification and purification of guanylate cyclases (GCs) in plants. Therefore, an assay was established to measure cGMP formation from plant protein extract from *A. thaliana* and *Hordeum vulgare* using a cGMP-enzyme immunoassay.

The third aim was the identification and characterization of cGMP target proteins in *A. thaliana* to reveal new insight into cGMP dependent pathways. An assay was established using a phosphodiesterase (PDE) resistant version of cGMP-agarose to purify cGMP binding proteins (CGBPs). After incubation of *A. thaliana* protein extracts with the cGMP-agarose, bound proteins were analyzed and quantified using mass spectrometry. To characterize potential cGMP binding proteins, T-DNA insertion lines of the candidate were used for phenotyping experiments.

2 Material and Methods

2.1 Materials

2.1.1 Plant Material and Soil

Arabidopsis thaliana ecotype Col-0 was used throughout this study. For the characterization of HP29b two *A. thaliana* mutant lines (SAIL_65_B07, SAIL_69_B02) of At3G61870 and the corresponding parental line N8846 were ordered from NASC (Nottingham, United Kingdom). For cNMP measurements after Dexamethasone (DEX) treatment *pDex::AvrRpm1-HA* mutant line was used (Breitenbach et al., 2014; Mackey et al., 2002). In addition, *Hordeum vulgare* cv. Golden Promise was used in this study.

For cultivation of *A. thaliana*, soil (Floraton 1, Floragard, Oldenburg, Germany) was mixed with silica sand in a 5:1 ratio. For cultivation of *H. vulgare* “Einheitserde Classic” (Einheitserde- und Humuswerke, Gebr. Patzer GmbH, Sinntal-Jossen, Germany) was used.

2.1.2 Bacterial and yeast strains

All bacterial strains used in this work are listed in Table 1. *Escherichia coli* strains were used for Gateway® cloning and protein expression, whereas *Azospirillum brasilense* was used to detect cGMP accumulation in the media.

Table 1: Bacterial strains used for cloning, protein expression and cGMP measurements

Species	Strain	Application	Source
Escherichia coli	DH5α	Gateway® cloning	Invitrogen, Karlsruhe, Germany
Escherichia coli	Rosetta™ 2(DE3)pLysS	Protein expression	Invitrogen, Karlsruhe, Germany
Escherichia coli	BL21(DE3)pLysS	Protein expression	Invitrogen, Karlsruhe, Germany
Azospirillum brasilense	AZ39	cGMP measurement	
Azospirillum brasilense	Sp7	cGMP measurement	

For protein expression the yeast *Saccharomyces cerevisiae* strain INVSc1 (Invitrogen, Karlsruhe, Germany) was used.

2.1.3 Vectors

All vectors used in this study are listed in Table 2. pDONR™221 was used as the entry vector for Gateway® cloning in all experiments. pDEST™17 and pET-DEST42 were used as destination vectors for expression in *E. coli* resulting in an either N- or C-terminal His-tagged protein. pYES-DEST52 was used as the destination vector for expression in *S. cerevisiae* resulting in a C-terminal His-tagged protein.

Table 2: Vectors used for Gateway® cloning

Name	Application	Source
Gateway® pDONR™221	Gateway® cloning	Invitrogen, Karlsruhe, Germany
Gateway® pDEST™17	Gateway® cloning	Invitrogen, Karlsruhe, Germany
Gateway® pET-DEST42	Gateway® cloning	Invitrogen, Karlsruhe, Germany
Gateway® pYES-DEST52	Gateway® cloning	Invitrogen, Karlsruhe, Germany

2.1.4 Chemicals

If not stated otherwise, all chemicals used in this thesis were of high purity grade and were purchased either from Sigma Aldrich (Taufkirchen, Germany), Carl Roth GmbH (Karlsruhe, Germany) or Merck (Darmstadt, Germany).

2.1.5 Enzymes for cDNA synthesis and Gateway® cloning

For cDNA synthesis for cloning purposes SuperScript™II Transcriptase was used. To verify the insertion of the PCR product into the different entry and destination vectors the restriction enzyme Eco88I was used. All enzymes used for cDNA synthesis, Gateway® cloning and restriction analysis are listed in Table 3.

Table 3: Enzymes used for cDNA-synthesis and Gateway® cloning

Name	Application	Source
Eco88I (AvaI)	Restriction analysis	Thermo Scientific, Bonn, Germany
SuperScript™II Transcriptase	cDNA-synthesis	Invitrogen, Karlsruhe, Germany
Gateway® BP Clonase™ Enzyme Mix	Gateway® cloning	Invitrogen, Karlsruhe, Germany
Gateway® LR Clonase™ Enzyme Mix	Gateway® cloning	Invitrogen, Karlsruhe, Germany

2.1.6 Enzymes for GC activity assay

Degradation of cGMP in GC activity assays was performed using PDE5A1 from human (Sigma, Taufkirchen, Germany).

2.1.7 Polymerases

For all PCR applications the Phusion® High Fidelity DNA Polymerase was used. In case of qPCR analysis the SensiMix™ SYBR Low-ROX Kit was used.

Table 4: DNA-Polymerases

Name	Specification	Source
Phusion® High Fidelity DNA Polymerase	Proof-reading polymerase	New England Biolabs, Norwich, England
SensiMix™ SYBR Low-ROX Kit	Polymerase used in qPCR analysis	Bioline, Luckenwalde, Germany

2.1.8 Antibiotics

For antibiotic selection on LB-agar plates either Ampicillin or Kanamycin was used. For sterilization of *H. vulgare* seeds a combination of Penicillin and Streptomycin was used. All stock- and working concentrations of the different antibiotics are listed in Table 5.

Table 5: Antibiotics for antibiotic selection and seed sterilization

	Stock concentration [mg/ml]	Working concentration [µg/ml]	Application	Source
Ampicillin	100	100	LB plates with antibiotic selection	Duchefa Biochemie, Haarlem, Netherland
Kanamycin	50	50	LB plates with antibiotic selection	Duchefa Biochemie, Haarlem, Netherland
Penicillin	100	600	Seed sterilization	GIBCO Laboratories
Streptomycin	25	250	Seed sterilization	Sigma, Taufkirchen, Germany

All Stock solutions were dissolved in ddH_2O and sterilized using 0.22 µm sterile filters (Millipore, Billerica, MA, United States). Aliquots were stored at -20 °C.

2.1.9 Primer

All primers used in this study are listed in Table 6.

Table 6: Primer

Name	Gene	Sequence	Application
C1 f	At3G61870	tgccacaatctctgttccaaga	Gateway® cloning
C1 r		tgatcgtttttccaccattattcca	
HP29b-cterm f	At3G61870	ggggacaagtttgtacaaaaaagcaggcttcga aggagatagaatggcgaccacacttcattgtct	Gateway® cloning
HP29b-cterm r		ggggaccactttgtacaagaaagctgggtctggc catttagtgaactcaa	
HP29b-nterm f	At3G61870	ggggacaagtttgtacaaaaaagcaggcttcga gaatctttattttcagggcgcgaccacacttcattg	Gateway® cloning
HP29b-nterm r		ggggaccactttgtacaagaaagctgggtctatg gccatttagtgaact	
M13 f	At3G61870	tgtaaaacgacggccagt	Sequencing
M13 r		caggaaacagctatgacc	BP reaction
LR- f	At3G61870	gcgaccacacttcattgtct	Sequencing

LR- r		tggccatttagtgaactcaaaga	LR reaction
HP29b SAIL f HP29b SAIL r SAIL LB	At3G61870	tatcgttccctttctgcattg cttcttcctcgcactcatcac gccttttcagaaatggataaatagccttgcttcc	Genotyping
TUB f TUB r	At4G20890	gtaccttgaagcttgctaatccta gtcaaaggtgcaaaaccaac	qPCR
S16 f S16 r	At2G09990	tttacgccatccgtcagagtat tctggtaacgagaacgagcac	qPCR

Table 7: Primer assays

Name	Gene	Ordering information
HP29b	At3G61870	At_AT3G61870_2_SG QuantiTect Primer Assay

The primer pair used in qPCR analysis for HP29b (At3G61870) was ordered from Qiagen (Hilden, Germany).

2.1.10 Antibodies

Table 8: Antibodies for western blot analysis

Name	Source
Primary Antibody Anti-His-tagged Protein Mouse mAb	Merck, Darmstadt, Germany
Secondary Antibody Anti Mouse IgG (H+L) AP	Promega, Mannheim, Germany

2.1.11 Nucleotides and cytokinin

Table 9: Nucleotides

Name	Source
ATP disodium salt hydrate	Sigma, Taufkirchen, Germany
ADP sodium salt	Sigma, Taufkirchen, Germany

GTP TRIS salt	Sigma, Taufkirchen, Germany
GDP sodium salt	Sigma, Taufkirchen, Germany
GMP disodium salt hydrate	Sigma, Taufkirchen, Germany
3'5'-cGMP sodium salt	Sigma, Taufkirchen, Germany
2'3'-cGMP sodium salt	BIOLOG, Bremen, Germany
Sp-8-AET-cGMPS-agarose (A010)	BIOLOG, Bremen, Germany
3'5'-cAMP sodium salt monohydrate	Sigma, Taufkirchen, Germany
c-di-GMP sodium salt	BIOLOG, Bremen, Germany
trans-Zeatin-riboside	Sigma, Taufkirchen, Germany

2.1.12 Solutions, media and kits

Table 10: Media used for plant cultivation

Name	Composition [per liter]	pH	Source
½ MS	2.2 g MS 10 g Sucrose	5.7 (KOH)	Duchefa Biochemie, Haarlem, Netherland
½ MS agar	2.2 g MS 10 g Sucrose 5 g Gelrite	5.7 (KOH)	Duchefa Biochemie, Haarlem, Netherland Duchefa Biochemie, Haarlem, Netherland
sterile plant growth media	4.4 g MS 10 g Sucrose 0.5 g MES	5.8 (KOH)	Duchefa Biochemie, Haarlem, Netherland
NB agar	8 g		

Table 11: Media used for bacterial cultivation

Name	Composition (per liter)	pH	Source
LB media	25 g LB broth high salt	7.0 (NaOH)	Duchefa Biochemie, Haarlem, Netherland
LB agar	LB media 12.5 g Agar for microbiology	7.0 (NaOH)	Sigma, Taufkirchen, Germany
M9 (1x)	200 ml M9 (5x) 2 mM $MgSO_4$ 0.1 mM $CaCl_2$ 20 mM D-Fructose		Sigma, Taufkirchen, Germany

Table 12: Media used for yeast cultivation

Name	Composition (per liter)	Source
YPD media	20 g Bacto™ Peptone 20 g Dextrose 10 g Yeast extract	BD Biosciences, Franklin Lakes, USA
YPD agar	YPD media 15 g Bacto™ Agar	BD Biosciences, Franklin Lakes, USA
Selective media	1.92 g Yeast Synthetic Drop-out Medium 20 g Raffinose	
Selective agar	Selective media 20 g 15 g Bacto™ Agar	BD Biosciences, Franklin Lakes, USA
Induction media	10 g Yeast extract 20 g Bacto™ Peptone 20 g Galactose	BD Biosciences, Franklin Lakes, USA

All plant, bacterial and yeast cultivation media were autoclaved after adjustment of the pH.

Table 13: Buffer for nucleic acid agarose gel

Name	Composition
TAE-buffer	40 mM TRIS 1 mM EDTA pH 8.0 (acetic acid)

For Size determination in all nucleic acid agarose gels, the GeneRuler 1kb DNA ladder from Fermentas (St. Leon-Rot, Germany) was used.

Table 14: Buffers and solutions for SDS-page, coomassie staining and western blot analysis

Application	Name	Composition
SDS-PAGE	TGS buffer	1x TGS buffer (Bio-Rad Laboratories GmbH, Munich, Germany)
Coomassie staining	Staining solution	400 ml Methanol 100 ml Acetic acid 500 ml ddH_2O 0.1 % Brilliant blue R-250
	Distaining solution	400 ml Methanol 100 ml Acetic acid 500 ml ddH_2O
Western blot	Blot buffer	25 mM TRIS 200 mM Glycin 0.1 % SDS 20 % Methanol
	TBS-buffer	10 mM TRIS 1 mM $MgCl_2$ 0.9 % NaCl pH 7.4 (HCl)
	TBST-buffer	TBS-buffer 0.5 % Tween20
	Block-solution	TBST-buffer 1 % (w/v) Skim milk powder 1 % (w/v) BSA

AP-buffer	100 mM TRIS 100 mM NaCl 5 mM MgCl2 pH 9.5 (HCl)

For all SDS-PAGE applications Mini-PROTEAN® TGX™ Precast Gels (4-15%) from Bio-Rad (Bio-Rad Laboratories GmbH, Munich, Germany) were used. As a protein size marker the PageRuler Plus Prestained Protein Ladder (Thermo Scientific, Bonn, Germany) was used.

Table 15: Solutions for silver staining

Name	Composition
Fixation	100 ml MeOH 76 ml ddH_2O 24 ml Acetic acid 100 µl Formaldehyde (37%)
Washing	150 ml EtOH 150 ml ddH_2O
Sensitizer	20 mg $Na_2S_2O_3$ 100 ml ddH_2O
Staining	200 mg $AgNO_3$ 100 ml ddH_2O 75 µl Formaldehyde (37%)
Development	6 g Na_2CO_3 97.5 ml ddH_2O 2.5 ml sensitizer 50 µl Formaldehyde (37%)
Stopping	100 ml MeOH 76 ml ddH_2O 24 ml Acetic acid
Storage	20 ml EtOH 77.5 ml ddH_2O 2.5 ml Glycerin (80 %)

Table 16: Buffers for protein purification via IMAC

Name	Composition
Buffer A	50 mM TRIS (pH 8.0) 300 mM NaCl 20 mM Imidazole 10 mM ß-Mercaptoethanol
Buffer A+	50 mM TRIS (pH 8.0) 1.3 M NaCl 20 mM Imidazole 10 mM ß-Mercaptoethanol
Buffer B	50 mM TRIS (pH 8.0) 300 mM NaCl 300 mM Imidazole 10 mM ß-Mercaptoethanol

Table 17: cNMP extraction buffers for FT-ICR and HPLC

Name	Composition
FT-ICR-MS extraction buffer	2 ml Acetic acid 80 ml Ethanol 18 ml ddH_2O
HPLC extraction buffer	40 ml Acetonitril 40 ml Methanol 20 ml ddH_2O

All components used for cNMP extraction were HPLC grade.

Table 18: Protein extraction buffers

Name	Composition
GC extraction buffer	175 mM Tris pH 8.0 20 mM Theophylline 1 % Protease inhibitor, Complete Mini EDTA free (Roche, Mannheim, Germany)
MOPS Buffer	200 mM MOPS pH 7.0

CGBP extraction buffer	20 mM MOPS pH 7.0 150 mM NaCl 10 mM MgCl2 5 mM EDTA 5 mM EGTA 200 mM Saccharose 5 mM ß-Mercaptoethanol 1 % protease inhibitor cocktail for plant cell and tissue extracts (Sigma, Taufkirchen, Germany)

GC activity assay was further performed using CelLytic™ P Cell Lysis Reagent (Sigma, Taufkirchen, Germany) instead of GC extraction buffer.

For the first extraction step of CGBPs, 1% Triton X-100 was added to CGBP extraction buffer to solubilize membrane associated proteins. For all following steps, CGBP extraction buffer without Triton X-100 was used.

Table 19: Kits used in this study

Name	Application	Source
RNeasy® Plant Mini Kit	RNA isolation from plant tissue	Qiagen GmbH, Hilden, Germany
QuantiTect® Reverse Transcription Kit	cDNA synthesis for qPCR	Qiagen GmbH, Hilden, Germany
QIAquick® Gel Extraction Kit	DNA extraction from agarose gel	Qiagen GmbH, Hilden, Germany
QIAprep® Spin Miniprep Kit	Plasmid DNA isolation from bacteria	Qiagen GmbH, Hilden, Germany
cGMP Enzyme Immunoassay Kit	Measurement of cGMP from plant extracts	Sigma, Taufkirchen, Germany
Extract-N-Amp™ Plant Tissue PCR Kit	Genomic DNA isolation from plant tissue for genotyping	Sigma, Taufkirchen, Germany
S.c. EasyComp™ Transformation Kit	Transformation of vectors into yeast	Invitrogen, Karlsruhe, Germany

2.2 Methods

2.2.1 Plant cultivation and treatments

Plant growth conditions

Soil grown plants of *A. thaliana* were always grown under long-day condition (14 h light; light intensity of 100 µE m^{-2} sec^{-1}; day 25 °C; night 18 °C; 70 % relative humidity) if not stated otherwise. After seeds were sown out on wet soil, plant pots were stratified at 4 °C for two days in the dark to synchronize germination. After stratification plant pots were transferred to the growth chamber.

Soil grown *H. vulgare* plants were grown under short-day condition (10 h light; light intensity of 100 µE $m^{-2}sec^{-1}$; day 25 °C; night 18 °C; 70 % relative humidity). Sterile grown *H. vulgare* and *A. thaliana* plants were grown as stated above.

For growth in liquid culture, approximately 30 sterilized seeds of *A. thaliana* were grown in 5 ml sterile plant growth media under permanent shaking at 80 rpm under short day condition.
After sterilization *H. vulgare* single seeds were transferred to sterile glass-vials filled with silica sand and ½ MS media. Plants were grown under short day condition.

Seed sterilization

All seeds of *A. thaliana* and *H. vulgare* grown in liquid culture or agar plates were sterilized.

For growth on agar plates *A. thaliana* seeds were placed in petri dishes containing two layers of filter paper saturated with 1.5 ml of 80 % ethanol. The ethanol was allowed to evaporate. The procedure was repeated twice. The dry seeds were then dispersed to square petri dishes containing ½ MS agar. Plates were sealed with parafilm and incubated in the dark at 4 °C for two days. Subsequently, the plates were transferred to a growth chamber and placed vertically.

For growth in liquid culture approximately 100 *A. thaliana* seeds were incubated with 1 ml of 80 % ethanol for 1 min. The ethanol was removed and seeds were incubated in 1 ml 50 % Danklorix (Colgate-Palmolive, Hamburg, Germany) for 15 min with moderate shaking. Seeds were then washed with 1.5 ml sterile ddH_2O for 5 times. After washing, seeds were incubated in the dark at 4 °C for two days and transferred to the sterile plant growth media.

Seed sterilization was performed by incubation of 50 *H. vulgare* seeds in 40 ml 70 % ethanol for 2 min slowly shaking. Afterwards the seeds were incubated in 30 ml sodium hypochlorite for 15 min with moderate shaking. The seeds were then washed five times with 40 ml sterile ddH_2O. Further, seeds were incubated in 30 ml of antibiotic solution (600 µg/ml Penicillin, 250 µg/ml Streptomycin) for 30 min, slowly shaking in the dark. The seeds were then placed on NB agar plates at room temperature until germination.

Dexamethasone (DEX)-treatment and NO_2-fumigation

For DEX-treatment, four week old soil grown *pDex:AvrRpm1-HA* plants were either sprayed with 30 µM DEX dissolved in 0.1 % methanol including 0.01 % Tween20 or methanol/ Tween20 as control. After 4 h, 150 mg of plant material was harvested in 1.5 ml reaction tubes filled with 12 1.7 – 2.0 mm glass beads (Carl Roth GmbH, Karlsruhe, Germany) and flash frozen in liquid nitrogen.

For fumigation with NO_2, four week old Col-0 plants were fumigated in a closed chamber with 30 ppm of NO_2 for 1 h. Control plants were untreated. After fumigation 150 mg of leaf material was harvested and frozen as described previously.

Sodium nitroprusside (SNP) - and indole-3-acetic acid (IAA) - treatment

SNP and IAA treatments were performed using 12 day old *A. thaliana* seedlings grown in sterile liquid culture. The growth media was renewed 2 days before the treatment. For SNP treatment a 500 mM stock solution was prepared. SNP was added to the growth media to a final concentration of 5 mM. As a negative control, exhausted SNP was used. A stock solution of 10 mM IAA was prepared in 0.5 % methanol. IAA was added to the growth media to a final concentration of 10 µM. For the negative control methanol was used.

UV-treatment

For UV experiments, four week old plants were transferred into a UV-chamber with long-day conditions (14 h light; light intensity of 130 µE m^{-2} sec^{-1}; day 25 °C; night 18 °C; 70 % relative humidity) with 0.4 W/m² of UV-B radiation during the light phase. Negative control plants were grown under the same conditions without UV-B radiation.

2.2.2 Autofluorescence detection

Detection of the UV-autofluorescence was performed using a hand-held UV lamp with a 365 nm longwave UV source (Blak-Ray B-100AP; UVP, Upland, USA). Emission of blue-green fluorescence was documented with a Nikon DC300 (Nikon, Tokyo, Japan).

2.2.3 cNMP measurements

12-Tesla FT-ICR-MS

Extraction of cNMPs was performed homogenizing 3x 150 mg of harvested flash frozen leaf material using the Silamat® S6 (Ivoclar Vivadent AG, Schaan, Liechtenstein) followed by incubation in 0.5 ml extraction buffer for 30 min at 4 °C (Table 17). Samples were centrifuged for 20 min at 4 °C and 15000 g and the supernatant was collected. Afterwards, the extraction was repeated using the pellet and another 1.5 ml of extraction buffer. All supernatants were pooled. For solid phase extraction an Oasis WAX 6cc solid phase extraction column (Waters) was used. The column was equilibrated by rinsing with 1 ml ultra-pure MeOH and 1 ml ddH_2O before the addition of the pooled leaf extract. The column was washed with 2 ml 2 % acetic acid. Secondary metabolites were eluted from the columns with 2 ml MeOH and 2 ml 5 % NH_4OH in MeOH. The samples were dried under vacuum, dissolved in 1 ml 70 % MeOH and centrifuged at 20800 g for 10 min. Before MS analysis, samples were diluted 1:200.

Identification and quantification of the cNMPs was performed in the research unit Analytical BioGeoChemistry (Helmholtz Zentrum München GmbH, Munich, Germany) by Prof. Dr. Schmitt-Kopplin and Dr. Kanawati. For this application a Solarix FT-ICR mass spectrometer (Bruker Daltonics, Billerica, USA) coupled to a 12 Tesla magnet (Magnex Scientific, Oxford, UK) was used as described previously (Wittek et al., 2014). Before non-targeted analysis, the results were normalized and the exact masses corresponding to the cNMPs were used for database searches with Metlin software. A cut-off of 1.5E+06 spectral counts per second was set as limit of quantification (LOQ).

HPLC–MS/MS

For cNMP extraction 150 mg of harvested flash frozen leaf material was homogenized as described previously and 800 µl of extraction buffer was added (Table 17). The samples were incubated at 95 °C for 15 min followed by 1 h freezing at -80 °C. Afterwards, samples were centrifuged at 20800 g for 10 min at 4 °C. The pellet was dried ON and was dissolved in 800 µl of 0.1 N NaOH. After heating to 95 °C for 15 min the protein concentration was determined by the method of Bradford (1976). 600 µl of the supernatant were dried under vacuum and stored at -20 °C. Before MS analysis samples were dissolved in 150 µl ddH_2O, centrifuged again at 20800 g for 10 min at 4 °C and the supernatant was used for further analysis.

HPLC–MS/MS was performed at the Research Core Unit Metabolomics (Hannover Medical School, Hannover, Germany) by Prof. Dr. Volkhard Kaever and Annette Garbe. Measurements were performed as described previously (Bähre & Kaever, 2014; Hartwig et

al., 2014) using a QTrap5500TM triple quadrupole mass spectrometer (ABSCIEX, Foster City, CA, USA). For the quantification of 2'3'-cNMPs the standards curves of the corresponding 3'5'-isomers were used.

2.2.4 GC activity assay

GC activity assay from plant material

For the guanylate-cyclase-activity-assay proteins from whole plants were extracted. Therefore plant material was ground in liquid nitrogen. GC-extraction buffer (Table 18) including 1% Triton X-100 was added and samples were homogenized on ice. The extracts were centrifuged at 4000 rpm for 10 min at 4 °C followed by a desalting step using PD10-desalting columns (GE Healthcare, Buckinghamshire, UK) using the GC-extraction buffer and following the gravity protocol. Proteins from the supernatant were quantified using the method of Bradford (1976). To measure GC-activity, each sample contained 200 µg of extracted protein, 20 mM $MgCl_2$ as GC-cofactor and 1 mM of the substrate GTP in a total reaction volume of 250 µl. The reactions were incubated for the indicated time under shaking at 350 rpm at 24 °C. In case of a cGMP degradation assay using PDE5A1 from human (Sigma, Taufkirchen, Germany), 400 units of the enzyme was added and samples were incubated for another 10 min at 37 °C under shaking at 350 rpm. To stop the reactions, 250 µl of 0.2M zinc acetate was added, followed by 250 µl of 0.2 M sodium carbonate. Samples were vortexed and frozen in liquid nitrogen for storage. To measure cGMP, samples were thawed and centrifuged at 6000 g for 10 min at room temperature. CGMP was measured from 100 µl supernatant with the cGMP Enzyme Immunoassay Kit following the manufacturer's instructions (Sigma Aldrich Taufkirchen, Germany). The standard curve was created using GC-extraction buffer.

GC activity assay from *Azospirillum brasilense*

To measure cGMP produced by *A. brasilense*, one colony from a NB agar plate was transferred to 20 ml NB media. Bacteria were cultured ON shaking at 200 rpm at 37 °C. On the next day 2 ml of bacteria culture was centrifuged at 4500 g for 5 min and the pellet was re-suspended in 1 ml of M9 media. 50 ml of M9 media was inoculated with the bacteria solution (Sp.7: 500 µl, AZ39: 1 ml). The bacteria solutions were kept at 37 °C under permanent shaking at 200 rpm. 1 ml samples were taken daily for 1 week and flash frozen in liquid nitrogen. After thawing, samples were centrifuged at 4500 g for 5 min. In case of a cGMP degradation assay 400 units of PDE5A1 from human (Sigma, Taufkirchen, Germany), added to 100 µl of sample followed by an incubation for 10 min at 37 °C under shaking at 350 rpm. cGMP content of 100 µl supernatant was measured using the cGMP Enzyme

Immunoassay Kit following the manufacturer's instructions (Sigma Aldrich Taufkirchen, Germany). The standard curve was created using M9 buffer.

2.2.5 CGBP pull-down

Plant material was ground in liquid nitrogen, followed by homogenization in CGBP extraction buffer with addition of 1 % Triton X-100 on ice. The protein solution was centrifuged at 12600 g for 25 min at 4 °C. The supernatant was transferred into a new tube and protein concentration was determined by the method of Bradford (1976). 4600 µg of extracted protein were used for downstream applications. For pre-incubation experiments the stated compounds were dissolved in 200 mM MOPS buffer (pH 7). If necessary the pH was adjusted to 7.0. Samples were mixed with the stated compound and the total volume of all samples was adjusted to 1.7 ml. In parallel 300 µl cGMP agarose (Sp-8-AET-cGMPS-agarose, BioLog, Bremen, Germany) was washed 3x with 1.5 ml CGBP extraction buffer. After incubation for 1.5 h at 4 °C the sample volume was adjusted to 3.5 ml and samples were incubated with the agarose for 2 h on a rotator at 4 °C. Samples were then centrifuged at 250 g for 1 min, supernatant was removed and the agarose was washed with 3.5 ml CGBP extraction buffer. The washing was repeated 5 x. Finally, supernatant was removed completely and 80 µl 2 x Laemmli SDS buffer (Sigma Aldrich Taufkirchen, Germany) was added directly to the agarose to elute the proteins bound to the agarose. Samples were boiled at 100 °C for 15 min shaking at 500 rpm. 20 µl of the supernatant of each sample were used to run a 1D SDS-PAGE. Another 20 µl were send for protein identification and quantification (PROT Core Facility Proteomics, Munich, Germany).

Silver staining

To visualize the proteins bound to the cGMP-agarose, silver staining of the 1D SDS-PAGE was performed. Therefore, proteins on the SDS-PAGE-gel were fixed by 2 x incubation of the gel in fixation solution for 15 min each. The gel was washed in 50 % ethanol 3 x for 10 min followed by incubation with the sensitizer solution for 1 min. After short washing in ddH_2O the gel was stained for 20 min followed by rinsing with ddH_2O. Afterwards, the gel was developed until the protein bands became visible. The reaction was then stopped by incubation with the stopping solution for 10 min.

2.2.6 Protein identification and quantification

Protein identification and quantification was performed in the core Facility Proteomics (Helmholtz Zentrum München GmbH, Munich, Germany) by Dr. von Törne. For the identification of proteins from silver stained gels, selected gel lanes were cut and trypsinized

overnight as described previously (Kempf et al., 2014). Peptides were extracted and acidified with 1% formic acid followed by analysis via mass spectrometry. For the identification and quantification of proteins from elution samples of the CGBP pull down, samples were subjected to tryptic digest applying a modified FASP procedure as described in detail in (Grosche et al., 2016).

Mass spectrometry

Dried gel samples were dissolved in 2% ACN/0.5% trifluoroacetic acid by incubation for 30 min at RT under agitation. Before loading, the samples were centrifuged at 4°C. LC-MS/MS analysis was performed as described previously on a LTQ-Orbitrap XL (Thermo Scientific) operated on a nano-HPLC (Ultimate 3000, Dionex) (von Toerne et al., 2013). From the mass spectrometry pre-scan, the 10 most abundant peptide ions were selected for fragmentation in the linear ion trap if they exceeded an intensity of at least 200 counts and were at least doubly charged. During fragment analysis a high-resolution (60000 full-width half maximum) MS spectrum was acquired in the Orbitrap with a mass range from 300 to 1500 Da.

Label free quantification

The acquired spectra of the different samples were loaded and analyzed using Progenesis QI software for proteomics (Version 2.0, Nonlinear Dynamics, Waters, Newcastle upon Tyne, United Kingdom) for label-free quantification as previously described (Hauck et al., 2010; Merl et al., 2012). All MS/MS spectra were exported from the Progenesis QI software as Mascot generic files (mgf) and used for peptide identification with Mascot (version 2.5.1) using the TAIR protein database (containing 35388 sequences). Search parameters used were 10 ppm peptide mass tolerance, 0.6 Da fragment mass tolerance, one missed cleavage allowed, carbamidomethylation was set as fixed modification, and methionine oxidation and deamidation of asparagine and glutamine as variable modifications. For gel bands Mascot ion score was set to 30 and false discovery rate (FDR) to 1%. For more complex eluates a Mascot integrated decoy database search was set to a false discovery rate (FDR) of 1% when searching was performed on the concatenated mgf files with a percolator ion score cut-off of 13 and an appropriate significance threshold p. Identifications were re-imported into Progenesis QI. For quantification, abundances of all unique peptides of an identified protein were summed up. All protein abundances were normalized to rubisco activase (AT2G39730).

2.2.7 Flavonol and chlorophyll measurements

After four weeks of growth under long day conditions plants (N8846, SAIL_65_B07, SAIL_69_B02) were transferred to sunsimulator and exposed to UV-B radiation. Flavonol

and chlorophyll contents were measured daily for one week. Measurements were performed non-invasively using the optical sensor Multiplex®3.6 (Force A, Orsay, France) as described in the manufacturer's instructions and elsewhere (Ben Ghozlen et al., 2010; Sytar et al., 2015). Depending on the measurement, excitation light of different wavelength was emitted by the Multiplex®3.6 and far-red and red chlorophyll fluorescence of the plant was measured (Table 20).

Table 20: Nomenclature of Multiplex® signals.
The name of each signal in the fluorescence excitation-emission matrix is defined by the abbreviation for its emission-light color separated by the underscore sign from the abbreviation for its excitation-light color: red (RF) and far-red (FRF) fluorescence, excited by ultraviolet (UV), or red (R) light. The central wavelength of each color is indicated in brackets(Ben Ghozlen et al., 2010).

	Excitation (nm)	
Emission (nm)	UV (373)	Red-orange (R) (635)
RF (685)		RF_R
FRF (735)	FRF_{UV}	FRF_R

The different signals measured were used to calculate indices for flavonol- (FLAV) and chlorophyll- (SFR_R) content (Table 21).

Table 21: Indices for determination of flavonols and chlorophyll

Flavonols	**Chlorophyll**
$FLAV = \log\left(\frac{FRF_R}{FRF_{UV}}\right)$	$SFR_R = \frac{FRF_R}{RF_R}$

2.2.8 Photosynthesis measurements

Measurements of the efficiency of PSII photochemistry in *A. thaliana* plants were performed using Pulse-Amplitude-Modulation (PAM) fluorometry with the MINI-PAM-II (Walz, Effeltrich, Germany) according to the manufacturer's instructions. Therefore, leafs of 4 week old plants (N8846, SAIL_65_B07, SAIL_69_B02) were dark-acclimated using the leaf clip DLC-8 from Walz (Effeltrich, Germany) by closing the shutter. After 30 min the shutter was opened for the measurement. A light curve was applied giving a saturation pulse every 20 sec with

increasing constant actinic light after each pulse (0, 24, 38, 55, 81, 122, 183, 262 and 367 µmol m^{-2} s^{-1}). The parameters measured for determination of the photosynthetic activity are listed in Table 22.

Table 22: Measured photosynthetic parameters.

Parameter	Description	Calculation
Ft	Corresponds to momentary fluorescence level (Ft) of an illuminates sample measured shortly before application of a saturation pulse	
F_m	Maximum fluorescence level elicited by a saturation pulse which closes all reaction centers.	
F'_m	Maximum fluorescence level of illuminated sample induced by saturation pulse; is decreased relative to F_M by non-photochemical quenching	
F_0	Minimum fluorescence level of dark adapted leaf	
PAR	Quantum flux density of photosynthetically active radiation (PAR) impinging on the sample	
ETR-Factor	Fraction of incident photons absorbed by sample; default value=0.84	
P_{PS2}/P_{PS1+2}	Relative distribution of absorbed PAR to photosystem II; default value=0.5	
$\frac{F_v}{F_m}$	Maximum photochemical quantum yield of PSII	$\frac{F_m-F0}{F_m}$
Y(II)	Effective photochemical quantum yield of PSII	$\frac{F'_m-Ft}{F'_m}$
Y(NPQ)	Quantum yield of light induced non photochemical fluorescence quenching	$\frac{F}{F'_m}-\frac{F}{F_m}$
ETR	Relative electron transfer rate	PAR*ETR-Factor *P_{PS2}/P_{PS1+2}*Y(II)

2.2.9 RNA isolation, genomic DNA isolation and cDNA synthesis

RNA isolation

Isolation of RNA was performed using the RNeasy® Plant Mini Kit following the protocol for "Purification of Total RNA from Plant Cells and Tissues" with addition of the "on column DNase digestion". The quality and concentration of the RNA was determined using the Nanodrop ND-1000 spectrophotometer (NanoDrop Technologies, Wilmington, USA). To identify impurities caused by proteins or phenolic compounds the absorption ration 260/280 was measured. The ratio may also vary with different pH. RNA was considered pure if the ration was between 1.8 and 2. Further, the 260/230 ratio was measured to detect contaminants which absorb at a wavelength of 230nm. To assure RNA integrity for downstream applications, RNA was analyzed in a 1 % agarose gel electrophoresis.

Genomic DNA isolation

Genomic DNA was isolated from tDNA-insertion lines and Col-0 to check for homozygous plants using the Extract-N-Amp™ Plant Tissue PCR Kit following the manufacturer's instructions. PCR was performed as indicated in the manual using gene-specific forward and reverse primer, as well as LBb1.3 primer (Table 6). The PCR product was analyzed in a 1 % agarose gel electrophoresis.

cDNA synthesis

Standard cDNA for cloning was synthesized using SuperScript™II Reverse Transcriptase following the manufacturer's instructions. For subsequent qPCR analysis cDNA was synthesized from 1 µg of total RNA using the QuantiTect® Reverse Transcription Kit following the manufacturer's instructions. Afterwards the cDNA was diluted 1:15 with ddH_2O.

2.2.10 PCR (Polymerase Chain Reaction) and qPCR (quantitative real-time-PCR)

Standard PCR

For the amplification of the desired gene products, a standard PCR was performed using gene specific primers Table 6. PCRs were performed using the Phusion® High-Fidelity DNA Polymerase following the manufacturer's instruction. The annealing temperatures of the gene-specific primers are indicated in Table 6. PCR was performed in a MJ Research PTC-200 Peltier Thermal Cycler. The PCR products were analyzed in a 1 % agarose gel electrophoresis.

qPCR

To quantify gene expression, transcript amounts of genes were accessed using semi-quantitative qPCR. In qPCR applications the amplification of target genes is monitored as the PCR reaction proceeds. In this work, cDNA of 12 day old seedlings was used as a template and transcript amounts were normalized to the stable expressed housekeeping genes S16 and Tubulin. For this application the 7500 Fast Real-Time PCR System (Applied Biosystems, Darmstadt, Germany) and SensiMix™ SYBR Low-ROX Kit (Bioline, Luckenwalde, Germany) was used (Table 4).

Nucleic acid agarose gel electrophoresis

To check RNA integrity and PCR amplification of genes, nucleic acids were separated by fragment size using gel electrophoresis. A 1 % agarose gel was casted (Table 13). Samples were mixed with 6x loading dye (Fermentas, St Leon-Rot, Germany) and gels were run at 120-140 V depending on the size of the gel. Afterwards, the separated fragments were visualized with UV light at a wavelength of 302nm using the GelDoc 2000 (Bio-Rad Laboratories GmbH, Munich, Germany).

2.2.11 Gateway cloning

Gel Extraction

After analysis of PCR products with an agarose gel electrophoresis, fragments were cut from the gel an extracted as directed in the QIAquick® Gel Extraction Kit guide (Qiagen, Hilden, Germany).

Preparation of the attB-flanked PCR Products

For cloning of the different DNA fragments with the Gateway system (Life Technologies, Darmstadt, Germany) specific primers were designed, containing attB-sites. For expression of the protein with a c-terminal 6x His tag, a Shine-Dalgarno sequence was introduced to the forward attB-primer. For n-terminal 6x His tag expression a TEV site was introduced. The PCR products isolated from the gel were flanked with the attB-sites using an additional standard PCR, followed by an additional gel extraction.

BP- and LR reaction

The BP- and LR-reaction was performed following the manufacturers instruction (Invitrogen, Karlsruhe, Germany) with minor changes. The reactions were downscaled to 5 µl total volume and the reaction time was elongated to ON incubation at 25 °C.

Transformation

Transformation was performed by mixing 2 µl of the reaction mixture of either the BP- or LR-reaction with 50 µl of *E. coli* DH5α competent cells. The reaction was incubated on ice for 30 min. After a heat-shock for 1 min at 42 °C, 250 µl LB media was added and a further incubation under moderate shaking at 37 °C for 1 h was performed. The bacteria were plated on LB-plates containing either kanamycin (BP-Reaction) or ampicillin (LR-reaction) for selection. After incubation ON at 37 °C colonies were picked and incubated ON in 4 ml antibiotic containing LB media. The plasmids were then extracted using the QIAprep® Spin Miniprep Kit (Qiagen, Hilden, Germany). Concentrations were measured using the Nanodrop ND-1000 spectrophotometer (NanoDrop Technologies, Wilmington, USA). Further, integration of the PCR products into the plasmids was checked by sequencing (Eurofins MWG operon, Ebersberg, Germany).

2.2.12 Protein expression

Protein expression in *E. coli*

For protein expression in *E. coli* the LR-reaction product was transformed into *E.coli* Rosetta™ 2(DE3)pLysS or BL21(DE3)pLysS strain as described previously using ampicillin for selection. After incubation in ampicillin containing LB media, 1 ml of bacteria solution was transferred to 250 ml LB media and bacteria grew until an OD of 0.6 – 0.8. The OD was measured photometrical (Ultraspec3100pro, GE Healthcare, Munich, Germany). Protein expression was induced with the addition of 1 mM IPTG followed by incubation ON at 18 °C. The cultures were centrifuged at 3200 g for 20 min at 4 °C. Cells were lysed using BugBuster® Master Mix (Merck, Darmstadt Germany) as directed in the manufacturer's instruction with addition of 1 % (w/v) Cocktail Protease Inhibitor (Sigma Aldrich Taufkirchen, Germany). After lysis, the extracts were centrifuged at 24000 g for 20 minutes at 4 °C.

Protein expression in yeast

For protein expression in *S. cerevisiae* INVSc1 was plated on YPD agar plates and incubated for two days at 28 °C. Single colonies were picked and transferred to 10 ml of YPD media followed by incubation at 28 °C ON under shaking at 250 rpm. Afterwards, the culture was diluted to an OD of 0.4 in YPD media and grown to an OD of 0.8. Generation of competent cells as well as transformation of the destination vectors into INVSc1 was performed using the S.c. EasyComp™ Transformation Kit following the manufacturer's instructions. The transformed cells were plated on selection agar plates and incubated at 28 °C for four days. Untransformed yeast cells as well as transformed cells only containing the empty vector were used as negative controls. Yeast cells from plate were inoculated and

transferred into 10 ml of selective media followed by incubation at 28 °C ON under shaking at 250 rpm. The culture was then added to 200 ml of selective media and grown for another 3 days followed by centrifugation at 1500 g. The pellet was resuspended in induction media to an OD of 0.4 and grown for 24 h. After centrifugation, cells were lysed using Y-PER™ Yeast Protein Extraction Reagent (Thermo Scientific, Bonn, Germany) as directed in the manufacturer's instruction.

Protein Purification via IMAC

To purify the expressed proteins 1 ml Ni-NTA agarose columns (Qiagen GmbH, Hilden, Germany) were prepared and equilibrated with 10 ml buffer A (Table 16) before samples were applied to the columns. Further, the columns were washed with 10 ml buffer A, 10 ml buffer A+ and 10 ml buffer A. Proteins were eluted with 500 µl buffer B.

Protein-Quantification

Protein quantification was performed according to the method of Bradford (1976) using the Protein Assay Dye Reagent Concentrate from Bio-Rad (Bio-Rad Laboratories GmbH, Munich, Germany).

SDS-PAGE

1D-SDS-PAGE (one-dimensional sodium dodecyl sulfate-polyacrylamide gel electrophoresis) was performed to separate and visualize proteins. Therefore protein samples were mixed 1:1 with 2x Laemmli sample buffer (Sigma Aldrich Taufkirchen, Germany), heated for 15 min at 95 °C and loaded into the gel pockets. Proteins were separated according to their molecular weight using precast Mini-PROTEAN® TGX™ Gels and the Mini-PROTEAN® Tetra Cell from Bio-Rad (Bio-Rad Laboratories GmbH, München, Germany). Gels were run at 200 V for 30 min. To visualize proteins on a SDS-PAGE, the gels were stained with coomassie solution for 1 h, and distained with distaining solution ON.

Western blot and Immunostaining

After the samples were run on a SDS-PAGE, the gel was blotted on a nitrocellulose membrane. The aperture was assembled as shown in Figure 10 and soaked with blot buffer (Table 14). It was assured that there are no air bubbles in between the layers.

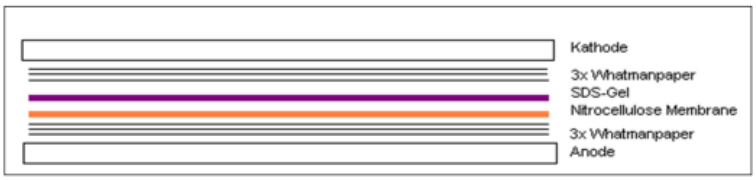

Figure 10: Western blot aperature.

The blot ran for 40 min with 2.5 mA/cm². The blotted membrane was then incubated in 50 ml block-solution for 1 h under moderate shaking at room temperature, followed by 1 h incubation at room temperature with 10 ml TBST containing the primary antibody (Table 8). The membrane was washed three times with 30 ml TBST buffer, 10 min each time. Afterwards, the membrane was incubated with 10 ml TBST containing the secondary antibody (Table 8). Incubation was performed at 4°C ON followed by two wash steps with 30 ml TBST buffer and one with 30 ml TBS buffer. In the end, the membrane was developed for 10 min using 200 µl of the NBT/BCIP Stock Solution (Sigma Aldrich Taufkirchen, Germany) diluted in 10 ml AP-buffer.

2.2.13 Programs and databases

All statistical analyses were performed using SigmaPlot 12.0 (Systat Software GmbH, Erkrath, Germany). To test if the datasets are normally distributed the Shapiro-Wilk test was applied. Datasets were considered normally distributed with a p-value >0.05. To determine significances, One way ANOVA was performed using the Holm-Sidak method for normally distributed datasets. If datasets were not normally distributed ANOVA on Ranks was performed using the Kruskal Wallis test. The datasets were considered significantly different with a p-value <0.05.

Band intensity analysis from silver stained SDS PAGE were performed using Image J (National Institutes of Health, Bethesda, USA).

All chemical structures were obtained from ChemIDplus, a toxicological data network provided by the U.S. National Library of Medicine (Bethesda, USA).

For GO-term analysis TAIR database (Phoenix Bioinformatics Corporation, Redwood City, USA) was used.

Prediction analysis of transmembrane domains was performed using the TMHMM server v. 2.0 (Center for Biological Sequence Analysis, Lyngby, Denmark).

Protein interaction predictions were accessed using STRING database Version 10.0 (http://string-db.org).

3 Results

3.1 Cyclic nucleotide measurements in *Arabidopsis thaliana*

In plants, cGMP is produced in response to various biotic and abiotic stimuli, including salt- and osmotic stress as well as pathogen infection and wounding (Donaldson et al., 2004; Grzegorzewska et al., 2012; Meier et al., 2009; Swiezawska et al., 2015). It was further linked to be involved in NO-induced cell death in *A. thaliana* suspension cultures (Clarke et al., 2000).

In this work cNMP signaling in two different cell death reactions was investigated. One of them was the simulation of a pathogen attack in *pDEX:AvrRPM1-HA* transgenic plants. These plants contain the *Pseudomonas avirulence* gene *AvrRPM1*, under the control of a dexamethasone (DEX)-inducible promotor. Four week old plants were sprayed with 30 µM DEX, inducing the expression of *AvrRPM1,* resulting in a HR (Breitenbach et al., 2014; Mackey et al., 2002).

The other system used was the fumigation with NO_2, since it was shown that NO_2 causes necrotic lesions when applied in high concentrations (Spierings, 1971; Taylor, 1966; Zeevaart, 1976). Therefore, four week old Col-0 plants were fumigated with 30 ppm NO_2 for 1 h.

Programmed cell death including HR was shown to be accompanied by the production of phenolic secondary metabolites (Gray et al., 1997; Hahlbrock, 1989; Overmyer et al., 2005; J. M. Stone et al., 2000). Therefore, plants were exposed to UV-light to detect the auto-fluorescence of phenolic compounds and chlorophyll. Phenolic compounds were shown to emit green-blue fluorescence, whereas chlorophyll emits red fluorescence (Talamond et al., 2015). As expected, the induction of HR in *pDEX:AvrRPM1-HA* transgenic plants resulted in the accumulation of phenolic compounds. This accumulation became visible 3 h after DEX treatment by an intense green-blue fluorescence compared to the control plants with a further increase after 4 h (Figure 11). In case of the NO_2-induced cell death, green-blue fluorescence was already visible directly after fumigation with no visible increase in the further time points. For both treatments, this effect was associated with a visible loss of turgor in the leaves.

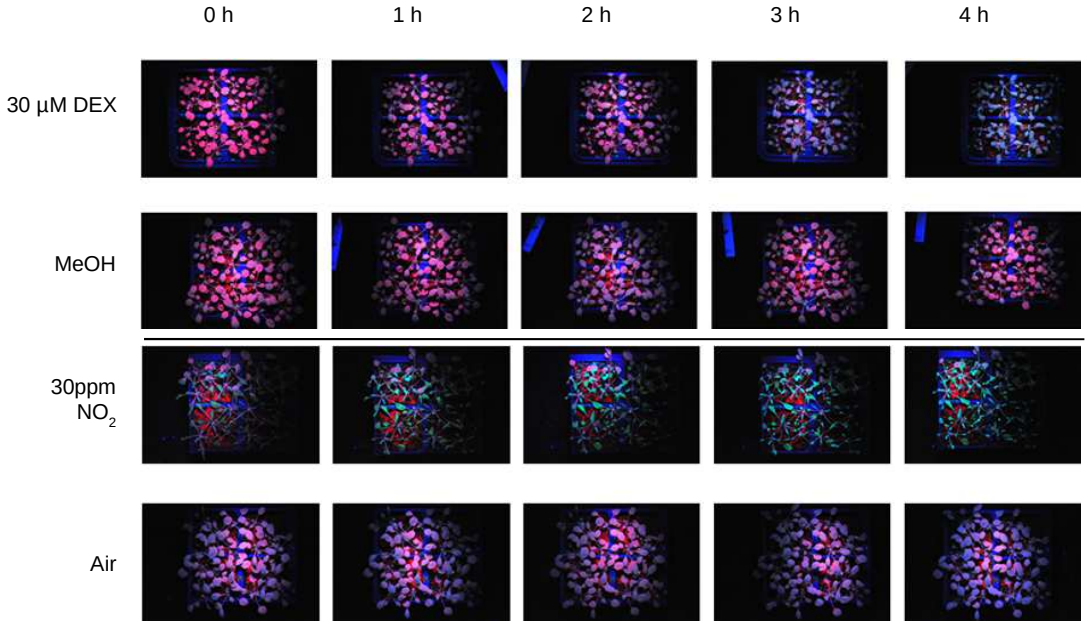

Figure 11: Accumulation of phenolic secondary metabolites during HR and cell death. Auto-fluorescence of phenolic compounds (green-blue) and chlorophyll (red) was monitored for 4 h spraying of *pDEX:AvrRPM1-HA* mutant plants with 30 µM DEX or after fumigation of Col-0 with 30 ppm NO_2. In case of the DEX-treatment of *pDEX:AvrRPM1-HA* mutant plants, red fluorescence in treated plants was strongly decreased compared to control plants after 3 h, whereas the intensity of green-blue fluorescence was increased. The same effect was visible directly after 1 h of NO_2 fumigation.

3.1.1 FT-ICR-MS

Treated and untreated plants were washed, flash frozen in liquid nitrogen and cNMPs were extracted from 150 mg leaf material. After solid phase extraction (SPE), cNMPs were measured using a fourier-transform-ion-cyclotron-resonance (FT-ICR) mass spectrometer coupled to a 12 Tesla magnet (Wittek et al., 2014). The cyclic nucleotides of >11 biological replicates of two independent experiments were measured and the threshold for identification and quantification was set to 1.5E+06 spectral counts per second. The levels of cGMP, cAMP and cUMP were increased after both treatments (Figure 12). For cGMP, 4h after spraying *pDEX:AvrRPM1-HA* mutant plants with DEX, a significant increase of 6.3-fold was detected (Table 23). 1 h after fumigation with NO_2 a 2.2-fold increase was observed. However, this increase was not significant. In case of cAMP, a 5.1- and 5.5-fold increase after DEX and NO_2 treatment was observed. The levels of cUMP were increased 3.0-fold after treatment with DEX and 4.0-fold after NO_2 fumigation. For cCMP, only after DEX treatment levels were increased above LOD, however this increase could not be observed in all samples.

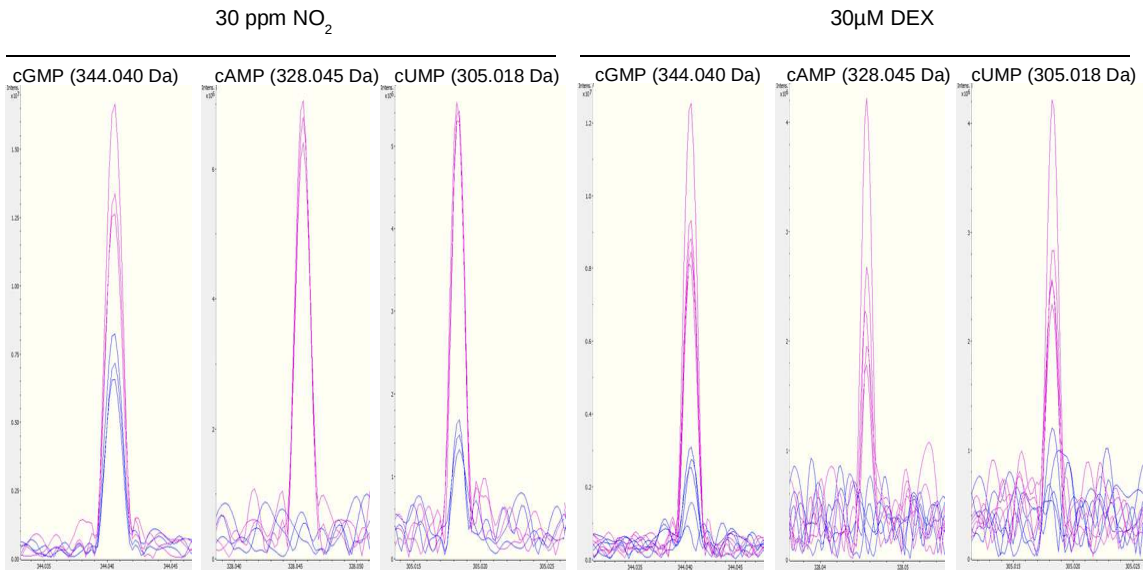

Figure 12: Relative quantification of cyclic nucleotides during HR and cell death using FT-ICR. cNMPs were measured after fumigation of Col-0 with 30 ppm NO_2 or spraying of *pDEX:AvrRPM1-HA* mutant plants with 30 µM DEX. Leaf samples of fumigated plants were taken directly after 1 h fumigation. DEX treated plants were harvested 4 h after treatment. Representative spectra of cGMP, cAMP and cUMP of control (blue) and treated (pink) plants from one experiment are shown.

Table 23: Nucleotide accumulation during NO_2-induced cell death and HR.

Annotation	Formula	Theoretical mass	Measured mass (m/z) $[M-H]^-$	Change in spectral count	
				30 ppm NO2	30 µM DEX
cAMP, cyclic adenosine monophosphate	$C_{10}H_{12}N_5O_6P$	328.0452	328.0452	5.5	5.1
cGMP, cyclic guanosine monophosphate	$C_{10}H_{12}N_5O_7P$	344.0402	344.0401	2.2	6.3
cCMP, cyclic cytidine monophosphate	$C_9H_{12}N_3O_7P$	304.0340	304.0339	0.0	1.3
cUMP, cyclic uridine monophosphate	$C_9H_{11}N_2O_8P$	305.0180	305.0180	4.0	3.0

3.1.2 HPLC–MS/MS

The detection method using a FT-ICR mass spectrometer is non-targeted and cNMPs can be identified by their exact individual mass. However, it is not possible to distinguish between the existing isomers of these cNMPs: the 3’5’- and the 2’3’-isomer. Therefore, a targeted high performance liquid chromatography tandem mass spectrometry (HPLC–MS/MS) method was applied, making it possible to separate the cNMPs by their specific masses and retention

time. After cNMP extraction, the samples were measured using a QTrap5500TM triple quadrupole mass spectrometer. For the quantification of 2'3'-cNMPs the standard curves of the corresponding 3'5'-isomers were used.

Figure 13 shows representative spectra of both isomers of cAMP and cGMP after NO_2 fumigation and DEX treatment compared to the corresponding negative controls. For the better demonstration of 3'5'-cNMPs the spectra of the cNMPs after each treatment were zoomed in. The retention time of the 3'5'-isomers were 3.73 min for cAMP and 3.0 min for cGMP. In case of the 2'3'-isomers, the retention times were 3.35 and 2.7 min for cAMP and cGMP, respectively. For both treatments a clear increase in the 2'3'- but not in the 3'5'-isoforms of both cNMPs can be observed.

Figure 14 shows all quantified cNMPs before and after the two treatments. In case of cAMP, a basal concentration of 2'3'-cAMP of 10-13 fmol/ µg protein was detected. This concentration was about 2-fold higher than concentrations of 3'5'-cAMP. For cGMP, basal levels of 2'3'-cGMP were detected in the range of 44-57 fmol/ µg protein, whereas the basal levels of 3'5'-cGMP could be detected but were below the limit of quantification (LOQ). The basal concentrations of between 40-58 fmol/ µg protein were detected for 2'3'-cCMP. In comparison, 3'5'-cCMP levels were below the limit of detection (LOD). In untreated plants, no 2'3'-cUMP could be detected (LOD), whereas a basal concentration of about 3 fmol/ µg protein was measured for 3'5'-cUMP.

Comparing the concentrations of cNMPs before and after the two treatments, no significant change in the levels of the 3'5'- cAMP was observed. 3'5'-cGMP was identified in most of the treated and untreated samples. However, based on the low signal the quantification was not possible. 3'5'-cCMP could not be identified in any of the samples. In case of 3'5'-cUMP a decrease after NO_2 fumigation was detected. The same trend was visible after treatment with DEX, whereas in this case it was not significant. In contrast, the investigation of the changes in the levels of the 2'3'-isomers showed a significant increase of cAMP, cGMP and cUMP for both treatments. An 11.8 and 28.7-fold increase after NO_2 and DEX treatment was measured for levels of 2'3'-cAMP. 2'3'-cGMP levels were increased 2.0 and 6.9-fold in both treatments, respectively. The levels of 2'3'-cUMP rose from below LOD to 5.6 fmol/ µg protein after fumigation with NO_2 and to 6.2 fmol/ µg protein after spraying with DEX. In contrast, a 26 % decrease in 2'3'-cCMP levels was observed after NO_2 fumigation. In case of DEX treatment a 4.2-fold increase was detected.

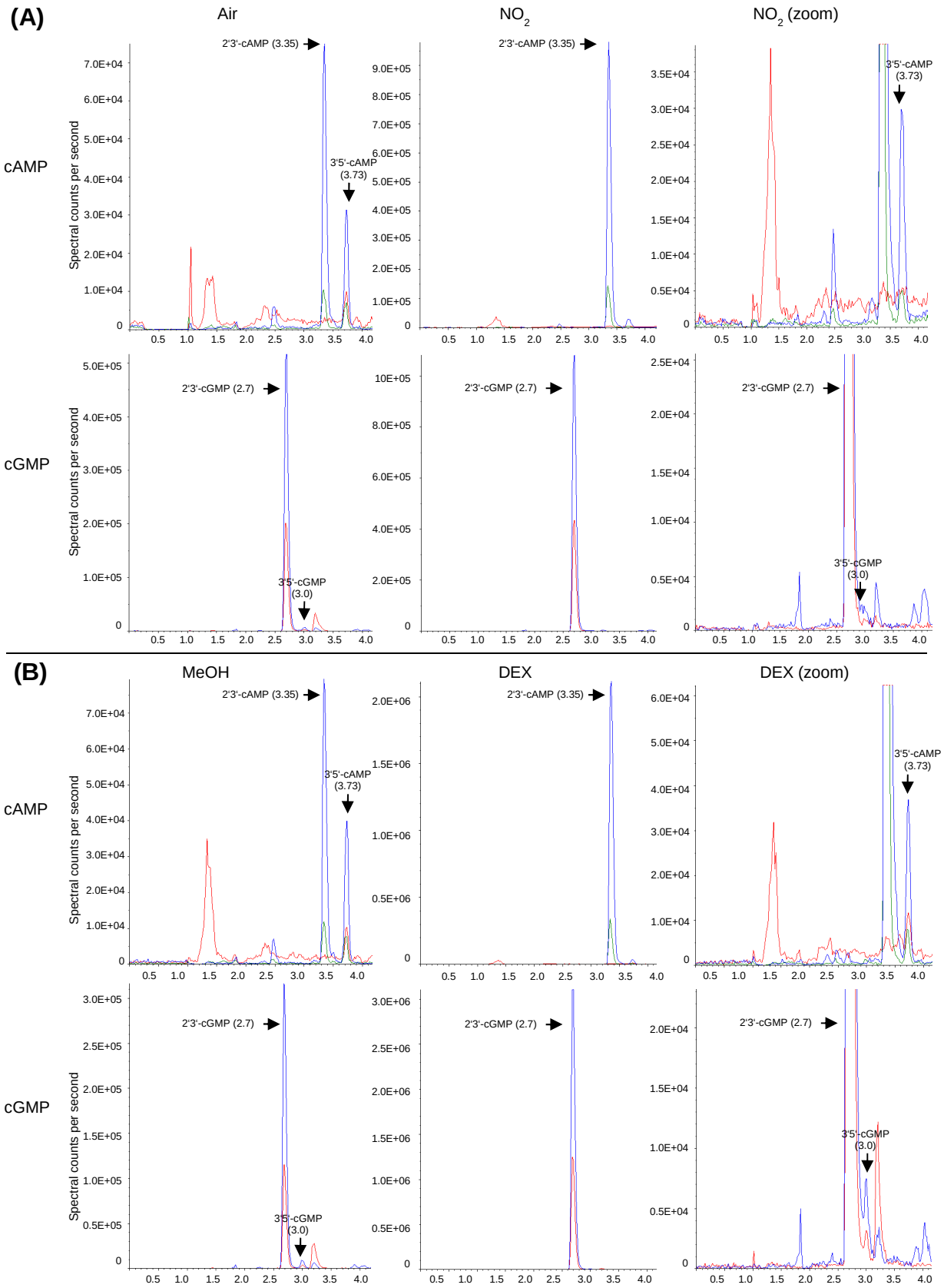

Figure 13: Representative spectra of cAMP and cGMP measured with HPLC–MS/MS.
CNMPs were measured using a QTrap5500TM triple quadrupole mass spectrometer after NO_2 fumigation (A) and DEX treatment (B). The 3'5'- and 2'3'-isoforms were separated by their retention time. The retention time of the 3'5'-isoforms were 3.73 and 3.0 for cAMP and cGMP and 3.35 and 2.7 for the 2'3'-isoforms, respectively. For both treatments a clear increase in the 2'3'- but not in the 3'5'- isoforms of both cNMPs was observed.

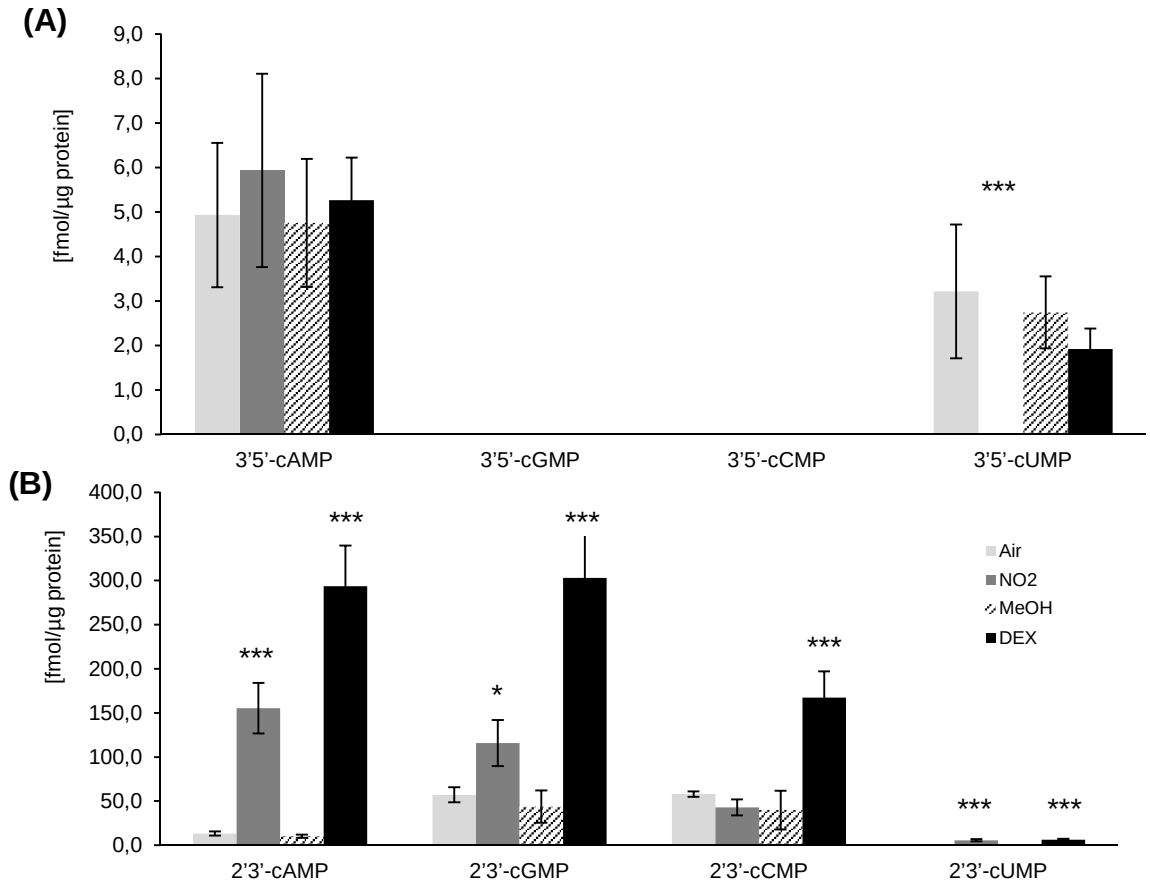

Figure 14: quantification of cyclic nucleotides during HR and cell death using HPLC–MS/MS. CNMPs were measured after fumigation of Col-0 with 30 ppm NO_2 or spraying of *pDEX:AvrRPM1-HA* mutant plants with 30 µM DEX. Leaf samples of fumigated plants were taken directly after 1 h fumigation. DEX treated plants were harvested 4 h after treatment. The cyclic nucleotides of were measured using a QTrap5500TM triple quadrupole mass spectrometer. Concentrations of 3'5'-cNMPs (A) and 2'3'-cNMPs (B) were measured. Columns represent the mean values. Error bars indicate the standard deviation. Asterisks indicate significant differences compared to control samples (Holm-Sidak-method, * P<0.05, ** P<0.01, *** P<0.001). (n>4)

In addition to cell death, cGMP levels have been shown to increase in response to treatment with the NO-donor SNP and the phytohormone auxin (Dubovskaya et al., 2011; Nan et al., 2014). NO was shown to be a stress signal in plants, as it induces the expression of defense genes in tobacco as well as HR in *A. thaliana* suspension cultures (Clarke et al., 2000; Durner et al., 1998). In contrast, auxin is an important signaling molecule. In response to physiological and environmental changes, it regulates plant growth and development, cell division and differentiation, as well as root and shoot architecture (Nan et al., 2014; Pagnussat et al., 2003; Seifertová et al., 2014). To investigate the role of the different cNMPs and their isomers in response to NO, liquid cultured *A. thaliana* Col-0 seedlings were incubated with 5 mM SNP for 3 h. CNMP levels in response to auxin were measured after treating liquid cultured seedling with 10 µM indole-3-acetic acid (IAA) for 1 h. Treated and untreated plants were washed, flash frozen in liquid nitrogen and cNMPs were extracted. In Figure 15 it is shown that after SNP treatment, no significant regulation of 3'5'-cAMP was observed. The levels of 3'5'-cGMP, -cCMP and -cUMP were below LOD. In case of the

2’3’-isomers, a significant upregulation of cAMP (2.1-fold) and cCMP (1.8-fold) levels was detected, whereas the upregulation of 2’3’-cGMP was not significant. After incubation with IAA, 2’3’-cCMP levels were significantly upregulated showing a 25 % increase.

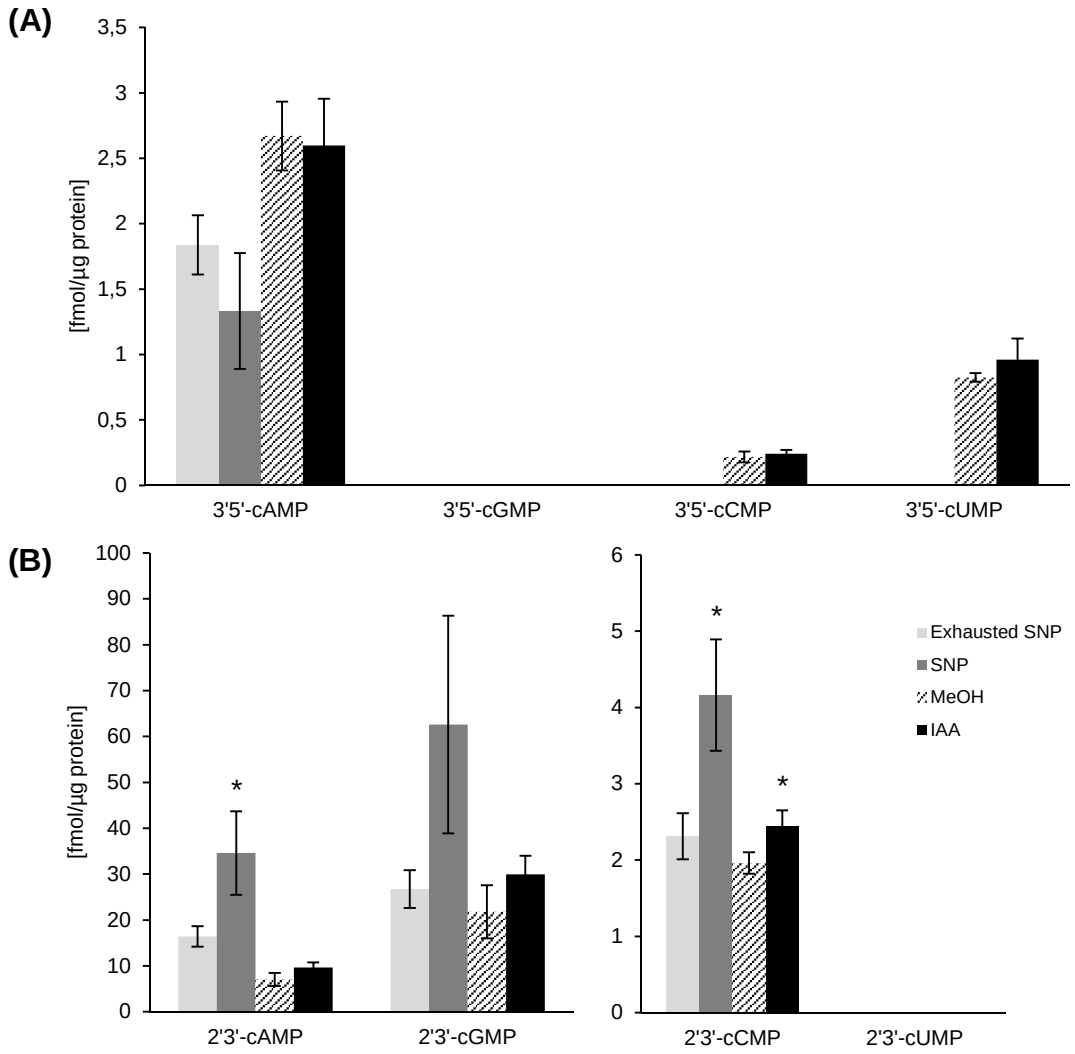

Figure 15: Quantification of cyclic nucleotides after SNP and IAA treatment using HPLC–MS/MS.
CNMPs were measured after incubation of 12 day old *A. thaliana* Col-0 seedlings from liquid culture with 5 mM SNP for 3 h or 10 µM IAA for 1 h. Samples were taken directly after the treatment. The cyclic nucleotide levels were measured using a QTrap5500TM triple quadrupole mass spectrometer. Concentrations of 3’5’-cNMPs (A) and 2’3’-cNMPs (B) were measured. Columns represent the mean values. Error bars indicate the standard deviation. Asterisks indicate significant differences compared to control samples (Holm-Sidak-method, * P<0.05, ** P<0.01, *** P<0.001). (n=3)

3.2 Detection of endogenous guanylyl cyclase (GC) enzyme activity in *H. vulgare* and *A. thaliana*

An assay was established to measure GC activity in soluble plant protein extracts. Therefore, cGMP formation in protein extracts was measured. Soluble proteins from either *H. vulgare* or *A. thaliana* were extracted, desalted and 200 µg of protein were incubated with the GC-substrate GTP and the GC-cofactor $MgCl_2$. After incubation for the indicated time points,

the cGMP formation was measured using a commercial cGMP-enzyme immunoassay. The negative controls were performed by incubation of the reaction mixture either without protein or without substrate.

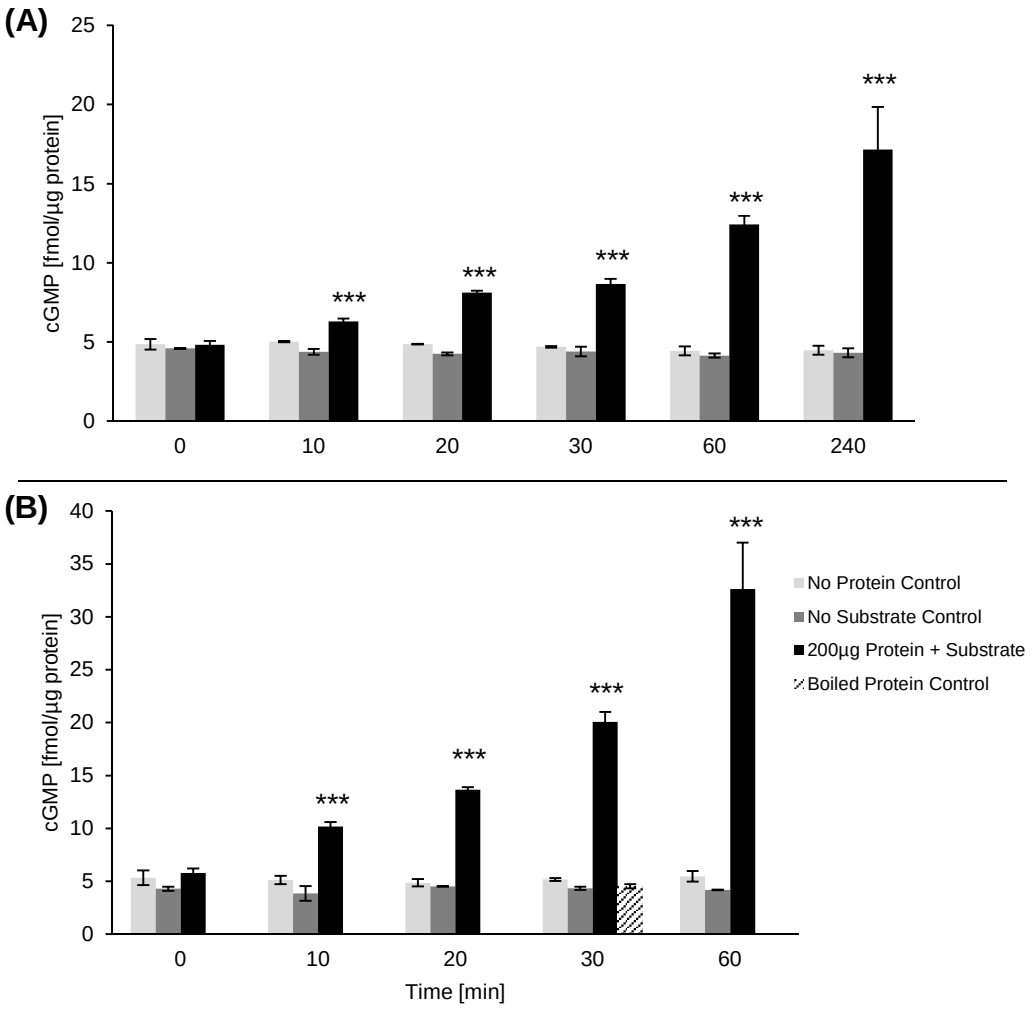

Figure 16: cGMP formation in protein extracts from *H. vulgare* and *A. thaliana*.
200 µg of soluble protein of *H. vulgare* (A) or *A. thaliana* (B) were incubated with 20 mM $MgCl_2$ and 1 mM GTP in a total reaction volume of 250 µl for the indicated time points. Reactions were stopped by addition of 250 µl 0.2M zinc acetate, followed by addition of 250 µl 0.2M sodium carbonate. After centrifugation cGMP content was measured from 100 µl supernatant with an enzyme immunoassay kit. Negative controls were prepared either without addition of protein (light grey) or substrate (dark grey). Additionally a boiled protein control was included for the 30 min incubation time point of *A. thaliana* (striped). Columns represent the mean values. Error bars indicate the standard deviation. Asterisks indicate significant differences compared to control samples (Holm-Sidak-method, * P<0.05, ** P<0.01, *** P<0.001).

Figure 16 shows the formation of cGMP in samples of *H. vulgare* (A) and *A. thaliana* (B) after incubation for the indicated time points. The formation of cGMP was detected only in samples containing protein and substrate. In the negative controls a background signal was observed which did not change in the different incubation times. The average activity in *H. vulgare* extracts was about 0.15 fmol/ µg protein/ min compared to an average activity in *A. thaliana* of about 0.5 fmol/ µg protein/ min. In the preparation of *A. thaliana* another negative control was included using boiled protein in the incubation mixture. No cGMP

formation was detected in these samples. Furthermore, before performing the activity assay, proteins of *H. vulgare* were extracted using detergent based CelLytic™ P Cell Lysis Reagent (Sigma, Taufkirchen, Germany). This extraction did not result in a higher activity (data not shown).

To confirm the production of cGMP in the different samples, a PDE was included in an additional preparation of *H. vulgare* protein (Figure 17). The samples were incubated for 1 h at 24 °C with a subsequent incubation with 400 units of PDE5A1 from human for 10 min at 37 °C under moderate shaking to maintain the optimal conditions for PDE activity. Figure 17 shows that the cGMP signal was completely degraded to no protein control levels by incubation of the extracts with the PDE.

To further investigate cGMP formation and purify GCs, the system was changed using sterile grown plants instead of soil grown plants. In case of *H. vulgare* as well as *A. thaliana* no cGMP formation was observed. Additionally, cGMP formation from soluble extracts of only leaf material was tested. In this case no cGMP production was detected. To exclude the possibility that cGMP formation was just significantly lower in sterile grown plants, both species were treated with compounds previously shown to induce cGMP formation in plants. These treatments included incubation with 5 mM SNP, 100 µM ABA and 100 µM IAA (Dubovskaya et al., 2011; Nan et al., 2014). No cGMP formation was observed in both species with none of the treatments.

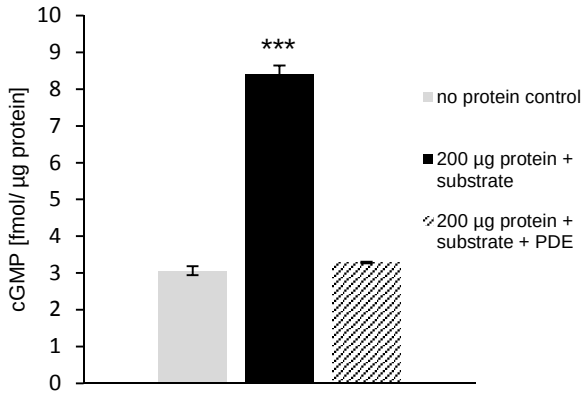

Figure 17: Degradation of cGMP by addition of a phosphodiesterase.
200 µg of soluble protein of *H. vulgare* were incubated with 20 mM $MgCl_2$ and 1 mM GTP in a total reaction volume of 250 µl for 1 h at 24 °C followed by 10 min incubation with 400 units of PDE5A1 at 37 °C. Reactions were stopped by addition of 250 µl 0.2 M zinc acetate, followed by addition of 250 µl 0.2M sodium carbonate. CGMP content was measured from 100 µl supernatant with an enzyme immunoassay kit. Columns represent the mean values. Error bars indicate the standard deviation. Asterisks indicate significant differences compared to control samples (Holm-Sidak-method, * P<0.05, ** P<0.01, *** P<0.001).

3.2.1 cGMP production by rhizosphere organisms

Formation of cGMP was observed in soil grown plants but not in sterile grown plants. Additionally, protein extracts from soil grown plants of both species were prepared using only

leaf material. Again, no cGMP formation was detected. Therefore it was assumed that cGMP formation could be the result of a contamination with proteins from rhizosphere organisms tightly attached to the plant root of soil grown plants. To examine this possibility, roots of soil grown *H. vulgare* plants were incubated in LB media for 10 min under moderate shaking. Afterwards, the LB media containing rhizosphere microorganisms was incubated ON at 37°C shaking at 200 rpm. On the next day the samples were centrifuged and the pellet was prepared for the GC purification assay in the same way as plant material. Consequently, cGMP formation was measured (Figure 18). A cGMP formation in protein extracts of the rhizosphere organisms was observed which was in a comparable range to that of protein extracts from soil grown *H. vulgare* plants (Figure 17).

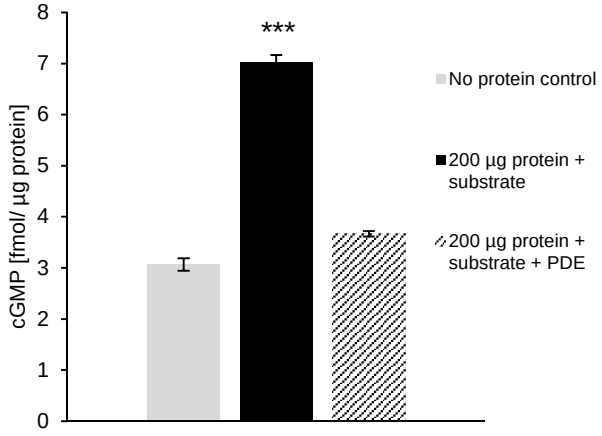

Figure 18: Formation of cGMP by rhizosphere and degradation by a phosphodiesterase.
200 µg of soluble protein of the rhizosphere were incubated with 20 mM $MgCl_2$ and 1 mM GTP in a total reaction volume of 250 µl for 1 h at 24 °C followed by 10 min incubation with 400 units of PDE5A1 at 37 °C. Reactions were stopped by addition of 250 µl 0.2 M zinc acetate, followed by addition of 250 µl 0.2 M sodium carbonate. CGMP content was measured from 100 µl supernatant with an enzyme immunoassay kit. Columns represent the mean values. Error bars indicate the standard deviation. Asterisks indicate significant differences compared to control samples (Holm-Sidak-method, * P<0.05, ** P<0.01, *** P<0.001).

To confirm that the cGMP produced in the soil grown plant preparations is the result of a contamination and was not formed from plant soluble protein extract another protein preparation was performed. Soil grown *H. vulgare* plants were either not rinsed and soil was roughly shaken off the roots or plant roots were washed extensively. Figure 19 shows that in case of well rinsed roots (A), a cGMP production of only about 3 fmol/ µg protein was detected. In comparison, samples of unrinsed roots showed a cGMP production of about 67 fmol/ µg protein after 1 h of incubation (B) resulting in a GC-activity of 1.1 fmol/ µg protein/ min.

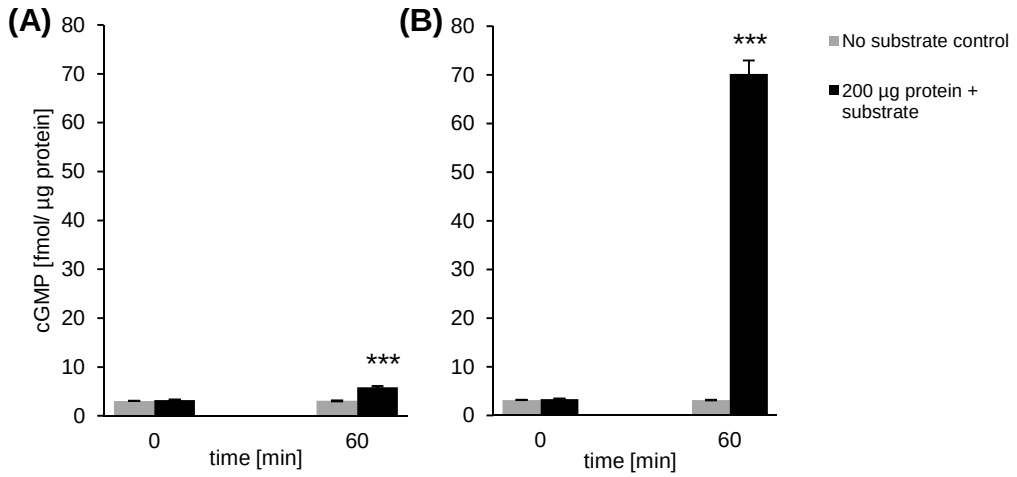

Figure 19: cGMP formation of rinsed and unrinsed soil grown *H. vulgare* plants.
200 µg soluble protein of either rinsed (A) or unrinsed (B) *H. vulgare* plants were incubated with 20 mM $MgCl_2$ and 1 mM GTP in a total reaction volume of 250 µl for 1 h at 24 °C. Reactions were stopped by addition of 250 µl 0.2 M zinc acetate, followed by addition of 250 µl 0.2 M sodium carbonate. CGMP content was measured from 100 µl supernatant with an enzyme immunoassay kit. Columns represent the mean values. Error bars indicate the standard deviation. Asterisks indicate significant differences compared to control samples (Holm-Sidak-method, * P<0.05, ** P<0.01, *** P<0.001).

3.2.2 Is cGMP produced by *Azospirillum brasilense*?

Further investigation of the production of cGMP by rhizosphere organisms was performed using *A. brasilense* based on previously shown cGMP production (Marden et al., 2011). The bacteria were cultivated in cyst inducing media (M9) and cGMP released to the media was measured. Figure 20 (A) shows that cGMP was produced continuously over time with a cGMP concentration of about 2 nM after 6 days of growth. In a further experiment, 7 nM of cGMP or 7 nM cGMP and a PDE was spiked to the samples before measurement. After incubation for 10 min at 37 °C cGMP content was measured from 100 µl media. The non-spiked sample showed a similar cGMP production compared to the first experiment. Figure 20 (B) shows that in case of the spiked samples with 7 nM cGMP and a PDE exactly the spiked amount of cGMP was degraded by the PDE.

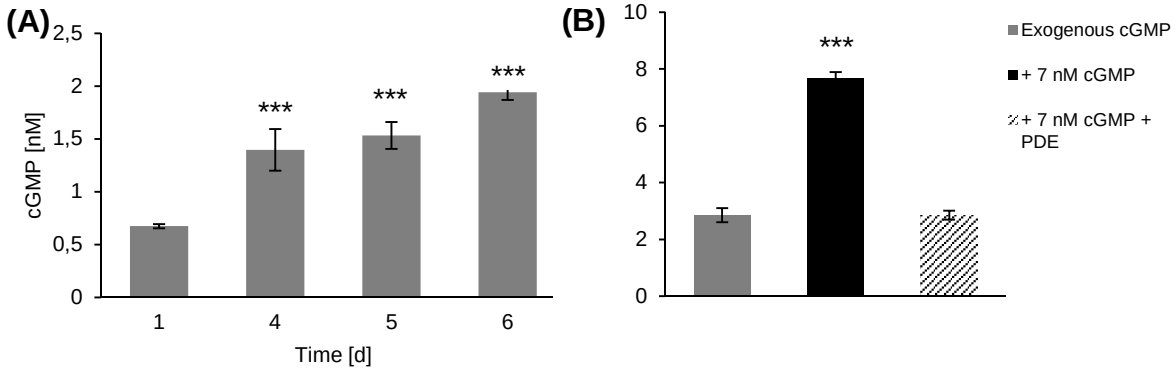

Figure 20: cGMP formation by *Azospirillum brasilense*.
A. Brasilense was grown for six days and exogenous cGMP was measured from the media (A). In a further experiment, samples from day six were spiked with 7 nM cGMP or 7 nM cGMP and 400 units of PDE5A1 (B). After 10 min of incubation at 37 °C samples flash frozen in liquid nitrogen, centrifuged and cGMP was measured from 100µl of the supernatant with an enzyme immunoassay kit. Columns represent the mean values. Error bars indicate the standard deviation. Asterisks indicate significant differences compared to control samples (Holm-Sidak-method, * P<0.05, ** P<0.01, *** P<0.001).

A. brasilense and other bacteria were shown to produce c-di-GMP (Romling et al., 2013; Russell et al., 2013). Therefore, the immunoassay kit was tested for cross reactivity with this compound. Figure 21 shows that c-di-GMP is detected by the kit. 100 µM of spiked c-di-GMP resulted in a 1000-fold lower cGMP signal of about 100 nM.

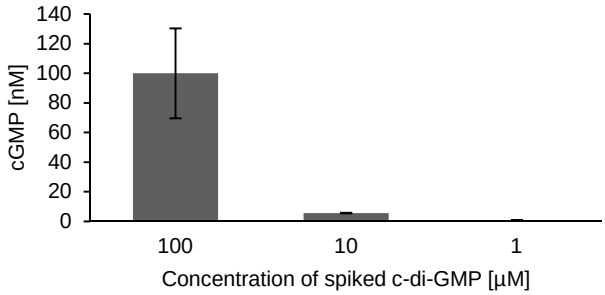

Figure 21: Detection of c-di-GMP with the enzyme immunoassay kit.
c-di-GMP was measured with the enzyme immunoassay kit. Concentrations used were 1, 10 and 100 µM. Columns represent the mean values. Error bars indicate the standard deviation.

3.3 Identification of cGMP binding proteins

cGMP immobilized on agarose by an aminoethylthio spacer attached to position eight of the ligand was used for the identification of proteins that are able to bind cGMP. The immobilized cGMP is stable and PDE resistant. The summarized workflow is shown in Figure 22. The first step in the CGBP identification process was the extraction of proteins from 12 day old *A. thaliana* seedlings. Subsequently, 4600 µg of the soluble protein extract were incubated with 300 µl of the cGMP-agarose to allow binding of the proteins. After incubation for 1.5 h, the cGMP-agarose was washed with CGBP extraction buffer to remove unattached proteins. Afterward, the supernatant was removed completely and 2 x Laemmli SDS buffer was added to the agarose to elute the bound proteins. After elution, the bound proteins were visualized on a 1D SDS-PAGE and further identified and quantified by mass spectrometry. This experiment was repeated twice.

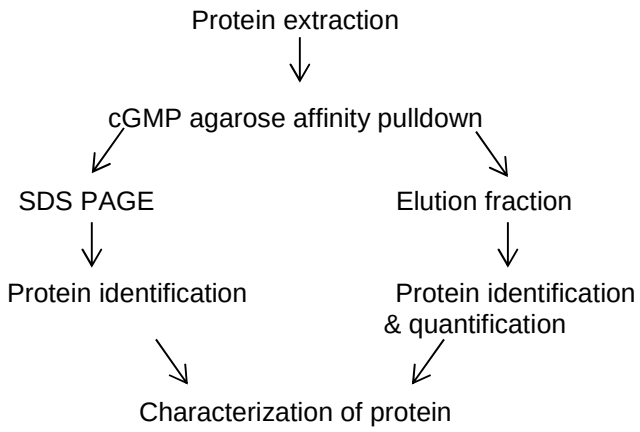

Figure 22: Summarized workflow of the identification of CGBPs.

The 20 most abundant proteins from all experiments were compared leading to 14 candidates present in all three preparations. Table 24 displays the candidates, with ten of them showing an annotated binding preference for different nucleotides or phosphate groups.

Table 24: Most abundant proteins eluted from cGMP-agarose.

Locus	Description	Binding preference
At4G09320	Nucleoside diphosphate kinase 1	ATP/ nucleoside diphosphate
At5G63310	Nucleoside diphosphate kinase 2	ATP/ nucleoside diphosphate
At4G28520	Cruciferin 3	DNA binding
At4G11010	Nucleoside diphosphate kinase 3	ATP/ GDP/ nucleoside diphosphate
At2G39730	Rubisco activase	ATP/ ADP
At3G53180	Glutamate-ammonia ligase	-
AtCG00480	ATP synthase subunit beta	ATP/ Nucleotide
AtCG00120	ATP synthase subunit alpha	ATP/ Nucleotide
At3G61870	unknown protein	-
At5G10160	Thioesterase superfamily protein	Possible binding to aminoethylthio spacer
AtCG00490	Ribulose-bisphosphate carboxylase	Phosphate
At1G04690	Potassium channel beta subunit 1	NADP
At2G22230	Thioesterase superfamily protein	-
At4G20360	RAB GTPase homolog E1B	GTP/ nucleotide

The majority of the bound proteins from the cGMP agarose have an affinity to bind nucleotides but no specific cGMP binding candidate was identified. Therefore, a negative control was included by pre-incubating the protein extract with 100 µM cGMP. In theory, the free cGMP should occupy the binding site of CGBPs and therefore prevent binding of CGBPs to the agarose. Figure 23 displays the elution profile of the 2’3’- and 3’5’-cGMP pre-incubated samples as well as the fraction without pre-incubation. The red arrow marks the band that was present in the fraction without pre-incubation but was less intense in the cGMP pre-incubated samples. The lower intensity was further confirmed by analysis of the band using “Image J”. The intensity of this band in each sample was normalized to the band marked by the blue arrow. The normalized band intensities of the cGMP pre-incubated samples were then compared to the band intensity of the sample without pre-incubation The result of this analysis revealed a 22 and 27 % lower band intensity after 2’3’- and 3’5’-cGMP pre-incubation, respectively (Supplementary Table 28).

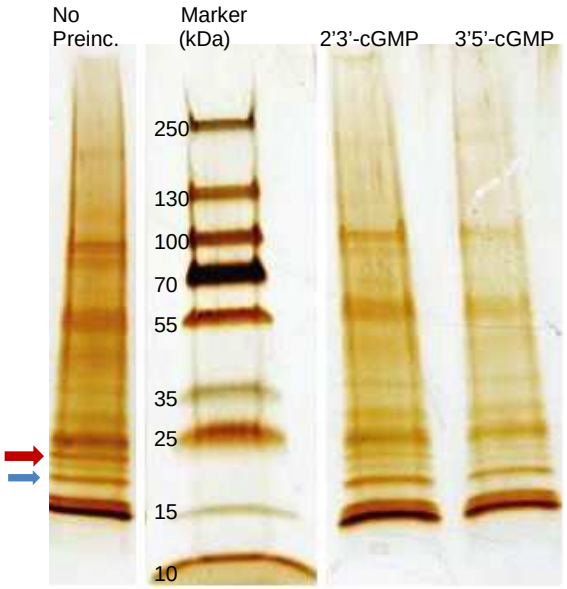

Figure 23: Elution profile of proteins bound to cGMP-agarose after cGMP pre-incubation.
Soluble protein extracts were pre-incubated with 100 µM of 2'3'- or 3'5'-cGMP before incubation with the cGMP-agarose. Bound proteins were eluted and analyzed on a 4-15% 1D SDS PAGE followed by silver staining. The red arrow marks the protein band which was present in the sample without pre-incubation but disappeared with cGMP pre-incubation. The blue arrow marks the band used for normalization of the band intensity.

To identify the protein that caused the indicated band (red arrow) in Figure 23, the band from the silver stained SDS PAGE was cut from the no pre-incubation fraction. Proteins present in the gel cuts were identified by mass spectrometry. This experiment was done three times. 11 proteins were shown to be present in all three experiments and were chosen for further analysis (Figure 24).

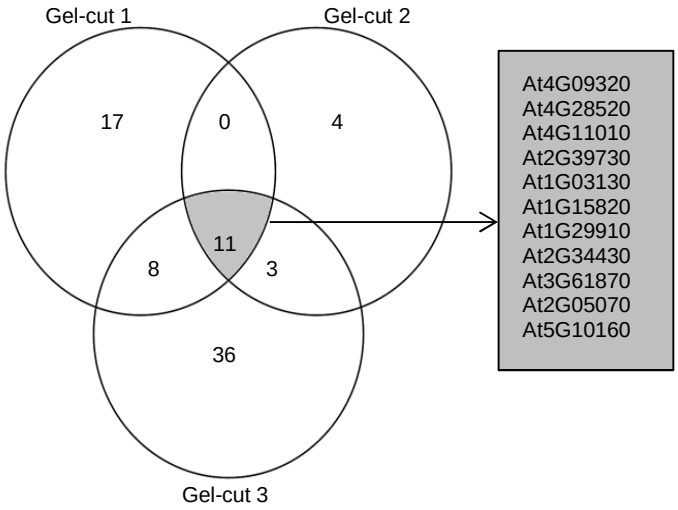

Figure 24: CGBP candidates from gel cuts.
The marked protein band of the no pre-incubation fraction of Figure 24 was cut and proteins were analyzed by LCMS/MS. The experiment was done three times. 11 proteins were found in all gel pieces (grey).

The proteins in the elution fraction of the 3’5’-cGMP pre-incubated sample, as well as the non-pre-incubated sample were analyzed and quantified. This experiment was repeated twice. Proteins showing an at least 1.5-fold lower abundance in the cGMP pre-incubated samples compared to the non-pre-incubated samples were considered potential CGBP candidates. In Figure 25 an overlap of the candidates of all three preparations and the candidates from the gel cut analysis is shown. This analysis resulted in a total of 32 candidates showing the expected binding behavior in at least two of three elutions (Supplementary Table 29). Furthermore, one candidate that was identified as a potential CGBP in the gel-cut analysis was also present in all three elution fraction preparations. This candidate was At3G61870.

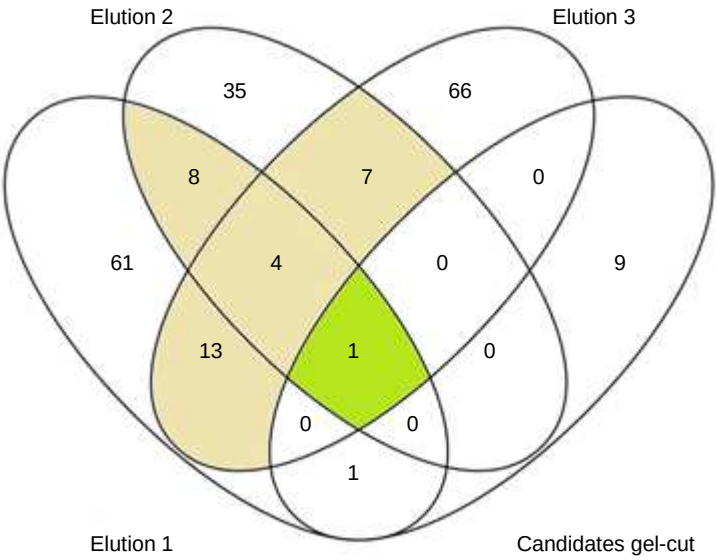

Figure 25: CGBP candidates from elution fraction and gel-cut analysis.
Candidates from the gel-cut analysis were overlapped with candidates from elution fractions of 3 individual experiments. Proteins of the elution fractions were considered putative CGBP candidates if the fold-change of the no pre-incubation fraction compared to cGMP pre-incubation was higher than 1.5 in at least 2 of 3 experiments (beige). This analysis resulted in 1 candidate (At3G61870) being present in all elution fraction preparations and in the gel-cut analysis (green).

For the identification of nonspecific binders, further negative controls were included. Protein extracts were pre-incubated with 100 µM of other nucleotides which show structural similarities to cGMP. These nucleotides included 3’5’-cAMP, ATP, GTP, GDP, GMP. After elution of the proteins from the agarose, proteins were analyzed on a SDS-PAGE. The elution profile of the proteins bound to the cGMP-agarose is shown in Figure 26. The red arrow marks the protein band present in all negative controls but absent in the cGMP pre-incubated sample, therefore presenting the expected binding behavior of a cGMP binding protein.

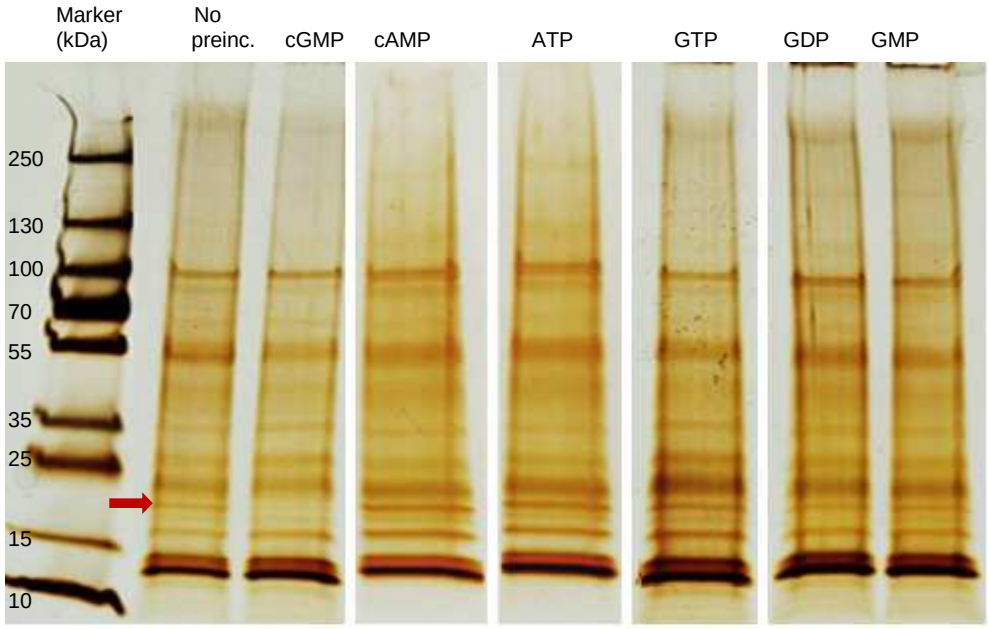

Figure 26: Elution profile of proteins bound to cGMP-agarose after pre-incubation.
Soluble protein extracts were pre-incubated with 100 µM of the indicated nucleotides before incubation with the cGMP-agarose. Bound proteins were eluted and analyzed on a 4-15% 1D SDS PAGE followed by silver staining. The red arrow marks the protein band which is present in all negative controls but disappears with cGMP pre-incubation.

The elution fractions of the cGMP-, GTP-, GDP and GMP pre-incubated samples as well as the one of the non-pre-incubated sample were analyzed and quantified via LCMS/MS. Table 25 displays the five most prominent candidates showing the highest fold changes over all negative controls. These proteins were shown to bind cGMP with a higher affinity than any other nucleotide tested in this study.

Table 25: Fold-changes of CGBP candidates of cGMP pre-incubated samples compared to negative controls from three individual experiments. (n.d.= not detected)

Locus	kDa	Description	No pre./cGMP	GTP/cGMP	GDP/ cGMP	GMP/cGMP
At3G61870	29.5	unknown protein HP29b	7.5/ 5.4/ 4.3	4.9/ 4.3/ 2.5	4.8/ 4.0/ 2.8	4.5/ 2.9/ 3.6
At3G56190	32.8	alpha-soluble nsf attachment protein 2	2.1/ 1.9/ 1.3	2.4/ 1.7/ 1.8	1.7/ 1.5/ 1.8	1.9/ 2.4/ 3.7
At3G15950	85.0	nai2, tsk-associating protein 1-like protein	3.9/ 4.7/ n.d.	3.8/ 3.0/ n.d.	2.2/ 1.8/ n.d.	3.6/ 2.4/ n.d.
At5G38480	28.6	general regulatory factor 3	n.d./ 2.4/ 2.1	n.d./ 1.6/ 1.9	n.d./ 2.7/ 1.8	n.d./ 1.9/ 2.0
At4G35450	38.1	ankyrin repeat-containing protein 2	2.0/ n.d./ 1.9	1.8/ n.d./ 1.7	2.0/ n.d./ 1.8	1.8/ n.d./ 1.7

3.4 Characterization of HP29b

At3G61870 (HP29b), a putative protein of unknown function, was chosen for further analysis. It was the only candidate present in all preparations and had the highest fold changes in the cGMP pre-incubation samples compared to all negative controls (Table 25). GO-term analysis indicate HP29b is an integral inner membrane protein localized in the inner envelop of chloroplasts, which was experimentally shown by Ferro et al. (2002) and Firlej-Kwoka (2008). Additionally, the protein contains four predicted transmembrane domains.

The analysis of potential interaction partners of HP29b revealed ten candidate proteins (Szklarczyk et al., 2015). All of these proteins are located in the chloroplast and the majority of them were shown to function in photosynthetic processes (Table 26).

Table 26: Predicted functional partners of HP29b.

Predicted functional partner	Description
PRXQ	peroxiredoxin q; role in the protection of the photosynthetic apparatus
SBPASE	Chloroplast enzyme sedoheptulose-1,7-bisphosphatase, involved in the carbon reduction of the calvin cycle
At3G47070	Located in chloroplast thylakoid membrane; unknown function
TLP18.3	Encodes a thylakoid lumen protein regulating photosystem ii repair cycle
At5G07020	Integral thylakoid membrane protein that interacts with PSII core complexes
CSP41A	Chloroplast stem-loop binding protein; protein with ribonuclease activity that is involved in plastid rRNA maturation
PGLP1	2-phosphoglycolate phosphatase 1; located in chloroplast stroma
CRB	Chloroplast RNA binding
PSB28	PSII reaction center
At4G02530	Chloroplast thylakoid lumen protein; unknown function

3.4.1 Expression of HP29b

For further characterization of HP29b, heterologous expression was performed in *E. coli* and *S. cerevisiae* (Figure 27). For expression in *E. coli* two different strains were used: BL21(DE3)pLysS and Rosetta™ 2(DE3)pLysS. HP29b was expressed with either a C- or N-terminal 6xHis-tag. Only the C-terminal His-tag expression in Rosetta™ 2(DE3)pLysS resulted in a western blot signal in the soluble fraction but not after Ni-NTA purification (Figure 27 A). In the membrane fraction, no anti-His western blot signal could be observed (data not shown). Therefore, the expression of the C-terminal His-tagged version of HP29b was repeated using *S. cerevisiae* strain INVSc1. No western blot signal could be detected in the soluble fraction. The preparation of the pellet resulted in a light smear in both, the HP29b expression sample and empty vector control sample (Figure 27 B).

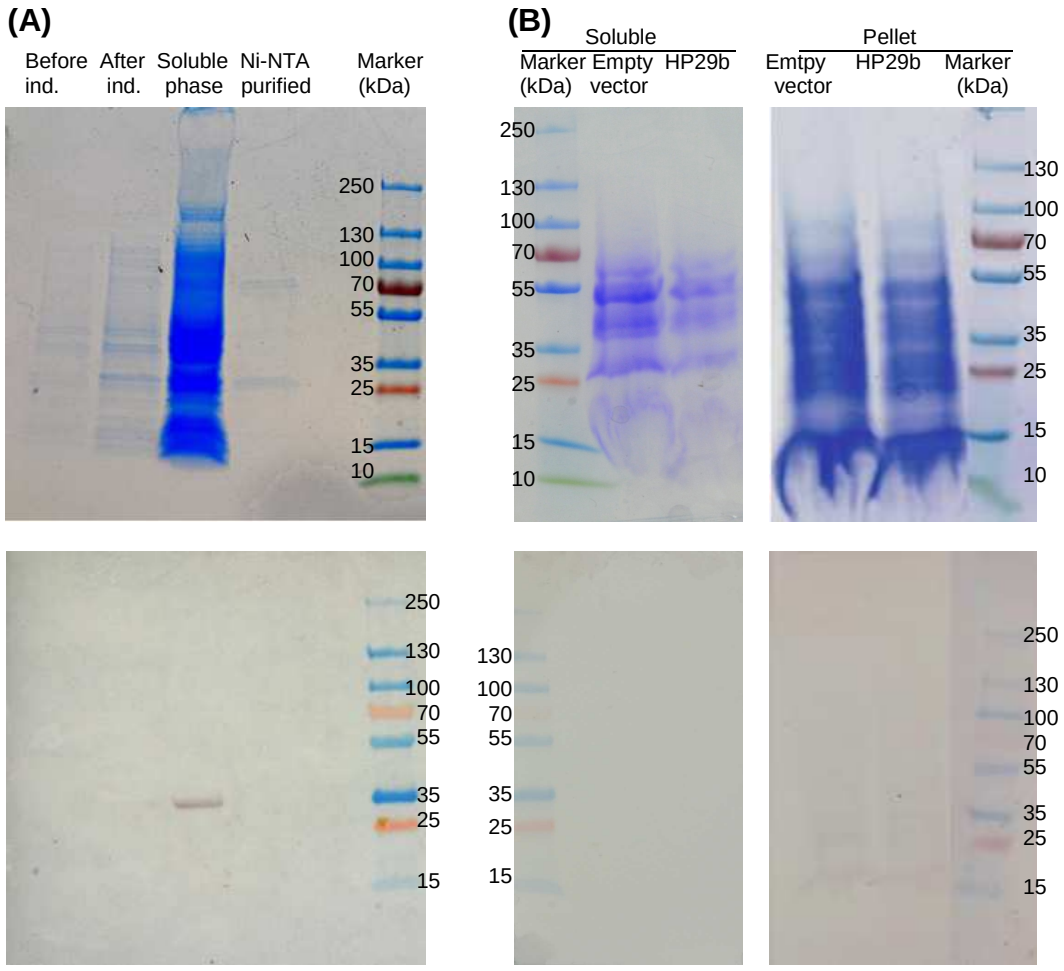

Figure 27: Heterologous expression of HP29b in *E. coli* and *S. cerevisiae*.
(A) Coomassie stained SDS-PAGE and anti-His western blot of C-terminal His-tagged HP29b expressed in *E. coli* Rosetta™ 2(DE3)pLysS cells. Samples were taken before and after induction, from the soluble phase after lysis and after Ni-NTA purification of the soluble fraction. (B) Coomassie stained SDS-PAGE and western blot of C-terminal His-tagged HP29b and empty vector control expressed in *S. cerevisiae* strain INVSc1. Samples were taken from soluble phase after lysis and from pellet.

3.4.2 Characterization of HP29b mutants

T-DNA insertion lines of HP29b were used for further experiments (SAIL_65_B07; SAIL_69_B02) together with their parental line (N8846) as the negative control. All lines have Col-3 background. Both mutant lines showed no phenotype under normal growth conditions (Figure 28).

Figure 28: Phenotype of N8846, SAIL_65_B07 and SAIL_69_B02 under normal growth conditions.
4 week old plants of N8846, SAIL_65_B07 and SAIL_69_B02. All plants were grown under long day conditions. No specific growth phenotype could be observed in both T-DNA insertion lines compared to the parental line.

Quantification of the transcript amount of *At3G61870* in the insertion lines compared to the parental line was done by qPCR analysis. Figure 29 B shows that expression of *At3G61870* was decreased to 51.9 % and 35 % in SAIL_65_B07 and SAIL_69_B02, respectively.

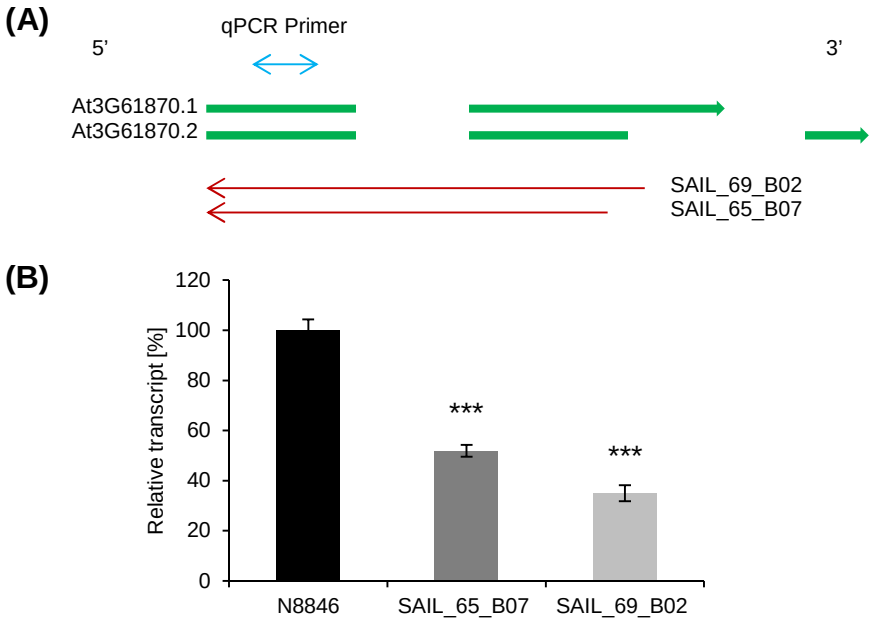

Figure 29: Relative gene expression of At3G61870 in T-DNA insertion lines.
(A) Both splicing variants of At3G61870 are shown (green). Disconnections of the arrows indicate introns. The red arrows demonstrate the T-DNA insertion site and direction of both mutants. The blue arrow marks the position of the transcript measured by qPCR. (B) Gene expression of *At3G61870* in 12 day old sterile grown plants of SAIL_65_B07, SAIL_69_B02 and N8846 was normalized to expression of S16 and Tubulin. Gene expression in the mutant is shown relative to expression in the parental line. Columns represent the mean values. Error bars indicate the standard deviation. Asterisks indicate significant differences compared to control samples of N8846 (Holm-Sidak-method, * P<0.05, ** P<0.01, *** P<0.001). (n=3)

To test whether HP29b was the candidate displaying the expected binding behavior in the protein preparations, soluble protein extracts were prepared from the parental line and both T-DNA insertion lines. It was expected that the marked protein band (Figure 26) would be present in the preparation of the parental line and absent in both mutants. All previous experiments were performed using *A. thaliana* Col-0 plants. Therefore, cGMP-pre-incubation experiments were repeated using the parental line of both mutants (N8846) (Figure 30 A). In Figure 30 B it is shown that in both mutant lines the indicated protein band was missing compared to the preparation of the parental line.

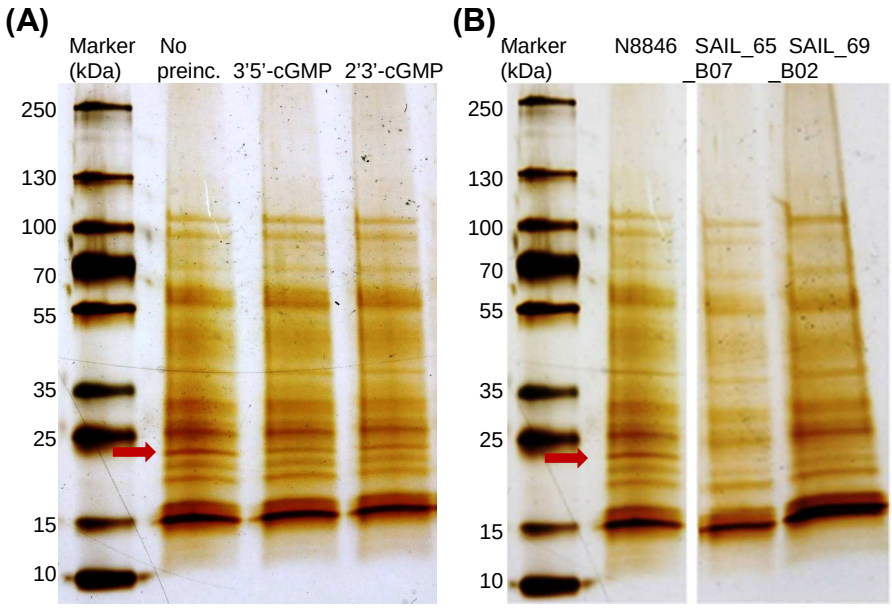

Figure 30: Elution profile of N8846, SAIL_65_B07 and SAIL_69_B02 from cGMP-agarose. Soluble protein extracts of N8846, SAIL_65_B07 and SAIL_69_B02 were prepared. (A) Elution profile of N8846 with no pre-incubation or pre-incubation with 100 µM 3'5'-/ or 2'3'-cGMP before incubation with the cGMP-agarose. (B) Elution profile of N8846, SAIL_65_B07 and SAIL_69_B02 without pre-incubation.

Determination of flavonol- and chlorophyll- content in mutant lines

HP29b was shown to be located in the chloroplast. Flavonoids are widely distributed in plant cell compartments including the chloroplasts (Agati et al., 2007). It was further shown that flavonoid contents increase in response to UV-B radiation and therefore protect the plant and its photosynthetic apparatus (Agati et al., 2011; Agati et al., 2007; J. Li et al., 1993). Moreover, increased chlorophyll contents have been observed in response to UV-B radiation (Jordan et al., 1998; Poulson et al., 2006). Consequently, the mutant lines were analyzed regarding their flavonol- and chlorophyll- contents in response to UV-B radiation. For the radiation experiments four week old plants were exposed to 0.4 W/m^2 of UV-B radiation for one week and flavonol- and chlorophyll- indices were measured daily. This experiment was performed twice.

Figure 31 A shows that under UV-B exposure the flavonol index increased in all three lines compared to control plants without UV exposure. No significant differences between the mutant lines and the parental line could be observed in the control plants. In contrast, with UV-B exposure significantly lower flavonol content was detected in both mutant lines compared to the parental line. In the mutant line SAIL_69_B02 this lower flavonol content was significant for all time points measured, whereas for the mutant line SAIL_65_B07 it became significant after 42 h and 56 h of UV exposure.

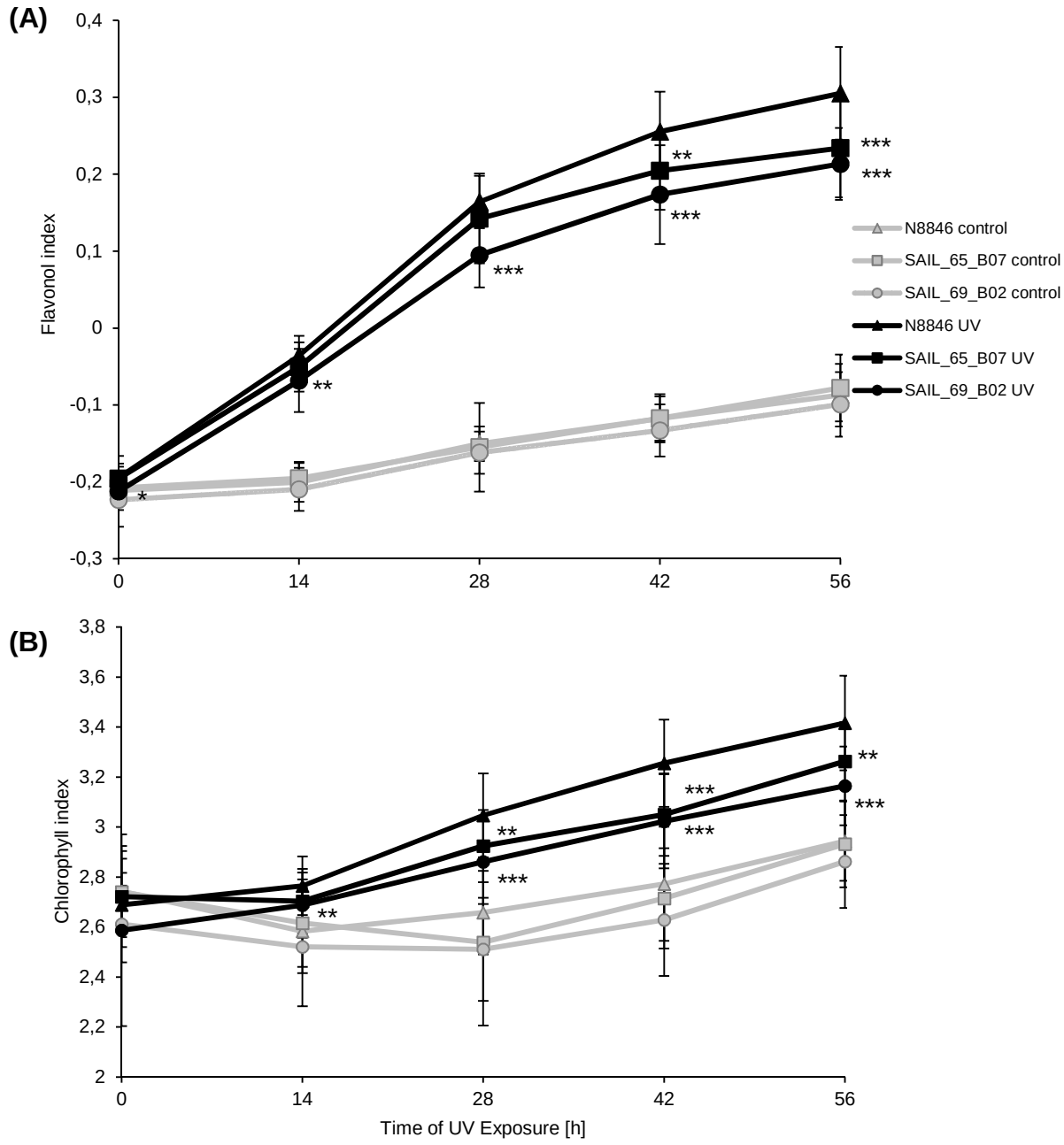

Figure 31: Flavonol- and chlorophyll-index in N8846, SAIL_65_B07 and SAIL_69_B02 after UV-exposure.
Four week old plants were exposed to 0.4 W/m² of UV-B radiation. Flavonol and chlorophyll contents were measured daily for one week. Control plants had same growth conditions without UV. Measurements were performed using the Multiplex®3.6 (Force A, Orsay, France). Flavonol index (A) and chlorophyll index (B) from two individual experiments are displayed. Error bars indicate the standard deviation. Error bars indicate the standard deviation. Asterisks indicate significant differences compared to the parental line N8846 (Holm-Sidak-method for normal distributed samples, Kruskal Wallis test in case of not normally distributed samples, * P<0.05, ** P<0.01, *** P<0.001). (n>15)

In case of chlorophyll measurements (Figure 31 B), plants exposed to UV-B radiation had higher chlorophyll contents compared to control plants in all lines. Without UV-B exposure, the plants of both mutant lines did not differ significantly compared to the parental line. In contrast, chlorophyll contents of both mutant lines were significantly lower compared to N8846 with UV-B exposure. In case of SAIL_69_B02 this lower chlorophyll content was significant after 14 h of UV-B exposure and in all following time points. For SAIL_65_B07 significantly lower chlorophyll content was detected after 28 h of UV-B exposure and in all following time points.

It was shown in previous publications that cGMP can induce an upregulation of genes involved in flavonoid biosynthesis (Durner et al., 1998; Pietrowska-Borek & Nuc, 2013; Suita et al., 2009). Further it was shown that cGMP can induce anthocyanin production in plants (Suita et al., 2009). The same was shown for the plant growth hormone class of cytokinins (Bhargava et al., 2013; Deikman & Hammer, 1995). To exclude that HP29b preferentially would bind cytokinins instead of cGMP another negative control was included in the CGBP pulldown. The protein extract was pre-incubated with trans-zeatin-riboside (Sigma Aldrich, Taufkirchen, Germany), a commercially available cytokinine. Figure 32 shows that 3'5'-cGMP but not trans-zeatin-riboside resulted in a decreased abundance of the marked protein band.

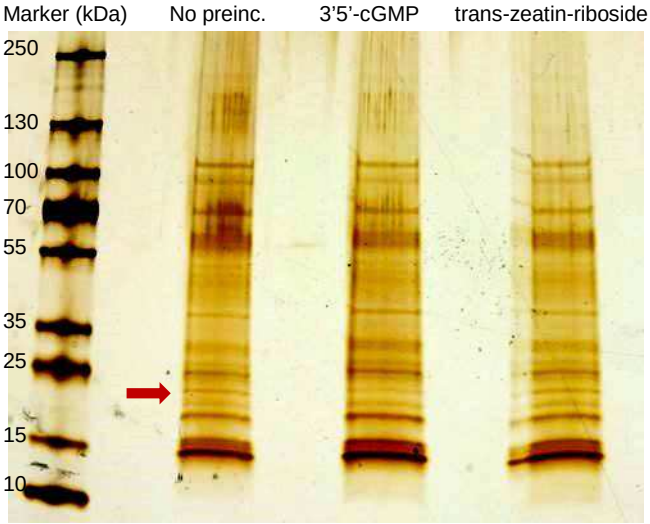

Figure 32: Elution profile of proteins bound to cGMP-agarose.
Soluble protein extracts from *A. thaliana* Col-0 plants were pre-incubated with either 100 µM of 3'5'-cGMP or trans-zeatin-riboside before incubation with the cGMP-agarose. Bound proteins were eluted and analyzed on a 4-15% 1D SDS PAGE followed by silver staining. The red arrow marks the protein band which is present in the negative controls but disappears with cGMP pre-incubation.

Determination of the efficiency of the PSII in mutant lines

To further investigate the role of HP29b, PSII efficiency measurements were performed using Pulse-Amplitude-Modulation (PAM) fluorometry. Parameters measured were the maximum

(F_v/F_m) and effective (Y(II)) photochemical quantum yield of PSII, quantum yield of light induced non photochemical fluorescence quenching (Y(NPQ)) and the relative electron transfer rate (ETR) (Figure 33). The different parameters were measured in five week old plants after 56 h of UV-B exposure over one week. The ETR was lower in both mutant lines compared to the parental line. However, this result was not significant. No differences were observed between the lines for all other parameters measured.

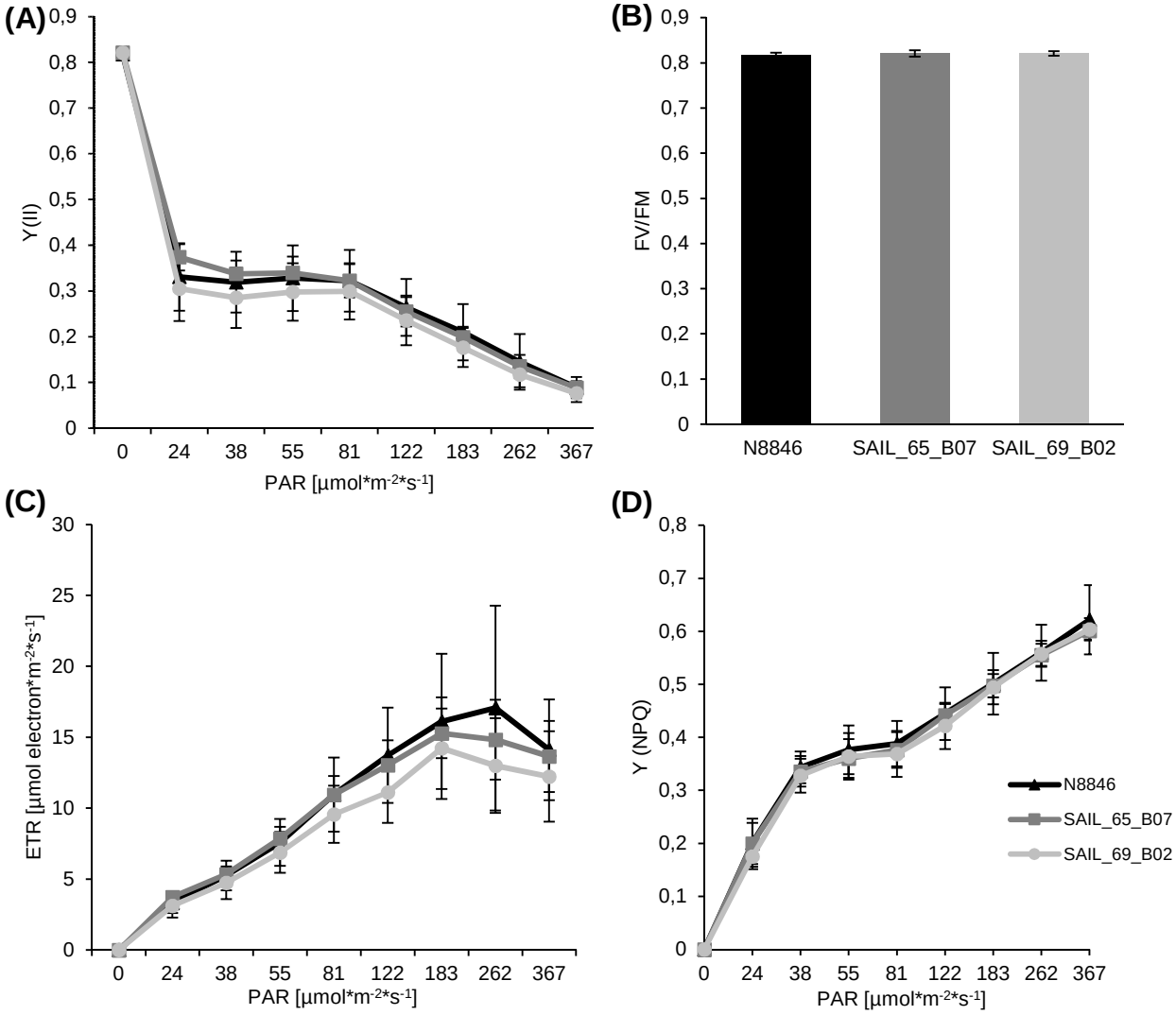

Figure 33: Efficiency of PSII measurements of N8846, SAIL_65_B07 and SAIL_69_B02.
Photosynthetic activity was measured in five week old dark-acclimated plants exposed to UV light. A light curve was applied giving a saturation pulse every 20 sec with increasing constant actinic light after each pulse. Parameters measured were the effective (A) and maximum (B) photochemical quantum yield of PSII, the relative electron transfer rate (C) and the quantum yield of light induced non photochemical fluorescence quenching (D). Columns represent the mean values. Error bars indicate the standard deviation. (n>8)

4 Discussion

The aim of this study was the investigation of cNMP signaling in plants and the identification of signaling components of the cGMP signaling cascade. To this end three experimental approaches were used:

1. Measurement of 3'5'- and 2'3'-cNMP levels in *A. thaliana* during HR and NO_2-induced cell death, as well as in response to treatment with the NO-donor SNP and the phytohormone IAA.

2. Identification of GCs by sequential fractionation of plant protein extracts.

3. Identification and characterization of target proteins of cGMP by affinity chromatography.

4.1 Measurement of cyclic nucleotides - potential role of 2'3'-cNMPs in signaling

Various stresses have been shown to increase cGMP levels in plants. In comparison, the number of reports on the regulation of cAMP, cCMP and cUMP levels is limited. In this thesis, cGMP, cAMP, cCMP and cUMP levels during HR and NO_2-induced cell death were investigated. Previous studies have shown that during cell death and HR reactions phenolic compounds are produced and these can be visualized by their green-blue auto-fluorescence under UV-light (Gray et al., 1997; Hahlbrock, 1989; Overmyer et al., 2005; J. M. Stone et al., 2000; Talamond et al., 2015). *pDEX:AvrRPM1-HA* mutant plants were treated with 30 µM DEX to induce HR. An intense green-blue fluorescence of phenolic compounds was detected 3 h after the treatment with an increase after 4 h suggesting a successful induction of HR (Figure 11). To induce cell death, *A. thaliana* Col-0 plants were fumigated with 30 ppm NO_2 for 1 h. In Figure 11 it is shown that directly after 1 h of fumigation an intense green-blue fluorescence was detected compared to the un-fumigated control plants, which indicates that cell death was induced. The fluorescence increased 1 h after fumigation. For both treatments, increased fluorescence of phenolic compounds was accompanied by an intense loss of turgor. These findings suggest that NO_2-induced cell death is similar to HR. However, the accumulation of phenolic compounds indicating cell death reactions was delayed in the DEX treated plants compared to the NO_2-fumigation experiment. Therefore, different

sampling time points were chosen for further experiments. Samples of treated *pDEX:AvrRPM1-HA* mutant plants were taken 4 h after treatment, whereas NO_2-fumigated plants were harvested directly after fumigation.

Using FT-ICR mass spectrometry, a significant upregulation of cAMP, cGMP and cUMP after DEX treatment of *pDEX:AvrRPM1-HA* mutant plants was observed, whereas only cAMP and cUMP levels are significantly increased after fumigation of Col-0 plants with NO_2. The detection method using a FT-ICR mass spectrometer is non-targeted and cNMPs were identified by their exact individual mass. However, it is not possible to distinguish between the 3'5'- and the 2'3'- positional isomers of the cNMPs.

HPLC–MS/MS was applied for measurements of the different cNMP-isomers after identification by their specific masses and retention times. In Figure 14, it is shown that for both treatments rather 2'3'-cNMP level were upregulated, but not 3'5'-cNMP levels. For 3'5'-cAMP no significant regulation was detected in response to both treatments used. In contrast, 2'3'-cAMP levels were about 12-fold and 29-fold increased after NO_2 fumigation or DEX treatment. A similar regulation was found for cGMP. 3'5'-cGMP was detected, but the levels were below LOQ, whereas 2'3'-cGMP levels showed a 2- and 7-fold increase after NO_2 fumigation or DEX treatment, respectively. These findings are consistent with the findings of Van Damme et al. (2014), who showed a significant upregulation of 2'3'-cAMP and -cGMP after cell death induction by wounding, but could not detect 3'5'-cAMP or -cGMP. Therefore it can be concluded that 3'5'-cAMP and -cGMP might not be part of a downstream signaling cascade in response to NO_2-induced cell death or HR.

Furthermore, in the present study levels of 2'3'-cNMPs are up to 60-fold higher compared to the 3'5'-isoforms. The same was found for 2'3'-cNMPs in diverse mice tissues, including heart, kidney and liver, showing an up to 5-fold higher 2'3'-cNMP content compared to the corresponding 3'5'-isomers (Burhenne et al., 2013). These results suggest that in case of NO_2-induced cell death and HR rather 2'3'-cNMPs but not 3'5'-cNMPs might play a dominant role. Different publications on 2'3'-cNMPs from the mammalian field proposed that 2'3'-cNMPs are acting as intracellular toxins derived from RNA degradation (Jackson, 2011; Jackson et al., 2009; Sokurenko et al., 2015). It was suggested that 2'3'-cAMP as well as 2'3'-cGMP play a role in apoptosis and necrosis by facilitating the opening of mitochondrial permeability transition pores (Jackson, 2011; Jackson et al., 2009; Sokurenko et al., 2015). From the present study it can be concluded that a similar mechanism is present in the plant system. Furthermore, 2'3'-cAMP was suggested to inhibit proliferation of vascular smooth muscle cells and glomerular mesangial cells in rat tissue (Jackson, 2011; Jackson et al., 2009). Considering the high concentrations of 2'3'-cNMPs compared to their 3'5'-isomers, it seems likely that these nucleotides are not just RNA degradation products, but might also play a role in plant signaling (Bähre & Kaever, 2014).

3’5’-cCMP was not detected in both treatments, leading to the conclusion that this particular cyclic nucleotide does not play a role in the investigated processes. In contrast, 2’3’-cCMP levels were above LOQ for both treatments, but showed an upregulation only after HR induction in the DEX treated plants. These findings support the presumption that 2’3’-cCMP has a distinct function in HR but does not play a role in NO_2-induced cell death.
In case of cUMP, the concentrations of the 3’5’- and the 2’3’-isomers were in the same range of about 2-6 fmol/ µg protein but showed a differential regulation. 3’5’-cUMP levels were decreased upon NO_2 fumigation as well as after DEX treatment. In comparison, 2’3’-cUMP levels increased after both treatments. Taken into account the suggested involvement of cUMP in cell death induction in mammals, these findings implicate that both isoforms indeed also play a role in the regulation of plant NO_2-induced cell death and HR (Beckert et al., 2014).
Taken together, a differential regulation of 2’3’-cNMPs in HR and NO_2-induced cell death was observed, whereas for 3’5’-cNMPs only cUMP showed a regulation upon NO_2 fumigation. However, for both treatments samples were taken at only one time point and UV-autofluorescence after 1 h of NO_2 fumigation already showed a considerably high level of cell death. Consequently, it cannot be excluded that 3’5’-cNMP regulation might occur in the earlier plant response. Therefore, additional time points for sample collection might give a better insight in cNMP signaling in HR and NO_2-induced cell death. Moreover, further investigation is necessary to confirm the second messenger function of 2’3’-cNMPs and to find target proteins and downstream components in the signaling cascade. Until now, the absence of commercially available cell permeable analogues of the different 2’3’- cyclic nucleotides is an essential obstacle hindering further progress in this field.

In addition to HR and NO_2-induced cell death, cNMP levels were monitored in response to stress and hormone treatment. Therefore the NO-donor SNP and the phytohormone IAA were used to treat 12 day old *A. thaliana* seedling. NO was shown to induce programmed cell death in *A. thaliana* suspension cultures and defense gene expression in tobacco (*Nicotiana tabacum*) leaves, both processes mediated by cGMP (Clarke et al., 2000; Durner et al., 1998). Increased levels of cGMP were observed in response to NO treatment measured in tobacco leaves and suspension cultures using a radioimmunoassay (Durner et al., 1998). In this thesis no significant regulation of 3’5’-cAMP in response to treatment with the NO-donor SNP was observed and 3’5’-cGMP, -cCMP and -cUMP could not be detected. Considering that at least basal 3’5’-cGMP and -cUMP levels were measured above LOD in leafs of four week old Col-0 plants, it can be concluded that cNMP signaling might be dependent on the age, cultivation method or the tissue of the plant. In comparison to the 3’5’-cNMPs, 2’3’- cAMP, -cCMP and -cGMP showed an upregulation 3 h after treatment.

This observation suggests that 2'3'-cNMPs could be signaling components not only in HR and NO_2-induced cell death but also in stress signaling in plants. Since different plant material and detection methods were used, these results might not be directly comparable to previous studies. However, further investigation comparing the different experimental results would probably contribute to the understanding of cGMP mediated NO-induced signaling in plants.

Another treatment used in this study was IAA. The phytohormone was shown to be involved in diverse biological processes, such as modulation of root and shoot architecture, growth regulation, or gravitropic responses (Nan et al., 2014; Woodward & Bartel, 2005). It was demonstrated that application of low concentrations, down to 100 nM led to an increase in cGMP levels, suggesting a role for cGMP in hormone related signaling apart from stress, NO_2-induced cell death and HR (Isner et al., 2012; Nan et al., 2014). CGMP concentrations were measured in roots and protoplasts. In roots, cGMP levels were determined using an enzyme immunoassay (Nan et al., 2014). Protoplasts were transformed with the fluorescent cGMP reporter δ-FlincG and cGMP levels were determined by fluorescence increase (Isner & Maathuis, 2011; Isner et al., 2012). In the present study treatment with IAA resulted in the upregulation of 2'3'-cCMP, whereas all other nucleotides show no significant changes. This result seems to be inconsistent with previous findings showing an upregulation of 3'5'-cGMP in response to IAA. However, in comparison to previous studies whole seedlings were used instead of protoplasts or only roots. Considering that cGMP might act locally and low concentrations were measured for example in roots (1.5 – 3.5 fmol/ mg fresh weight), it is likely that measurements using whole seedlings led to a dilution of cGMP resulting in levels below LOD (Nan et al., 2014).

To further investigate the role of cGMP in IAA and NO mediated signaling, different plant compartments should be analyzed separately and the extraction could be improved by the use of more plant material, leading to a cGMP signal above LOQ. Taken together cNMP level analysis, it can be concluded that the different cyclic nucleotides have distinct roles in stress- as well as hormone related signal transduction processes.

4.2 Detection of GC enzyme activity in *H. vulgare* and *A. thaliana*

So far, 3'5'-cGMP is one of the most studied cNMPs in plant, but the key components of the signaling cascade remain to be identified. Although it was demonstrated that 3'5'-cGMP levels seem to be tightly regulated in terms of production and degradation, little is known about the corresponding enzymes, the GCs and PDEs (Dubovskaya et al., 2011). Bioinformatics approaches suggested several GC candidates using a partially variable

14 amino acid search motif (Kwezi et al., 2007; Meier et al., 2010; Mulaudzi et al., 2011; Qi et al., 2010). However, these candidates still remain controversial because of their comparably low or irreproducible activities (Ashton, 2011; Bojar et al., 2014). Therefore another aim of this thesis was the biochemical purification of plant GCs from soluble plant extracts.

Prior to the purification of plant GCs, an assay was established to measure GC activity in plant protein extracts by monitoring cGMP formation over time. In Figure 16 it is shown that in total soluble protein extracts derived from root and vegetative tissue of soil grown *H. vulgare* as well as *A. thaliana* plants a stable linear cGMP formation was observed over time. Mammalian PDE5A1, specific for cGMP degradation, was included in the assay, showing a degradation of the measured signal down to background levels. Therefore it can be concluded that the measured signal represents the formation of cGMP and is not the result of a non-specific cross reaction with the immunoassay kit. However, this result was not reproducible using protein extracts from sterile grown plant material. Furthermore, total protein extract from only leaf material of soil grown *H. vulgare* and *A. thaliana* plants showed no cGMP formation in soluble protein extracts. These findings led to the conclusion that the observed cGMP formation in protein extracts from soil grown plants might have been the result of a contamination with proteins from rhizosphere organisms.

To test if the measured cGMP formation was the result of a contamination, roots from soil grown plants were incubated in LB media and rhizosphere organisms were cultured and analyzed for GC activity in protein extracts. In Figure 18 it is shown that cGMP formation does occur in this preparation in the same range as it was detected in soil grown plant preparations. This result suggested that the cGMP formation in soluble plant protein extracts was the result of a contamination with rhizosphere organisms. This assumption is supported by the fact that in another preparation comparing the cGMP formation in rinsed and unrinsed *H. vulgare* plants it was demonstrated that a significantly higher cGMP level was observed in protein extracts from unrinsed plants after 1 h (Figure 19). One common rhizosphere organism which was previously shown to produce exogenous cGMP during cyst formation is *A. brasilense* (Marden et al., 2011). This experiment was successfully repeated in the present study detecting an increasing signal using the immunoassay kit. However, this signal was not degradable with addition of a PDE, suggesting the measured signal was not the result of a cGMP formation but rather an unknown compound produced by *A. brasilense* cross reacting with the immunoassay kit.

One compound having a similar structure to cGMP is c-di-GMP, a canonical bacterial second messenger (Romling et al., 2013; Russell et al., 2013). The kit was tested for cross reactivity with c-di-GMP. It could be demonstrated that c-di-GMP is detected by the kit but results in a signal 1000 times lower than spiked. Still, this cross reactivity might be generally crucial for cGMP measurements in bacteria since intracellular concentrations of c-di-GMP have been

measured in the high nano- or low micro-molar range (Paul et al., 2004; Romling et al., 2013; Simm et al., 2004; Weinhouse et al., 1997). The measured cGMP concentration in the present study of about 2 nM after 6 days of incubation could therefore be the result of a concentration of 2 µM c-di-GMP. However, in this study exogenous cGMP was measured in the growth media and known c-di-GMP levels are estimated as intracellular concentrations. One way to identify the compound causing a cross reactivity with the immune kit could be the analysis of the growth medium via HPLC. Another cross reactivity with 3'5'-cGMP immunoassay kits was shown for 2'3'-cGMP (Sokurenko et al., 2015). In this study 2'3'-cGMP formation resulting from an enzymatic reaction was measured using a 3'5'-cGMP immunoassay kit. The concentrations measured were in the low µM- range.

Since in sterile grown plants no cGMP formation could be detected, it was assumed that potential GCs in the extract might be highly diluted with other plant proteins resulting in a cGMP formation below the detection limit of the immunoassay kit. Therefore, plants were treated with SNP and IAA since previous studies demonstrated increased GC activity upon these treatments (Dubovskaya et al., 2011; Nan et al., 2014). Additionally, plants were treated with the phytohormone ABA, which was shown to induce cGMP production in plants (Dubovskaya et al., 2011). However, inconsistent to these studies none of the treatments resulted in a detectable cGMP formation.

For the purification of GCs in plants the immunoassay kit was not suitable to detect cGMP formation from plant protein extracts. The measurement of cGMP from soluble protein extracts using an enzyme immunoassay was performed in a previous study showing a cGMP content of 5 fmol/ µg protein after 10 minutes of incubation (Dubovskaya et al., 2011). However, no negative controls were performed in this study, e.g. no substrate control or addition of a PDE. Furthermore, compared to the present study the measured cGMP concentration would be in the range of the measured background signal. Other studies measured GC activity from plant protein expressed in *E. coli* using an immunoassay (Mulaudzi et al., 2011; Qi et al., 2010; Szmidt-Jaworska et al., 2009). In these cases, cGMP producing enzymes are highly concentrated resulting in a higher cGMP level compared to a soluble protein extract from whole seedlings used in the present study. Consequently, one explanation that no cGMP formation could be detected in the present study could be a high grade of dilution of the protein extract with other plant proteins. This dilution then resulted in a cGMP formation which was below the detection limit of the immunoassay.

To overcome the described problems, highly sensitive HPLC-MS/MS based method to detect cGMP formation could be applied. Moreover, protein extraction could be performed from different plant tissue since cGMP was shown to functions in local tissue, for example in roots and guard cells (Maathuis, 2006; Maathuis & Sanders, 2001; Pagnussat et al., 2003; Wang et al., 2013). Additionally, cGMP formation might be detected in membrane fractions, since

several pGCs have been proposed to be present in plants (Kwezi et al., 2007; Kwezi et al., 2011; Meier et al., 2010). Taken together these findings, cGMP measurements using enzyme immunoassay kits should be analyzed with care and PDE controls are crucial for the unambiguous confirmation that cGMP is the compound causing a signal in the assay.

4.3 Identification of cGMP binding proteins

Another aim of this study was the identification of cGMP binding proteins using an affinity purification approach. Therefore, soluble protein extracts from *A. thaliana* were incubated with cGMP immobilized on agarose and the bound proteins were analyzed. Several proteins tightly bound to the cGMP agarose were identified (Table 24). GO-term analysis revealed that the majority of these proteins are known to bind different nucleotides, suggesting that the pull down assay was successfully established. However, none of these candidates were shown to specifically bind cGMP.

Another critical point was the identification of non-specific interactions of proteins with the agarose. It is likely that many bound proteins might bind non-specific to the matrix or to the linker between cGMP and the agarose (Hanke et al., 2011). Furthermore, proteins can interact with only a part of the bound cGMP, e.g. the cyclic phosphate or the guanine. To decipher non-specific interactions from specific ones, pre-incubation of the soluble protein extracts with different nucleotides were performed before the extracts were incubated with the agarose. The pre-incubation with 3’5’- and 2’3’-cGMP was performed to occupy the binding site of CGBPs and therefore prevent binding of these proteins to the cGMP-agarose (Figure 23). Using this approach, one protein band appeared less intense in the pre-incubated samples compared to the samples with no pre-incubation. This finding suggests that the protein causing the observed pattern in the different samples is a potential cGMP binding candidate. Analysis of this protein band resulted in the identification of 11 proteins. Furthermore, candidates from the whole elution fractions were analyzed and compared with the candidates from the gel cut analysis. This approach identified one candidate (At3G61870) showing a lower binding affinity in cGMP-pre-incubated samples compared to non-pre-incubated samples and being present in the analyzed gel cuts. This result gives strong evidence that At3G61870 is indeed a CGBP and is the candidate causing the observed protein pattern. Additionally, 32 further candidates have been identified showing the expected affinity pattern in the soluble fractions (Figure 25).

To exclude the possibility of a non-specific binding of the identified proteins, further pre-incubation experiments were performed using nucleotides which show structural similarities to cGMP. These nucleotides included 3’5’-cAMP, GTP, GDP, GMP and ATP (Figure 26).

In total, five prominent candidates were identified showing a lower affinity to the cGMP-agarose after cGMP-pre-incubation compared to all other pre-incubated and the non-pre-incubated samples (Table 25). The most prominent candidate in the previous experiments, At3G61870, was also confirmed to have a specific cGMP binding preference. In Table 27 the identified CGBP candidates and their functional GO terms are shown. Considering that these proteins were shown to bind cGMP, it seems likely that cGMP is involved in the indicated processes. Some of these processes have already been described to be affected by cGMP. For example, in mammals cGMP can activate PKGs leading to phosphorylation of target proteins. In plants, cGMP has been shown to be involved in protein phosphorylation processes (Isner et al., 2012; Ordoñez et al., 2014). The general regulatory factor 3 is a 14-3-3 protein. These proteins have been shown to play a key role in signal transduction processes and were shown to interact with kinases (Pfam domain: PF00244). Since no PKG has been clearly identified in plants so far it seems likely that compared to the mammalian system other proteins, such as the general regulatory factor 3, are participating in the signal transduction process. Another explanation for the appearance of this protein as a cGMP binding candidate in this assay would be that it was co-purified, meaning that it was bound to a cGMP-binding protein.

Another GO-term from the ankyrin repeat-containing protein 2 is the involvement in defense responses to bacteria. Increased cGMP concentrations have been observed in response to treatment of *A. thaliana* with virulent and avirulent *Pseudomonas syringae* (Meier et al., 2009). Further experiments are crucial to understand the connection between cGMP increase in response to bacteria and the role of ankyrin repeat-containing protein 2.

The most abundant candidate on the cGMP-agarose, showing the highest fold changes in cGMP pre-incubated samples compared to all negative controls was HP29b (At3G61870), a chloroplast protein with unknown function. Therefore this candidate was chosen for further investigation.

Table 27: CGBP candidates from cGMP-agarose pull down.

Description	GO-term
HP29b	Unknown function
alpha-soluble nsf attachment protein 2	Intracellular protein transport
nai2, tsk-associating protein 1-like protein	Endoplasmic reticulum body organization
general regulatory factor 3	Protein phosphorylated amino acid binding

ankyrin repeat-containing protein 2	Defense response to bacteria, post-embryonic development, protein folding, protein targeting to chloroplast

4.4 Characterization of HP29b

To further investigate the binding affinity of HP29b and to analyze its crystal structure, heterologous expression was performed in *E. coli* and *S. cerevisiae*. However, in both systems expression failed (Figure 27). HP29b was shown to be a membrane protein located in the inner envelope of chloroplasts (Ferro et al., 2002; Firlej-Kwoka, 2008). Bioinformatics sequence analysis revealed four transmembrane domains in this protein. It was shown that the expression of eukaryotic membrane proteins in a prokaryotic system is sometimes problematic, mostly because of the differences in membrane composition, protein folding and posttranslational modifications between the eukaryotic and the prokaryotic system (Bernaudat et al., 2011; Blum et al., 2000; Freigassner et al., 2009; Opekarova & Tanner, 2003).

Another problem is the comparably fast expression of proteins in prokaryotes leading to exposure of hydrophobic segments, protein aggregation and formation of inclusion bodies (Bernaudat et al., 2011; Freigassner et al., 2009; Miroux & Walker, 1996). To overcome these problems, a weaker promotor could be used or growth conditions can be modified, e.g. lowering growth temperature (Freigassner et al., 2009; Quick & Wright, 2002; Wagner et al., 2008). In the present study, two different *E. coli* expression strains were used to express the protein with either an N- or C-terminal His-tag. Furthermore, different growth conditions and IPTG concentrations for the induction of expression were tested. However, none of these attempts resulted in a sufficient protein expression.

Another system for heterologous protein expression is yeast. This eukaryote is capable of protein processing similar to higher eukaryotes, including posttranslational modifications (Freigassner et al., 2009). However, the lipid compositions of yeast membranes is still different compared to higher eukaryotes and therefore might affect protein expression and function (Freigassner et al., 2009). Considering the different membrane composition, it seems likely that in the present study protein expression in *S. cerevisiae* failed. For further investigation the expression of HP29b might be performed in a plant system, such as transient protein expression in *A. thaliana* or tobacco leaves. In these systems all components important for plant membrane protein expression, such as proper folding as well as protein targeting and transport, are available.

Further investigation of HP29b was performed using two different mutant lines and their parental line as a negative control. Gene expression analysis was performed and a decreased expression in both mutants was observed. Both mutant lines were used in another pulldown experiment with cGMP-agarose. It was expected that the protein band which showed the previously discussed lower binding capacity after cGMP-pre-incubation is missing in the protein preparation of the mutant lines compared to the parental line. Figure 30 B shows that expected binding pattern was confirmed.

4.4.1 The role of HP29b in flavonoid-biosynthesis

Flavonoids are secondary metabolites derived from the phenylpropanoid pathway (Figure 34). They have been shown to be involved in plant protection processes, e.g. UV-B absorption, scavenging of reactive oxygen species (ROS), as well as protection from pathogen and herbivore attacks (Agati et al., 2011; Ferreyra et al., 2012; Ryan et al., 2002; B. Winkel-Shirley, 2002). Moreover, flavonoids are important for flower coloration and therefore act as attractors of pollinators (Ferreyra et al., 2012; Mol et al., 1998). Additionally it was shown that flavonoids are involved in the induction of root nodulation in response to symbiosis with nitrogen fixing bacteria (Wasson et al., 2006; Zhang et al., 2009).

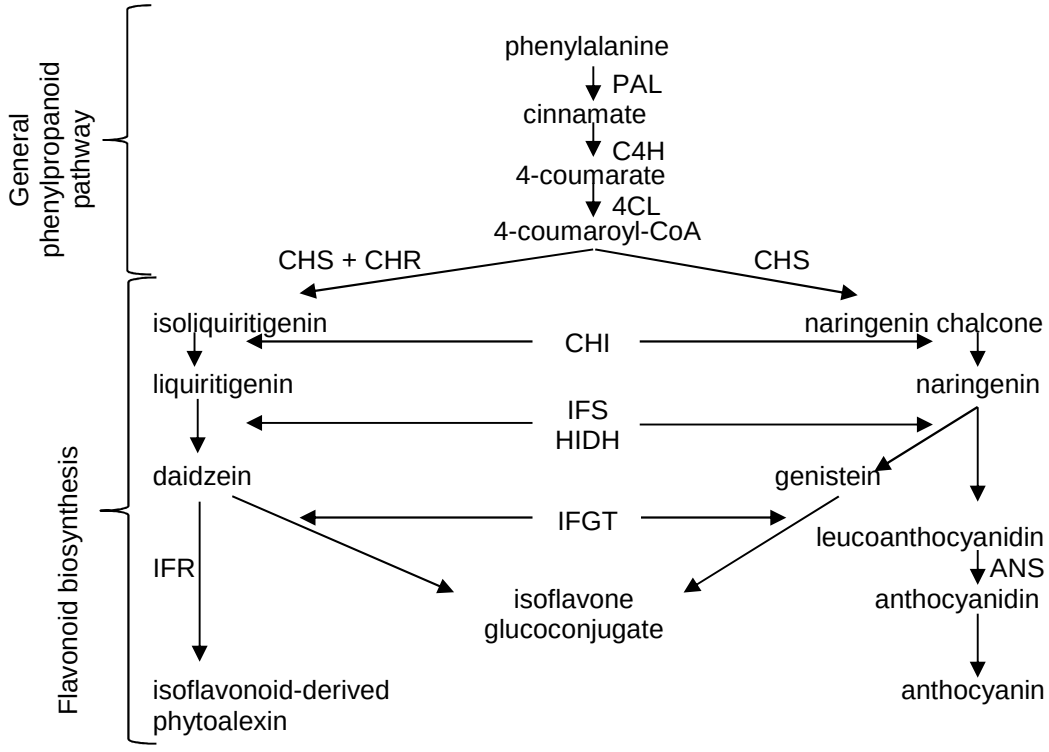

Figure 34: The flavonoid biosynthetic pathway.
The phenylpropanoid pathway and the flavonoid biosynthetic pathway are illustrated. PAL, phenylammonia-lyase; C4H, cinnamic acid 4-hydrolase; 4CL, 4-coumarate:CoA ligase; CHS, chalcone synthase; CHR, chalcone reductase; CHI, chalcone isomerase; IFS, 2-Hydroxyisoflavanone synthase; HIDH, 2-Hydroxyisoflavanone dehydratase; IFGT, UDP-glucose:isoflavone 7-O-glucosyltransferase; IFR, Isoflavone reductase; ANS, Anthocyanidin synthase. Figure modified after Suita et al. (2009).

In the flavonoid biosynthetic pathway phenylalanine is transformed into 4-coumaroyl-CoA. Upon activation, the chalcone synthase then produces chalcone scaffolds from which all flavonoids derive (Ferreyra et al., 2012). Different biotic and abiotic stresses have been shown to activate the phenylpropanoid pathway and lead to increased flavonoid levels in order to protect the plant, including wounding, viral-, fungal- and bacterial infection, as well as UV-B-radiation, heavy metal and nutrient stress and low temperatures (Dixon & Paiva, 1995; Ferrer et al., 2008; Ferreyra et al., 2012; Moura et al., 2010; Pietrowska-Borek & Nuc, 2013; Posmyk et al., 2009; Brenda Winkel-Shirley, 2001).

In addition to environmental stresses, the second messenger cGMP was shown to directly activate the transcription of almost all genes involved in the phenylpropanoid pathway, including phenylammonia-lyase (PAL), 4-coumarate:CoA ligase (4CL) and the chalcone synthase (CHS) (Bowler et al., 1994; Durner et al., 1998; Pietrowska-Borek & Nuc, 2013; Suita et al., 2009). Further, it was demonstrated, that cGMP treatment results in the accumulation of cinnamic acid in tobacco- and anthocyanins in soybean cell culture (Durner et al., 1998; Suita et al., 2009). Although it was demonstrated that cGMP is involved in the phenylpropanoid- and flavonoid- biosynthesis, the exact role of cGMP in this pathways needs to be investigated.

Because of the described role of cGMP in flavonoid biosynthesis, the two transgenic lines of HP29b, a cGMP binding protein, were analyzed regarding their flavonol- content in response to UV-B-radiation. No obvious phenotype in both mutant lines was observed under non-stress conditions relative to the parental line (Figure 28). Interestingly upon moderate UV-B exposure, the increase of the flavonol content was partially impaired in both mutant lines (Figure 31 A). Therefore, it can be concluded that HP29b is involved in UV-B induced cGMP dependent signal transduction leading to the activation of the flavonoid biosynthetic pathway. To further investigate the role of HP29b in flavonol biosynthesis, gene expression analysis of genes involved in the phenylpropanoid pathway could be applied comparing parental line and mutant lines of HP29b in response to cGMP treatment.

It was previously shown that not only cGMP but also cytokinins are able to induce the expression of genes involved in flavonoid biosynthesis and induce anthocyanin production (Bhargava et al., 2013; Deikman & Hammer, 1995). To exclude that HP29b preferentially would bind cytokinins instead of cGMP, the cGMP-agarose pulldown was repeated pre-incubating the protein extracts of Col-0 with a commercially available cytokinin (trans-zeatin-riboside). In Figure 32 it is shown that 3’5’-cGMP but not cytokinin pre-incubation led to a decrease in the binding affinity of HP29b to the cGMP-agarose. This result supports the assumption that HP29b has a specific binding affinity for cGMP.

4.4.2 The role of HP29b in chlorophyll-biosynthesis

It was previously shown that cGMP plays a role in photosynthesis as well as phytochrome mediated phototransduction processes. In photosynthesis, light is absorbed by light-harvesting complexes of the photosystem II (PSII), which are proteins including chlorophyll a and b molecules. The resulting energy is used to split H_2O into O_2, protons and electrons. The protons are transferred from the stroma to the thylakoid lumen which leads to the formation of a proton gradient used by the ATP-synthase to synthesize ATP from adenosine-diphosphate (ADP) and phosphate (Pi). The electrons are transferred via the electron transport chain, first to the cytochrome-b6f-complex and second to the photosystem I (PSI) where they are used in the reduction process of NADP to NADPH. The energy from ATP and NADPH is then used in the calvin cycle to convert CO_2 into sugars (Lambers et al., 2008). It was demonstrated that upon treatment with cell-permeable cGMP analogues, the transcript of two genes of the PSII are upregulated (Herrera, 2012). Furthermore, it is suggested that cGMP together with Ca^{2+} is involved in the expression of the PS I as well as the cytochrome-b6f-complex upon activation of phytochrome signaling (Figure 35) (Bowler et al., 1994; Chory, 1994). Additionally, chlorophyll contents have been shown to increase in response to UV-B radiation (Jordan et al., 1998; Poulson et al., 2006).

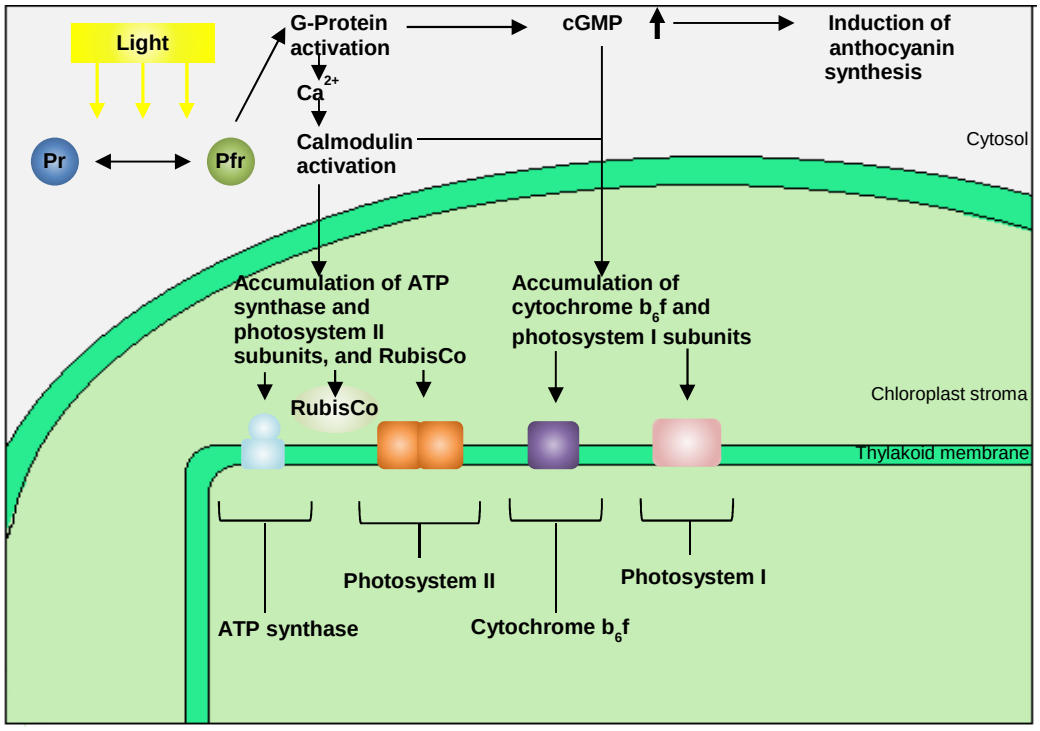

Figure 35: phytochrome-A mediated signal-transduction pathways.
Light induces the transformation of phytochrome from its inactive form (Pr) to its active form (Pfr) leading to the activation of G-proteins. G-proteins stimulate chloroplast development by elevation of cGMP and Ca^{2+} levels resulting in the accumulation of the cytochrome-b6f-complex and Photosystem I. Figure modified after Chory (1994).

The analysis of potential interaction partners of HP29b revealed ten candidate proteins (Table 26). All of these proteins are located in the chloroplast and the majority of them were shown to function in photosynthetic processes. Based on these interactions and the known function of cGMP in photosynthesis and phytochrome mediated phototransduction processes, chlorophyll contents of the mutant lines and the parental line were investigated in response to UV-B radiation (Figure 31 B). It was shown that the chlorophyll content increased in all lines in response to UV-B radiation compared to control plants. This result is consistent with previous studies applying ambient UV-B radiation (Boeger & Poulson, 2006; Jordan et al., 1998; Poulson et al., 2006). Interestingly, the chlorophyll content of both mutant lines was significantly lower compared to the parental line after UV-B exposure, suggesting a putative function of HP29b in phytochrome mediated phototransduction or chlorophyll biosynthesis. Although the exact function remains unclear, it is known that HP29b is a chloroplast protein located in the inner envelope (Ferro et al., 2002; Firlej-Kwoka, 2008). Presuming that HP29b might be part of the phytochrome signal transduction process by binding cGMP, a knock down of this protein could likely result in an impaired signal transduction, resulting in a decreased chlorophyll content or in incomplete chloroplast development and function (Figure 35). However, to confirm this hypothesis further experiments need to be performed.

4.5 Outlook

In this study it was found that 2‘3‘-cNMPs are highly upregulated in response to the induction of HR and NO_2-induced cell death as well as in response to NO and IAA, indicating an important role for 2’3’-cNMPs in these processes. Previous studies on 3’5’-cNMPs in plants have studied the *in vivo* effects of these cyclic nucleotides using readily available cell permeable analogous (Dubovskaya et al., 2011; Jiang et al., 2005; Maathuis, 2006; Pietrowska-Borek & Nuc, 2013). Unfortunately, for 2’3’-cNMPs cell permeable analogous do not exist to date. Only the development of such would allow phenotypic studies correlating the increased *in vivo* concentrations with the discussed signaling pathways. Additionally, the development of 2’3’-cNMP-agaroses would possibly allow the identification of potential downstream targets of these nucleotides.

The biochemical purification of potential GCs failed due to non-detectable GC activity in *A. thaliana* and *H. vulgare*. A possible reason for that are the low activities of GCs in plants resulting in cGMP formation outside the detection limit of the immunoassay. Therefore, other

methods, for example HPLC-MS/MS should be applied to measure 3’5’-cGMP. This highly sensitive method would improve the detection and therefore open the possibility to biochemically purify potential GCs from plant protein extract by tracking GC activity. Additionally, cGMP formation might be detected in membrane fractions, since several pGCs have been proposed to be present in plants (Irving et al., 2012). Furthermore, additional methods and compounds could be applied to investigate the activation process of GCs in plants.

To further address 3’5’-cGMP signaling in plants, PDE-resistant cGMP-agarose was used to identify potential cGMP binding candidates. An assay was successfully established and several candidates were identified. However, the heterologous expression in *E. coli* and *S. cerevisiae* of the most prominent one, HP29b, failed. To further investigate the function of this protein, to analyze the binding affinity to cGMP and to access possible cGMP dependent activity, expression should be performed in a natural environment of this protein using a plant expression system. Phenotypic mutant analysis revealed a potential function for HP29b in flavonol biosynthetic processes. It was shown that upon treatment with cGMP, the expression of genes involved in flavonoid biosynthesis was induced (Durner et al., 1998; Pietrowska-Borek & Nuc, 2013; Suita et al., 2009). To further investigate the role of HP29b in this process, gene expression analysis of these genes could be performed comparing parental line and mutant lines of HP29b upon treatment with cGMP. Flavonoids have been shown to be produced in response to various different stresses, including wounding, viral-, fungal- and bacterial infection, as well as nutrient stress and low temperatures (Dixon & Paiva, 1995). Therefore, different stress treatments should be performed followed by phenotypic analysis of the mutant plants to further investigate the potential role of HP29b in these processes.

5 Literature

Abel, S., Nürnberger, T., Ahnert, V., Krauss, G., & Glund. (2000). Induction of an extracellular cyclic nucleotide phosphodiesterase as an accessory ribonucleolytic activity during phosphate starvation of cultured tomato cells. *Plant Physiology, 122*(2), 543-552.

Agati, G., Biricolti, S., Guidi, L., Ferrini, F., Fini, A., & Tattini, M. (2011). The biosynthesis of flavonoids is enhanced similarly by UV radiation and root zone salinity in L. vulgare leaves. *Journal of Plant Physiology, 168*(3), 204-212. doi:10.1016/j.jplph.2010.07.016

Agati, G., Matteini, P., Goti, A., & Tattini, M. (2007). Chloroplast-located flavonoids can scavenge singlet oxygen. *New Phytol, 174*(1), 77-89. doi:10.1111/j.1469-8137.2007.01986.x

Akimoto, M., Zhang, Z., Boulton, S., Selvaratnam, R., VanSchouwen, B., Gloyd, M., . . . Melacini, G. (2014). A mechanism for the auto-inhibition of hyperpolarization-activated cyclic nucleotide-gated (HCN) channel opening and its relief by cAMP. *Journal of Biological Chemistry, 289*(32), 22205-22220.

Anderson, J. A., Huprikar, S. S., Kochian, L. V., Lucas, W. J., & Gaber, R. F. (1992). Functional expression of a probable Arabidopsis thaliana potassium channel in Saccharomyces cerevisiae. *Proceedings of the National Academy of Sciences, 89*(9), 3736-3740.

Apel, K., & Hirt, H. (2004). Reactive oxygen species: metabolism, oxidative stress, and signal transduction. *Annu. Rev. Plant Biol., 55*, 373-399.

Ashton, A. R. (2011). Guanylyl cyclase activity in plants? *Proc Natl Acad Sci U S A, 108*(19), E96; author reply E97-98. doi:10.1073/pnas.1101007108

Astier, J., & Lindermayr, C. (2012). Nitric oxide-dependent posttranslational modification in plants: an update. *Int J Mol Sci, 13*(11), 15193-15208. doi:10.3390/ijms131115193

Bähre, H., Danker, K. Y., Stasch, J.-P., Kaever, V., & Seifert, R. (2014). Nucleotidyl cyclase activity of soluble guanylyl cyclase in intact cells. *Biochemical and biophysical research communications, 443*(4), 1195-1199.

Bähre, H., & Kaever, V. (2014). Measurement of 2',3'-cyclic nucleotides by liquid chromatography-tandem mass spectrometry in cells. *J Chromatogr B Analyt Technol Biomed Life Sci, 964*, 208-211. doi:10.1016/j.jchromb.2014.02.046

Bastian, R., Dawe, A., Meier, S., Ludidi, N., Bajic, V. B., & Gehring, C. (2010). Gibberellic acid and cGMP-dependent transcriptional regulation in Arabidopsis thaliana. *Plant Signaling & Behavior, 5*(3), 224-232.

Beavo, J. A., & Brunton, L. L. (2002). Cyclic nucleotide research -- still expanding after half a century. *Nat Rev Mol Cell Biol, 3*(9), 710-718. doi:10.1038/nrm911

Beavo, J. A., Hardman, J. G., & Sutherland, E. W. (1970). Hydrolysis of cyclic guanosine and adenosine 3',5'-monophosphates by rat and bovine tissues. *J Biol Chem, 245*(21), 5649-5655.

Beckert, U., Grundmann, M., Wolter, S., Schwede, F., Rehmann, H., Kaever, V., . . . Seifert, R. (2014). cNMP-AMs mimic and dissect bacterial nucleotidyl cyclase toxin effects. *Biochemical and biophysical research communications, 451*(4), 497-502.

Ben Ghozlen, N., Cerovic, Z. G., Germain, C., Toutain, S., & Latouche, G. (2010). Non-destructive optical monitoring of grape maturation by proximal sensing. *Sensors (Basel), 10*(11), 10040-10068. doi:10.3390/s101110040

Bernaudat, F., Frelet-Barrand, A., Pochon, N., Dementin, S., Hivin, P., Boutigny, S., . . . Rolland, N. (2011). Heterologous expression of membrane proteins: choosing the appropriate host. *PLoS One, 6*(12), e29191. doi:10.1371/journal.pone.0029191

Beste, K. Y., Burhenne, H., Kaever, V., Stasch, J.-P., & Seifert, R. (2011). Nucleotidyl cyclase activity of soluble guanylyl cyclase α1β1. *Biochemistry, 51*(1), 194-204.

Beste, K. Y., & Seifert, R. (2013). cCMP, cUMP, cTMP, cIMP and cXMP as possible second messengers: development of a hypothesis based on studies with soluble guanylyl cyclase α1β1. *Biological chemistry, 394*(2), 261-270.

Bhargava, A., Clabaugh, I., To, J. P., Maxwell, B. B., Chiang, Y. H., Schaller, G. E., . . . Kieber, J. J. (2013). Identification of cytokinin-responsive genes using microarray meta-analysis and RNA-Seq in Arabidopsis. *Plant Physiol, 162*(1), 272-294. doi:10.1104/pp.113.217026

Blum, A., Martin, H. J., & Maser, E. (2000). Human 11beta-hydroxysteroid dehydrogenase 1/carbonyl reductase: recombinant expression in the yeast Pichia pastoris and Escherichia coli. *Toxicology, 144*(1-3), 113-120.

Boeger, M. R. T., & Poulson, M. (2006). Efeitos da radiação ultravioleta-B sobre a morfologia foliar de Arabidopsis thaliana (L.) Heynh.(Brassicaceae). *Acta Botanica Brasilica*.

Bojar, D., Martinez, J., Santiago, J., Rybin, V., Bayliss, R., & Hothorn, M. (2014). Crystal structures of the phosphorylated BRI1 kinase domain and implications for brassinosteroid signal initiation. *Plant J, 78*(1), 31-43. doi:10.1111/tpj.12445

Bolwell, G. P. (1992). A role for phosphorylation in the down-regulation of phenylalanine ammonia-lyase in suspension-cultured cells of French bean. *Phytochemistry, 31*(12), 4081-4086.

Bowler, C., Neuhaus, G., Yamagata, H., & Chua, N. H. (1994). Cyclic GMP and calcium mediate phytochrome phototransduction. *Cell, 77*(1), 73-81.

Bradford, M. M. (1976). A Rapid and Sensitive Method for the Quantitation Microgram Quantities of Protein Utilizing the Principle of Protein-Dye Binding. *Analytical biochemistry, 254*, 248-254.

Breitenbach, H. H., Wenig, M., Wittek, F., Jorda, L., Maldonado-Alconada, A. M., Sarioglu, H., . . . Vlot, A. C. (2014). Contrasting Roles of the Apoplastic Aspartyl Protease APOPLASTIC, ENHANCED DISEASE SUSCEPTIBILITY1-DEPENDENT1 and LEGUME LECTIN-LIKE PROTEIN1 in Arabidopsis Systemic Acquired Resistance. *Plant Physiol, 165*(2), 791-809. doi:10.1104/pp.114.239665

Bridges, D., Fraser, M. E., & Moorhead, G. B. G. (2005). Cyclic nucleotide binding proteins in the Arabidopsis thaliana and Oryza sativa genomes. *BMC bioinformatics, 6*, 6-6. doi:10.1186/1471-2105-6-6

Brown, E. G., Al-Najafi, T., & Newton, R. (1975). Partial-purification of adenosine 3'-5'-cyclic monophosphate phosphodiesterase from Phaseolus vulgaris L. associated activator and inhibitors. *Biochemical Society Transactions, 3*(3), 393-395.

Brown, E. G., Al-Najafi, T., & Newton, R. (1977). Cyclic nucleotide phosphodiesterase activity in Phaseolus vulgaris. *Phytochemistry, 16*(9), 1333-1337.

Brown, E. G., Edwards, M. J., Newton, R., & Smith, C. (1979). Plurality of cyclic nucleotide phosphodiesterase in Spinacea oleracea: subcellular distribution, partial purification, and properties. *Phytochemistry, 18*(12), 1943-1948.

Brown, E. G., Edwards, M. J., Newton, R., & Smith, C. (1980). The cyclic nucleotide phosphodiesterases of spinach chloroplasts and microsomes. *Phytochemistry, 19*(1), 23-30.

Burhenne, H., Beste, K., Spangler, C., Voigt, U., Kaever, V., & Seifert, R. (2011). *Determination of cytidine 3', 5'-cyclic monophosphate and uridine 3', 5'-cyclic monophosphate in mammalian cell systems and in human urine by high-performance liquid chromatography/mass spectrometry.* Paper presented at the NAUNYN-SCHMIEDEBERGS ARCHIVES OF PHARMACOLOGY.

Burhenne, H., Tschirner, S., Seifert, R., & Kaever, V. (2013). Identification and quantitation of 2, 3-cGMP in murine tissues. *BMC Pharmacology and Toxicology, 14*(1), 1.

Cheung, W. Y. (1971). Cyclic 3 ', 5 '-nucleotide phosphodiesterase. Effect of divalent cations. *Biochim Biophys Acta, 242*(2), 395-409.

Choi, Y.-E., & Xu, J.-R. (2010). The cAMP signaling pathway in Fusarium verticillioides is important for conidiation, plant infection, and stress responses but not fumonisin production. *Molecular plant-microbe interactions, 23*(4), 522-533.

Chory, J. (1994). Plant phototransduction. Phytochrome signal transduction. *Curr Biol, 4*(9), 844-846.

Clarke, A., Desikan, R., Hurst, R. D., Hancock, J. T., & Neill, S. J. (2000). NO way back: nitric oxide and programmed cell death in Arabidopsis thaliana suspension cultures. *The Plant Journal, 24*(5), 667-677.

Cousson, A. (2010). Indolyl-3-butyric acid-induced Arabidopsis stomatal opening mediated by 3',5'-cyclic guanosine-monophosphate. *Plant Physiol Biochem, 48*(12), 977-986. doi:10.1016/j.plaphy.2010.09.007

Cousson, A., & Vavasseur, A. (1998). Putative involvement of cytosolic Ca 2+ and GTP-binding proteins in cyclic-GMP-mediated induction of stomatal opening by auxin in Commelina communis L. *Planta, 206*(2), 308-314. doi:10.1007/s004250050405

Daniel, P. B., Walker, W. H., & Habener, J. F. (1998). Cyclic AMP signaling and gene regulation. *Annual review of nutrition, 18*(1), 353-383.

de Alda, J. A. O., Ajlani, G., & Houmard, J. (2000). Synechocystis Strain PCC 6803cya2, a Prokaryotic Gene That Encodes a Guanylyl Cyclase. *Journal of Bacteriology, 182*(13), 3839-3842.

Deikman, J., & Hammer, P. E. (1995). Induction of Anthocyanin Accumulation by Cytokinins in Arabidopsis thaliana. *Plant Physiol, 108*(1), 47-57.

Derbyshire, E. R., & Marletta, M. A. (2012). Structure and regulation of soluble guanylate cyclase. *Annual review of biochemistry, 81*, 533-559. doi:10.1146/annurev-biochem-050410-100030

Desch, M., Schinner, E., Kees, F., Hofmann, F., Seifert, R., & Schlossmann, J. (2010). Cyclic cytidine 3′, 5′-monophosphate (cCMP) signals via cGMP kinase I. *FEBS letters, 584*(18), 3979-3984.

Dixon, R. A., & Paiva, N. L. (1995). Stress-induced phenylpropanoid metabolism. *The Plant cell, 7*(7), 1085.

Donaldson, L., Ludidi, N., Knight, M. R., Gehring, C., & Denby, K. (2004). Salt and osmotic stress cause rapid increases in Arabidopsis thaliana cGMP levels. *FEBS Lett, 569*(1-3), 317-320. doi:10.1016/j.febslet.2004.06.016

Dubovskaya, L. V., Bakakina, Y. S., Kolesneva, E. V., Sodel, D. L., McAinsh, M. R., Hetherington, A. M., & Volotovski, I. D. (2011). cGMP-dependent ABA-induced stomatal closure in the ABA-insensitive Arabidopsis mutant abi1-1. *New Phytologist, 191*(1), 57-69.

Dubovskaya, L. V., & Volotovski, I. D. (2004). AFFINITY CHROMATOGRAPHY ISOLATION AND CHARACTERIZATION OF SOLUBLE cGMP-BINDING PROTEINS FROM AVENA SATIVA L . SEEDLINGS. *Bulgarian Journal of Plant Physiology, 30*, 14-24.

Durner, J., Wendehenne, D., & Klessig, D. F. (1998). Defense gene induction in tobacco by nitric oxide, cyclic GMP, and cyclic ADP-ribose. *Proc Natl Acad Sci U S A, 95*(17), 10328-10333.

Ederli, L., Meier, S., Borgogni, A., Reale, L., Ferranti, F., Gehring, C., & Pasqualini, S. (2008). cGMP in ozone and NO dependent responses. *Plant Signal Behav, 3*(1), 36-37.

Ehsan, H., Reichheld, J.-P., Roef, L., Witters, E., Lardon, F., Van Bockstaele, D., . . . Van Onckelen, H. (1998). Effect of indomethacin on cell cycle dependent cyclic AMP fluxes in tobacco BY-2 cells. *FEBS letters, 422*(2), 165-169.

Ferrer, J.-L., Austin, M., Stewart, C., & Noel, J. (2008). Structure and function of enzymes involved in the biosynthesis of phenylpropanoids. *Plant Physiology and Biochemistry, 46*(3), 356-370.

Ferreyra, M. L. F., Rius, S. P., & Casati, P. (2012). Flavonoids: biosynthesis, biological functions, and biotechnological applications. *Frontiers in plant science, 3*.

Ferro, M., Salvi, D., Riviere-Rolland, H., Vermat, T., Seigneurin-Berny, D., Grunwald, D., . . . Rolland, N. (2002). Integral membrane proteins of the chloroplast envelope: identification and subcellular localization of new transporters. *Proc Natl Acad Sci U S A, 99*(17), 11487-11492. doi:10.1073/pnas.172390399

Firlej-Kwoka, E. (2008). *Protein import into the inner envelope membrane of chloroplasts.* lmu.

Freigassner, M., Pichler, H., & Glieder, A. (2009). Tuning microbial hosts for membrane protein production. *Microb Cell Fact, 8*, 69. doi:10.1186/1475-2859-8-69

Fröhlich, A., & Durner, J. (2011). The hunt for plant nitric oxide synthase (NOS): is one really needed? *Plant Sci, 181*(4), 401-404. doi:10.1016/j.plantsci.2011.07.014

Furchgott, R. F., & Zawadzki, J. V. (1980). The obligatory role of endothelial cells in the relaxation of arterial smooth muscle by acetylcholine. *Nature, 288*(5789), 373-376.

Gille, A., Lushington, G. H., Mou, T.-C., Doughty, M. B., Johnson, R. A., & Seifert, R. (2004). Differential inhibition of adenylyl cyclase isoforms and soluble guanylyl cyclase by purine and pyrimidine nucleotides. *Journal of Biological Chemistry, 279*(19), 19955-19969.

Goridis, C., & Morgan, I. G. (1973). Guanyl cyclase in rat brain subcellular fractions. *FEBS Lett, 34*(1), 71-73.

Gray, J., Close, P. S., Briggs, S. P., & Johal, G. S. (1997). A novel suppressor of cell death in plants encoded by the Lls1 gene of maize. *Cell, 89*(1), 25-31.

Grosche, A., Hauser, A., Lepper, M. F., Mayo, R., von Toerne, C., Merl-Pham, J., & Hauck, S. M. (2016). The Proteome of Native Adult Muller Glial Cells From Murine Retina. *Mol Cell Proteomics, 15*(2), 462-480. doi:10.1074/mcp.M115.052183

Gross, I., & Durner, J. (2016). In Search of Enzymes with a Role in 3′, 5′-Cyclic Guanosine Monophosphate Metabolism in Plants. *Frontiers in plant science, 7*.

Grzegorzewska, W., Swieżawska, B., Szewczuk, P., & Szmidt-Jaworska, A. (2012). Cyclic nucleotides are involved in the defense response against mechanical wounding and pathogen attack in Hippeastrum. *Acta Biochim Pol, 59*(Suppl 3, P6. 9), 165.

Hahlbrock, K. (1989). [Gene technology and biological safety]. *Naturwissenschaften, 76*(12), 560-564.

Hamet, P., Tremblay, J., Pang, S. C., Garcia, R., Thibault, G., Gutkowska, J., . . . Genest, J. (1984). Effect of native and synthetic atrial natriuretic factor on cyclic GMP. *Biochem Biophys Res Commun, 123*(2), 515-527.

Hanke, S. E., Bertinetti, D., Badel, A., Schweinsberg, S., Genieser, H. G., & Herberg, F. W. (2011). Cyclic nucleotides as affinity tools: phosphorothioate cAMP analogues address specific PKA subproteomes. *N Biotechnol, 28*(4), 294-301. doi:10.1016/j.nbt.2010.12.001

Hardman, J. G., & Sutherland, E. W. (1969). Guanyl cyclase, an enzyme catalyzing the formation of guanosine 3', 5'-monophosphate from guanosine triphosphate. *Journal of Biological Chemistry, 244*(23), 6363-6370.

Hartwig, C., Bahre, H., Wolter, S., Beckert, U., Kaever, V., & Seifert, R. (2014). cAMP, cGMP, cCMP and cUMP concentrations across the tree of life: High cCMP and cUMP levels in astrocytes. *Neurosci Lett, 579*, 183-187. doi:10.1016/j.neulet.2014.07.019

Hasan, A., Danker, K. Y., Wolter, S., Bähre, H., Kaever, V., & Seifert, R. (2014). Soluble adenylyl cyclase accounts for high basal cCMP and cUMP concentrations in HEK293 and B103 cells. *Biochemical and biophysical research communications, 448*(2), 236-240.

Hauck, S. M., Dietter, J., Kramer, R. L., Hofmaier, F., Zipplies, J. K., Amann, B., . . . Ueffing, M. (2010). Deciphering membrane-associated molecular processes in target tissue of autoimmune uveitis by label-free quantitative mass spectrometry. *Mol Cell Proteomics, 9*(10), 2292-2305. doi:10.1074/mcp.M110.001073

He, X.-l., Chow, D.-c., Martick, M. M., & Garcia, K. C. (2001). Allosteric activation of a spring-loaded natriuretic peptide receptor dimer by hormone. *Science, 293*(5535), 1657-1662.

Herrera, N. M. (2012). *Physiological and Molecular Effects of the Cyclic Nucleotides cAMP and cGMP on Arabidopsis thaliana.*

Humbert, P., Niroomand, F., Fischer, G., Mayer, B., Koesling, D., Hinsch, K. D., . . . Bohme, E. (1990). Purification of soluble guanylyl cyclase from bovine lung by a new immunoaffinity chromatographic method. *Eur J Biochem, 190*(2), 273-278.

Ignarro, L. J., Buga, G. M., Wood, K. S., Byrns, R. E., & Chaudhuri, G. (1987). Endothelium-derived relaxing factor produced and released from artery and vein is nitric oxide. *Proceedings of the National Academy of Sciences, 84*(24), 9265-9269.

Irving, H. R., Kwezi, L., Wheeler, J. I., & Gehring, C. (2012). Moonlighting kinases with guanylate cyclase activity can tune regulatory signal networks Do not distribute . © 2012 Landes Bioscience. *Plant Signaling & Behavior*(February), 201-204.

Isner, J. C., & Maathuis, F. J. M. (2011). Measurement of cellular cGMP in plant cells and tissues using the endogenous fluorescent reporter FlincG. *Plant J, 65*(2), 329-334. doi:10.1111/j.1365-313X.2010.04418.x

Isner, J. C., Nühse, T., & Maathuis, F. J. M. (2012). The cyclic nucleotide cGMP is involved in plant hormone signalling and alters phosphorylation of Arabidopsis thaliana root proteins. *Journal of Experimental Botany, 63*(8), 3199-3205. doi:10.1093/jxb/ers045

Jackson, E. K. (2011). The 2′, 3′-cAMP-adenosine pathway. *American Journal of Physiology-Renal Physiology, 301*(6), F1160-F1167.

Jackson, E. K., Gillespie, D. G., & Dubey, R. K. (2011). 2′-AMP and 3′-AMP inhibit proliferation of preglomerular vascular smooth muscle cells and glomerular mesangial cells via A2B receptors. *Journal of Pharmacology and Experimental Therapeutics, 337*(2), 444-450.

Jackson, E. K., Ren, J., & Mi, Z. (2009). Extracellular 2′, 3′-cAMP is a source of adenosine. *Journal of Biological Chemistry, 284*(48), 33097-33106.

Janistyn, B. (1988). Stimulation by manganese (II) sulphate of a cAMP-dependent protein kinase from Zea mays seedlings. *Phytochemistry, 27*(9), 2735-2736.

Janistyn, B. (1989). cAMP promoted protein phosphorylation of dialysed coconut milk. *Phytochemistry, 28*(2), 329-331.

Jiang, J., Fan, L. W., & Wu, W. H. (2005). Evidences for involvement of endogenous cAMP in Arabidopsis defense responses to Verticillium toxins. *Cell research, 15*(8), 585-592.

Jordan, B. R., James, P. E., & A. H-Mackerness, S. (1998). Factors affecting UV-B-induced changes in Arabidopsis thaliana L. gene expression: the role of development, protective pigments and the chloroplast signal. *Plant Cell Physiol, 39*(7), 769-778.

Kakiuchi, S., Yamazaki, R., & Teshima, Y. (1971). Cyclic 3',5'-nucleotide phosphodiesterase, IV. Two enzymes with different properties from brain. *Biochem Biophys Res Commun, 42*(5), 968-974.

Kamisaki, Y., Saheki, S., Nakane, M., Palmieri, J., Kuno, T., Chang, B., . . . Murad, F. (1986). Soluble guanylate cyclase from rat lung exists as a heterodimer. *Journal of Biological Chemistry, 261*(16), 7236-7241.

Kaplan, B., Sherman, T., & Fromm, H. (2007). Cyclic nucleotide-gated channels in plants. *FEBS letters, 581*(12), 2237-2246.

Kato, R., Uno, I., Ishikawa, T., & Fujii, T. (1983). Effects of cyclic AMP on the activity of soluble protein kinases in Lemna paucicostata. *Plant and cell physiology, 24*(5), 841-848.

Kempf, S. J., Buratovic, S., von Toerne, C., Moertl, S., Stenerlow, B., Hauck, S. M., . . . Tapio, S. (2014). Ionising radiation immediately impairs synaptic plasticity-associated cytoskeletal signalling pathways in HT22 cells and in mouse brain: an in vitro/in vivo comparison study. *PLoS One, 9*(10), e110464. doi:10.1371/journal.pone.0110464

Kim, E.-K., & Park, J.-M. (2003). Identification of novel target proteins of cyclic GMP signaling pathways using chemical proteomics. *BMB Reports, 36*(3), 299-304.

Kimura, H., & Murad, F. (1974). Evidence for two different forms of guanylate cyclase in rat heart. *J Biol Chem, 249*(21), 6910-6916.

Kimura, H., & Murad, F. (1975a). Increased particulate and decreased soluble guanylate cyclase activity in regenerating liver, fetal liver, and hepatoma. *Proc Natl Acad Sci U S A, 72*(5), 1965-1969.

Kimura, H., & Murad, F. (1975b). Two forms of guanylate cyclase in mammalian tissues and possible mechanisms for their regulation. *Metabolism, 24*(3), 439-445.

Koesling, D., Harteneck, C., Humbert, P., Bosserhoff, A., Frank, R., Schultz, G., & Böhme, E. (1990). The primary structure of the larger subunit of soluble guanylyl cyclase from

bovine lung Homology between the two subunits of the enzyme. *FEBS letters, 266*(1-2), 128-132.
Kots, A. Y., Martin, E., Sharina, I. G., & Murad, F. (2009). A short history of cGMP, guanylyl cyclases, and cGMP-dependent protein kinases. *Handb Exp Pharmacol*(191), 1-14. doi:10.1007/978-3-540-68964-5_1
Kurosaki, F., Tsurusawa, Y., & Nishi, A. (1987). The elicitation of phytoalexins by Ca2+ and cyclic AMP in carrot cells. *Phytochemistry, 26*(7), 1919-1923.
Kwezi, L., Meier, S., Mungur, L., Ruzvidzo, O., Irving, H., & Gehring, C. (2007). The Arabidopsis thaliana brassinosteroid receptor (AtBRI1) contains a domain that functions as a guanylyl cyclase in vitro. *PLoS One, 2*(5), e449-e449. doi:10.1371/journal.pone.0000449
Kwezi, L., Ruzvidzo, O., Wheeler, J. I., Govender, K., Iacuone, S., Thompson, P. E., . . . Irving, H. R. (2011). The phytosulfokine (PSK) receptor is capable of guanylate cyclase activity and enabling cyclic GMP-dependent signaling in plants. *The Journal of biological chemistry, 286*(25), 22580-22588. doi:10.1074/jbc.M110.168823
Labrecque, J., Deschênes, J., McNicoll, N., & De Léan, A. (2001). Agonistic induction of a covalent dimer in a mutant of natriuretic peptide receptor-A documents a juxtamembrane interaction that accompanies receptor activation. *Journal of Biological Chemistry, 276*(11), 8064-8072.
Lambers, H., Chapin III, F. S., & Pons, T. L. (2008). Photosynthesis *Plant physiological ecology* (pp. 11-99): Springer.
Laue, S., Winterhoff, M., Kaever, V., van den Heuvel, J. J., Russel, F. G., & Seifert, R. (2014). cCMP is a substrate for MRP5. *Naunyn-Schmiedeberg's archives of pharmacology, 387*(9), 893-895.
Lemtiri-Chlieh, F., Thomas, L., Marondedze, C., Irving, H., & Gehring, C. (2011). *Cyclic nucleotides and nucleotide cyclases in plant stress responses*: InTech Rijeka.
Li, J., Ou-Lee, T. M., Raba, R., Amundson, R. G., & Last, R. L. (1993). Arabidopsis Flavonoid Mutants Are Hypersensitive to UV-B Irradiation. *Plant Cell, 5*(2), 171-179. doi:10.1105/tpc.5.2.171
Li, S., & Xue, L. (2010). The interaction between H2O2 and NO, Ca2+, cGMP, and MAPKs during adventitious rooting in mung bean seedlings. *In Vitro Cellular & Developmental Biology - Plant, 46*(2), 142-148. doi:10.1007/s11627-009-9275-x
Lin, P. P.-C., & Varner, J. E. (1972). Cyclic nucleotide phosphodiesterase in pea seedlings. *Biochimica et Biophysica Acta (BBA)-Enzymology, 276*(2), 454-474.
Lucas, K. A., Pitari, G. M., Kazerounian, S., Ruiz-Stewart, I., Park, J., Schulz, S., . . . Waldman, S. A. (2000). Guanylyl cyclases and signaling by cyclic GMP. *Pharmacol Rev, 52*(3), 375-414.
Ludidi, N., & Gehring, C. (2003). Identification of a novel protein with guanylyl cyclase activity in Arabidopsis thaliana. *The Journal of biological chemistry, 278*(8), 6490-6494. doi:10.1074/jbc.M210983200
Maathuis, F. J. M. (2006). cGMP modulates gene transcription and cation transport in Arabidopsis roots. *Plant J, 45*(5), 700-711. doi:10.1111/j.1365-313X.2005.02616.x
Maathuis, F. J. M., & Sanders, D. (2001). Sodium uptake in Arabidopsis roots is regulated by cyclic nucleotides. *Plant Physiol, 127*(4), 1617-1625.
Mackey, D., Holt, B. F., 3rd, Wiig, A., & Dangl, J. L. (2002). RIN4 interacts with Pseudomonas syringae type III effector molecules and is required for RPM1-mediated resistance in Arabidopsis. *Cell, 108*(6), 743-754.
Marden, J. N., Dong, Q., Roychowdhury, S., Berleman, J. E., & Bauer, C. E. (2011). Cyclic GMP controls Rhodospirillum centenum cyst development. *Molecular microbiology, 79*(3), 600-615. doi:10.1111/j.1365-2958.2010.07513.x
Marondedze, C., Wong, A., Thomas, L., Irving, H., & Gehring, C. (2015). Cyclic Nucleotide Monophosphates in Plants and Plant Signaling.
Meier, S., Madeo, L., Ederli, L., Donaldson, L., Pasqualini, S., & Gehring, C. (2009). Deciphering cGMP signatures and cGMP-dependent pathways in plant defence. *Plant Signal Behav, 4*(4), 307-309.

Meier, S., Ruzvidzo, O., Morse, M., Donaldson, L., Kwezi, L., & Gehring, C. (2010). The Arabidopsis wall associated kinase-like 10 gene encodes a functional guanylyl cyclase and is co-expressed with pathogen defense related genes. *PLoS One, 5*(1), e8904-e8904. doi:10.1371/journal.pone.0008904

Merl, J., Ueffing, M., Hauck, S. M., & von Toerne, C. (2012). Direct comparison of MS-based label-free and SILAC quantitative proteome profiling strategies in primary retinal Muller cells. *Proteomics, 12*(12), 1902-1911. doi:10.1002/pmic.201100549

Miroux, B., & Walker, J. E. (1996). Over-production of proteins in Escherichia coli: mutant hosts that allow synthesis of some membrane proteins and globular proteins at high levels. *J Mol Biol, 260*(3), 289-298. doi:10.1006/jmbi.1996.0399

Mittler, R., Vanderauwera, S., Gollery, M., & Van Breusegem, F. (2004). Reactive oxygen gene network of plants. *Trends in plant science, 9*(10), 490-498.

Mol, J., Grotewold, E., & Koes, R. (1998). How genes paint flowers and seeds. *Trends in plant science, 3*(6), 212-217.

Monzel, M., Kuhn, M., Bahre, H., Seifert, R., & Schneider, E. H. (2014). PDE7A1 hydrolyzes cCMP. *FEBS Lett, 588*(18), 3469-3474. doi:10.1016/j.febslet.2014.08.005

Moura, J. C. M. S., Bonine, C. A. V., De Oliveira Fernandes Viana, J., Dornelas, M. C., & Mazzafera, P. (2010). Abiotic and biotic stresses and changes in the lignin content and composition in plants. *Journal of integrative plant biology, 52*(4), 360-376.

Mulaudzi, T., Ludidi, N., Ruzvidzo, O., Morse, M., Hendricks, N., Iwuoha, E., & Gehring, C. (2011). Identification of a novel Arabidopsis thaliana nitric oxide-binding molecule with guanylate cyclase activity in vitro. *FEBS letters, 585*(17), 2693-2697. doi:10.1016/j.febslet.2011.07.023

Nakane, M., Saheki, S., Kuno, T., Ishii, K., & Murad, F. (1988). Molecular cloning of a cDNA coding for 70 kilodalton subunit of soluble guanylate cyclase from rat lung. *Biochemical and biophysical research communications, 157*(3), 1139-1147.

Nan, W., Wang, X., Yang, L., Hu, Y., Wei, Y., Liang, X., . . . Bi, Y. (2014). Cyclic GMP is involved in auxin signalling during Arabidopsis root growth and development. *Journal of Experimental Botany, 65*(6), 1571-1583. doi:10.1093/jxb/eru019

Neuhaus, G., Bowler, C., Hiratsuka, K., Yamagata, H., & Chua, N. H. (1997). Phytochrome-regulated repression of gene expression requires calcium and cGMP. *The EMBO journal, 16*(10), 2554-2564.

Newton, R. (1995). Cytidine 3′, 5′-Cyclic Monophosphate: A Third Cyclic Nucleotide Secondary Messenger? *Nucleosides, Nucleotides & Nucleic Acids, 14*(3-5), 743-747.

Newton, R., Chiatante, D., Ghosh, D., Brenton, A. G., Walton, T. J., Harris, F. M., & Brown, E. G. (1989). Identification of cyclic nucleotide constituents of meristematic and non-meristematic tissue of Pisum sativum roots. *Phytochemistry, 28*(9), 2243-2254.

Newton, R., & Smith, C. (2004). Cyclic nucleotides. *Phytochemistry, 65*(17), 2423-2437. doi:10.1016/j.phytochem.2004.07.026

Opekarova, M., & Tanner, W. (2003). Specific lipid requirements of membrane proteins--a putative bottleneck in heterologous expression. *Biochim Biophys Acta, 1610*(1), 11-22.

Ordoñez, N. M., Marondedze, C., Thomas, L., Pasqualini, S., Shabala, L., Shabala, S., & Gehring, C. (2014). Cyclic mononucleotides modulate potassium and calcium flux responses to H2O2 in Arabidopsis roots. *FEBS letters, 588*(6), 1008-1015. doi:10.1016/j.febslet.2014.01.062

Overmyer, K., Brosche, M., Pellinen, R., Kuittinen, T., Tuominen, H., Ahlfors, R., . . . Kangasjarvi, J. (2005). Ozone-induced programmed cell death in the Arabidopsis radical-induced cell death1 mutant. *Plant Physiol, 137*(3), 1092-1104. doi:10.1104/pp.104.055681

Pagnussat, G. C., Lanteri, L., & Lamattina, L. (2003). Nitric Oxide and Cyclic GMP Are Messengers in the Indole Acetic Acid-Induced Adventitious Rooting Process 1. *Plant Physiology, 132*, 1241-1248. doi:10.1104/pp.103.022228.mals

Pasqualini, S., Meier, S., Gehring, C., Madeo, L., Fornaciari, M., Romano, B., & Ederli, L. (2009). Ozone and nitric oxide induce cGMP-dependent and -independent

transcription of defence genes in tobacco. *New Phytol, 181*(4), 860-870. doi:10.1111/j.1469-8137.2008.02711.x

Paul, R., Weiser, S., Amiot, N. C., Chan, C., Schirmer, T., Giese, B., & Jenal, U. (2004). Cell cycle-dependent dynamic localization of a bacterial response regulator with a novel di-guanylate cyclase output domain. *Genes Dev, 18*(6), 715-727. doi:10.1101/gad.289504

Penson, S. P., Schuurink, R. C., Fath, a., Gubler, F., Jacobsen, J. V., & Jones, R. L. (1996). cGMP Is Required for Gibberellic Acid-Induced Gene Expression in Barley Aleurone. *The Plant cell, 8*(12), 2325-2333. doi:10.1105/tpc.8.12.2325

Pfeiffer, S., Janistyn, B., Jessner, G., Pichorner, H., & Ebermann, R. (1994). Gaseous nitric oxide stimulates guanosine-3′, 5′-cyclic monophosphate (cGMP) formation in spruce needles. *Phytochemistry, 36*(2), 259-262.

Pharmawati, M., Billington, T., & Gehring, C. (1998). Stomatal guard cell responses to kinetin and natriuretic peptides are cGMP-dependent. *Cellular and Molecular Life Sciences CMLS, 54*(3), 272-276.

Pharmawati, M., Maryani, M. M., Nikolakopoulos, T., Gehring, C. A., & Irving, H. R. (2001). Cyclic GMP modulates stomatal opening induced by natriuretic peptides and immunoreactive analogues. *Plant Physiology and Biochemistry, 39*(5), 385-394. doi:Doi 10.1016/S0981-9428(01)01252-9

Pietrowska-Borek, M., & Nuc, K. (2013). Both cyclic-AMP and cyclic-GMP can act as regulators of the phenylpropanoid pathway in Arabidopsis thaliana seedlings. *Plant physiology and biochemistry : PPB / Société française de physiologie végétale, 70*, 142-149. doi:10.1016/j.plaphy.2013.05.029

Polya, G., Chung, R., & Menting, J. (1991). Resolution of a higher plant protein kinase similar to the catalytic subunit of cyclic AMP-dependent protein kinase. *Plant Science, 79*(1), 37-45.

Posmyk, M., Kontek, R., & Janas, K. (2009). Antioxidant enzymes activity and phenolic compounds content in red cabbage seedlings exposed to copper stress. *Ecotoxicology and Environmental Safety, 72*(2), 596-602.

Potter, L. R., & Hunter, T. (2001). Guanylyl cyclase-linked natriuretic peptide receptors: structure and regulation. *Journal of Biological Chemistry, 276*(9), 6057-6060.

Poulson, M. E., Boeger, M. R., & Donahue, R. A. (2006). Response of photosynthesis to high light and drought for Arabidopsis thaliana grown under a UV-B enhanced light regime. *Photosynth Res, 90*(1), 79-90. doi:10.1007/s11120-006-9116-2

Qi, Z., Verma, R., Gehring, C., Yamaguchi, Y., Zhao, Y., Ryan, C. A., & Berkowitz, G. A. (2010). Ca2+ signaling by plant Arabidopsis thaliana Pep peptides depends on AtPepR1, a receptor with guanylyl cyclase activity, and cGMP-activated Ca2+ channels. *Proc Natl Acad Sci U S A, 107*(49), 21193-21198. doi:10.1073/pnas.1000191107

Quick, M., & Wright, E. M. (2002). Employing Escherichia coli to functionally express, purify, and characterize a human transporter. *Proc Natl Acad Sci U S A, 99*(13), 8597-8601. doi:10.1073/pnas.132266599

Rapoport, R. M., Draznin, M. B., & Murad, F. (1983). Endothelium-dependent relaxation in rat aorta may be mediated through cyclic GMP-dependent protein phosphorylation. *Nature, 306*(5939), 174-176.

Rapoport, R. M., & Murad, F. (1983). Agonist-induced endothelium-dependent relaxation in rat thoracic aorta may be mediated through cGMP. *Circ Res, 52*(3), 352-357.

Rauch, A., Leipelt, M., Russwurm, M., & Steegborn, C. (2008). Crystal structure of the guanylyl cyclase Cya2. *Proceedings of the National Academy of Sciences, 105*(41), 15720-15725.

Richards, H., Das, S., Smith, C., Pereira, L., Geisbrecht, A., Devitt, N. J., . . . Newton, R. (2002). Cyclic nucleotide content of tobacco BY-2 cells. *Phytochemistry, 61*(5), 531-537.

Romling, U., Galperin, M. Y., & Gomelsky, M. (2013). Cyclic di-GMP: the first 25 years of a universal bacterial second messenger. *Microbiol Mol Biol Rev, 77*(1), 1-52. doi:10.1128/MMBR.00043-12

Russell, M. H., Bible, A. N., Fang, X., Gooding, J. R., Campagna, S. R., Gomelsky, M., & Alexandre, G. (2013). Integration of the second messenger c-di-GMP into the chemotactic signaling pathway. *MBio, 4*(2), e00001-00013. doi:10.1128/mBio.00001-13

Ryan, K. G., Swinny, E. E., Markham, K. R., & Winefield, C. (2002). Flavonoid gene expression and UV photoprotection in transgenic and mutant Petunia leaves. *Phytochemistry, 59*(1), 23-32.

Schaap, P. (2005). Guanylyl cyclases across the tree of life. *Front Biosci, 10*, 1485-1498.

Seifert, R. (2015). cCMP and cUMP: emerging second messengers. *Trends in biochemical sciences, 40*(1), 8-15.

Seifertová, D., Skůpa, P., Rychtář, J., Laňková, M., Pařezová, M., Dobrev, P. I., . . . Zažímalová, E. (2014). Characterization of transmembrane auxin transport in Arabidopsis suspension-cultured cells. *Journal of Plant Physiology, 171*(6), 429-437. doi:10.1016/j.jplph.2013.09.026

Simm, R., Morr, M., Kader, A., Nimtz, M., & Romling, U. (2004). GGDEF and EAL domains inversely regulate cyclic di-GMP levels and transition from sessility to motility. *Mol Microbiol, 53*(4), 1123-1134. doi:10.1111/j.1365-2958.2004.04206.x

Smith, C. (1996). Tansley Review No. 86 Accumulation of phytoalexins: defence mechanism and stimulus response system. *New Phytologist, 132*(1), 1-45.

Sokurenko, Y. V., Zelenikhin, P., Ulyanova, V., Kolpakov, A., Muller, D., & Ilinskaya, O. (2015). Identification of 2′, 3′-cGMP as an intermediate of RNA catalytic cleavage by binase and evaluation of its biological action. *Russian Journal of Bioorganic Chemistry, 41*(1), 31-36.

Spierings, F. H. F. G. (1971). Influence of fumigations with NO~ on growth and yield of tomato plants. *Netherlands Journal of Plant Pathology, 77*, 194-200.

Stone, J. M., Heard, J. E., Asai, T., & Ausubel, F. M. (2000). Simulation of fungal-mediated cell death by fumonisin B1 and selection of fumonisin B1-resistant (fbr) Arabidopsis mutants. *Plant Cell, 12*(10), 1811-1822.

Stone, J. R., & Marletta, M. A. (1994). Soluble guanylate cyclase from bovine lung: activation with nitric oxide and carbon monoxide and spectral characterization of the ferrous and ferric states. *Biochemistry, 33*(18), 5636-5640.

Suita, K., Kiryu, T., Sawada, M., Mitsui, M., Nakagawa, M., Kanamaru, K., & Yamagata, H. (2009). Cyclic GMP acts as a common regulator for the transcriptional activation of the flavonoid biosynthetic pathway in soybean. *Planta, 229*(2), 403-413.

Swiezawska, B., Jaworski, K., Szewczuk, P., Pawelek, A., & Szmidt-Jaworska, A. (2015). Identification of a Hippeastrum hybridum guanylyl cyclase responsive to wounding and pathogen infection. *Journal of Plant Physiology, 189*, 77-86. doi:10.1016/j.jplph.2015.09.014

Sytar, O., Bruckova, K., Hunkova, E., Zivcak, M., Konate, K., & Brestic, M. (2015). The application of multiplex fluorimetric sensor for the analysis of flavonoids content in the medicinal herbs family Asteraceae, Lamiaceae, Rosaceae. *Biol Res, 48*, 5. doi:10.1186/0717-6287-48-5

Szklarczyk, D., Franceschini, A., Wyder, S., Forslund, K., Heller, D., Huerta-Cepas, J., . . . von Mering, C. (2015). STRING v10: protein-protein interaction networks, integrated over the tree of life. *Nucleic Acids Res, 43*(Database issue), D447-452. doi:10.1093/nar/gku1003

Szmidt-Jaworska, A., Jaworski, K., Pawełek, A., & Kopcewicz, J. (2009). Molecular cloning and characterization of a guanylyl cyclase, PNGC-1, involved in light signaling in Pharbitis nil. *Journal of plant growth regulation, 28*(4), 367-380.

Talamond, P., Verdeil, J. L., & Conejero, G. (2015). Secondary metabolite localization by autofluorescence in living plant cells. *Molecules, 20*(3), 5024-5037. doi:10.3390/molecules20035024

Taylor, O. C. E., F.M. (1966). Suppression of Plant Growth by Nitrogen Dioxide'. *Plant Physiology, 41*, 132-135.

Thompson, W. J., & Appleman, M. M. (1971). Characterization of cyclic nucleotide phosphodiesterases of rat tissues. *J Biol Chem, 246*(10), 3145-3150.

Tresguerres, M., Levin, L. R., & Buck, J. (2011). Intracellular cAMP signaling by soluble adenylyl cyclase. *Kidney international, 79*(12), 1277-1288.

Van Damme, T., Blancquaert, D., Couturon, P., Van Der Straeten, D., Sandra, P., & Lynen, F. (2014). Wounding stress causes rapid increase in concentration of the naturally occurring 2′, 3′-isomers of cyclic guanosine-and cyclic adenosine monophosphate (cGMP and cAMP) in plant tissues. *Phytochemistry, 103*, 59-66.

von Toerne, C., Kahle, M., Schafer, A., Ispiryan, R., Blindert, M., Hrabe De Angelis, M., . . . Hauck, S. M. (2013). Apoe, Mbl2, and Psp Plasma Protein Levels Correlate with Diabetic Phenotype in NZO Mice - An Optimized Rapid Workflow for SRM-Based Quantification. *J Proteome Res, 12*(3), 1331-1343. doi:10.1021/pr3009836

Wagner, S., Klepsch, M. M., Schlegel, S., Appel, A., Draheim, R., Tarry, M., . . . de Gier, J. W. (2008). Tuning Escherichia coli for membrane protein overexpression. *Proc Natl Acad Sci U S A, 105*(38), 14371-14376. doi:10.1073/pnas.0804090105

Waldman, S. A., Rapoport, R. M., & Murad, F. (1984). Atrial natriuretic factor selectively activates particulate guanylate cyclase and elevates cyclic GMP in rat tissues. *J Biol Chem, 259*(23), 14332-14334.

Wang, Y.-F., Munemasa, S., Nishimura, N., Ren, H.-M., Robert, N., Han, M., . . . Schroeder, J. I. (2013). Identification of cyclic GMP-activated non-selective Ca2+-permeable cation channels and associated CNGC5 & CNGC6 genes in Arabidopsis guard cells. *Plant Physiology, 163*(October), 578-590. doi:10.1104/pp.113.225045

Wasson, A. P., Pellerone, F. I., & Mathesius, U. (2006). Silencing the flavonoid pathway in Medicago truncatula inhibits root nodule formation and prevents auxin transport regulation by rhizobia. *Plant Cell, 18*(7), 1617-1629. doi:10.1105/tpc.105.038232

Weinhouse, H., Sapir, S., Amikam, D., Shilo, Y., Volman, G., Ohana, P., & Benziman, M. (1997). c-di-GMP-binding protein, a new factor regulating cellulose synthesis in Acetobacter xylinum. *FEBS Lett, 416*(2), 207-211.

Winkel-Shirley, B. (2001). Flavonoid biosynthesis. A colorful model for genetics, biochemistry, cell biology, and biotechnology. *Plant Physiology, 126*(2), 485-493.

Winkel-Shirley, B. (2002). Biosynthesis of flavonoids and effects of stress. *Curr Opin Plant Biol, 5*(3), 218-223.

Wittek, F., Hoffmann, T., Kanawati, B., Bichlmeier, M., Knappe, C., Wenig, M., . . . Vlot, A. C. (2014). Arabidopsis ENHANCED DISEASE SUSCEPTIBILITY1 promotes systemic acquired resistance via azelaic acid and its precursor 9-oxo nonanoic acid. *Journal of Experimental Botany, 65*(20), 5919-5931. doi:10.1093/jxb/eru331

Wolter, S., Dove, S., Golombek, M., Schwede, F., & Seifert, R. (2014). N4-monobutyryl-cCMP activates PKA RIα and PKA RIIα more potently and with higher efficacy than PKG Iα in vitro but not in vivo. *Naunyn-Schmiedeberg's archives of pharmacology, 387*(12), 1163-1175.

Wolter, S., Golombek, M., & Seifert, R. (2011). Differential activation of cAMP-and cGMP-dependent protein kinases by cyclic purine and pyrimidine nucleotides. *Biochemical and biophysical research communications, 415*(4), 563-566.

Woodward, A. W., & Bartel, B. (2005). Auxin: regulation, action, and interaction. *Ann Bot, 95*(5), 707-735. doi:10.1093/aob/mci083

Yoshioka, H., Asai, S., Yoshioka, M., & Kobayashi, M. (2009). Molecular mechanisms of generation for nitric oxide and reactive oxygen species, and role of the radical burst in plant immunity. *Molecules and cells, 28*(4), 321-329.

Zeevaart, A. J. (1976). Some effects of fumigating plants for short periods with NO2. *Environmental Pollution, 11*, 97-108.

Zhang, J., Subramanian, S., Stacey, G., & Yu, O. (2009). Flavones and flavonols play distinct critical roles during nodulation of Medicago truncatula by Sinorhizobium meliloti. *Plant J, 57*(1), 171-183. doi:10.1111/j.1365-313X.2008.03676.x

Zong, X., Krause, S., Chen, C.-C., Krüger, J., Gruner, C., Cao-Ehlker, X., . . . Biel, M. (2012). Regulation of hyperpolarization-activated cyclic nucleotide-gated (HCN) channel activity by cCMP. *Journal of Biological Chemistry, 287*(32), 26506-26512.

6 Supplement

Table 28: Band intensity measurements using ImageJ.

Figure	Lane-name	MGV* (red band)	MGV (blue band, control)	MGV blue band/ MGV red band	% of "no-preincubation"
Figure 23	No preincubation	104.08	112.55	1.08	100.00
	100 µM 2'3' cGMP	144.37	121.42	0.84	77.77
	100 µM 3'5'-cGMP	179.7	142.31	0.79	73.23
Figure 26	No preincubation	140.82	146.29	1.04	100.00
	100 µM 3'5'-cGMP	168	134.15	0.80	76.87
	100 µM 3'5'-cAMP	112.52	114.66	1.02	98.09
	100 µM ATP	110.21	121.12	1.10	105.79
	100 µM GTP	105.43	101.04	0.96	92.25
	100 µM GDP	120.06	114.36	0.95	91.69
	100 µM GMP	114.03	114.67	1.01	96.80
Figure 30 (A)	No preincubation	131.12	163.27	1.25	100.00
	100 µM 3'5'-cGMP	176.12	166.07	0.94	75.73
	100 µM 2'3' cGMP	179.92	179.84	1.00	80.27
Figure 30 (B)	N8846	107.61	127.1	1.18	100.00
	SAIL_65_B07	173.01	152.3	0.88	74.53
	SAIL_69_B02	137.9	122.33	0.89	75.11
Figure 32	No preincubation	182.622	165.39	0.91	100.00
	100 µM 3'5'-cGMP	191.14	142.91	0.75	82.56
	100 µM trans-zeatin-riboside	182.73	157.78	0.86	95.34

*MGV= mean gray value

Table 29: Common elements of the indicated preparations.
All candidates of the 3 preparations with a fold-change >1.5 and the candidates from the gel cut analysis were compared (Figure 25).

Elution 1 **Elution 2** **Elution 3** **Gel-cut candidates**	**Elution 1** **Elution 2** **Elution 3**	**Elution 1** **Elution 2**	**Elution 1** **Elution 3**	**Elution 2** **Elution 3**
AT3G61870	AT5G54160	AT3G56190	AT5G37510	AT2G20990
	AT4G24190	AT5G20890	AT5G52840	AT5G54770
	AT5G16620	AT5G13430	AT2G33220	AT5G37360
	AT1G65260	AT4G17530	AT1G57720	AT5G38480
		AT2G44060	AT3G42050	AT3G20050
		AT1G56190	AT2G35490	ATCG00350
		AT4G35260	ATCG00720	AT5G56010
		AT3G15950	AT3G08940	
			AT3G26650	
			AT1G12900	
			AT5G08060	
			AT4G35450	
			AT3G18190	

Acknowledgements

Without the support of many people, I could have never carried out this thesis. Therefore, I would like to thank all these people for their help, encouragement and advices.

First of all, I would like to express my sincere gratitude to Prof. Dr. Jörg Durner, for giving me the opportunity to carry out my thesis in his research group and for his guidance and continuous scientific and personal support.

I would also like to thank Prof. Dr. Brigitte Poppenberger-Sieberer for her participation in my thesis committee and for her helpful ideas and comments regarding this project.

Moreover, I want to thank Dr. Frank Gaupels and Dr. Inonge Gross for their help, suggestions and encouragement during this thesis. It was very pleasant to have such optimistic supervisors.

Further, I want to thank Dr. Christine von Törne for the protein identification and quantification service and Dr. Daniela Bertinetti for the support in establishing the protein pull-down assay. Additionally, I would like to thank Prof. Dr. Volkhard Kaever and Annette Garbe for the measurements of cNMPs.

For all their suggestions, ideas and the enjoyable working atmosphere I want to thank all of my colleagues. It was a pleasure working with you. Especially I want to thank Claudia Scheler and Dörte Kasten for their personal support and their ability to make me laugh even on the worst days.

A special thanks goes to my parents, for their support, encouragement and their trust in me. I would have never gotten so far without you!

Finally, I want to thank Raymond Kempkens. You are my one and only, the love of my life and my best friend. You raised me up when I was down, you supported me in every decision and you made me believe in myself. Ich liebe dich!